Master Thesis

M. Admiraal

Decentralized sewage treatment by ceramic Microfiltration

A study in the RINEW project concept

TU Delft

QSENZ water- en gasanalyse

Evides waterbedrijf

Master of Science Thesis in Civil Engineering

Decentralized sewage water treatment by ceramic Microfiltration

By:

Ing. M. Admiraal

Graduation Committee

Prof. Dr. ir. J.B. (Jules) van Lier

Dr. ir. S.G.J. (Bas) Heijman

Prof. Dr. ir. J.S. (Hans) Vrouwenvelder

Dr. ir. P. (Paula) van den Brink

Delft University of Technology

Faculty of Civil Engineering and Geosciences

Department of Water Management

Sanitary Engineering Section

24-07-2017

Preface

Bernoulli's principle states:

'an increase in the speed of a fluid occurs simultaneously with a decrease in pressure or a fluid's potential energy'

After reading and understanding Bernoulli's principle in the first year of my applied science study Civil Engineering, my love for water was born. Finalizing my thesis in 2013 I got in touch with water technology. I asked myself the question: What is required to directly close the urban water cycle in order to create a sustainable living and working area? I thought by myself: Membranes! Well, here I am, enthusiastically graduating the master study 'Watermanagement' at the TU Delft as part of the RINEW project. RINEW uses membrane technologies to study different ways to recover valuable substances directly from sewage water.

For seven months I cycled to the RINEW pilot near the Merwehaven in Rotterdam. Finding my way within the pilot hall, creating interesting research questions and performing the corresponding experiments. Therefore, I would like to thank Han van der Griek and Tessa Steenbakker who supported me in setting-up and executing my experimental work.

I would like to thank the committee members; prof. Jules van Lier, prof. Hans Vrouwenvelder and dr. Paula van der Brink but especially my day-to-day supervisor dr. Bas Heijman. Bas helped me throughout the whole graduation process enabling me to obtain my master title.

At last I would like to thank my girlfriend, sister and parents for the necessary moral support and distraction.

Max Admiraal

Delft, August 2017

Abstract

The increase in greenhouse gas emissions change the precipitation behaviour causing either extreme wet- or dry weather. This impacts the fresh water supply for clean water production. Evides B.V., one of the Dutch water companies, anticipates to these changes with the sewer mining concept called 'RINEW' (Rotterdam Innovative Nutrients and Energy Watermanagement). RINEW studies various ways to recover valuable substances in direct decentralized sewage treatment. The treatment scheme involves the pre-treatment microscreen, coagulation and ceramic Microfiltration (cMF) for the water purification step Reverse Osmosis (RO). Since the application of cMF for sewage treatment is a novel concept, the objective of present thesis is to gain insight into technical aspects of cMF (a cMF fouling indicator and effect of oxygen on RO biofouling) and potential financial feasibility of the RINEW concept in the Netherlands.

To study the potential of a fouling indicator for the cMF, irreversible fouling rates and feed water quality results are obtained over a two month period. The feed water quality is digitally monitored and characterized on COD, NTU and EC. The parameter 'COD' (chemical oxygen demand) is considered the most suitable as fouling indicator due to the relative large particle size of organic matter and sticky properties of biopolymers. Relating the fouling rates to the feed water quality results in a linear trend where higher irreversible fouling rates occur at higher COD concentrations. Yet, the trend result is scattered significantly since the operational flux was highly instable over time. The feed pump is originally designed for a Nanofiltration (NF) application which may explain the deviant cMF operation.

The effect of oxygen in cMF permeate is studied on the (bio)fouling development on spiral wound Reverse Osmosis (RO). The study is done in duplicate each time using two parallel Membrane Fouling Simulator (MFS) which are fed by cMF permeate. In one MFS setup the water is depleted from oxygen by adding Sodium Bisulfite ($NaHSO_3$). The pressure drop results in the MFS fed by aerobic water indicate a significant unstable fouling rate. The fouling rates obtained from the MFS fed by oxygen depleted water compare to similar studies done with NF permeate and tap water. This suggest a significant stable RO biofouling can be obtained if Sodium Bisulfite treatment is applied to RO feed water.

The potential financial feasibility is studied via a concept study. Concept 1 is the RINEW concept providing high quality water (e.g. demi water) to an industry. Since it is a sewer mining concept the water transport costs are neglected. In concept 2 an equal high quality water flow is produced from secondary effluent by a MF/UF+RO combination at a central Sewage Treatment Plant (SWTP). The water transport from the central SWTP to the industry is taken into account in concept 2. The difference in specific costs [EURm-3] between the two concepts is estimated which is recalculated into a breakeven the high quality water transport distance of approximately 20 km. In other words, if an industry demands high quality water and sewage is the only water source, concept 2 is more financial feasible within a range of 20 km from a SWTP. In relation to the Netherlands the SWTP density is discussed as too high for the RINEW concept to be financial feasible. Similar realized treatment plants in the Netherlands show higher importance to aspects like water source, current expertise and existing facilities in the decision-making of treatment plant.

Table of contents

List of figures

Chapter 1

Introduction

1.1 Background

Climate change dominates scientific, politic, and public discussions all over the world. Increased greenhouse gas emissions warm the planet we are living on which leads to a change in regional and global hydrological cycles (Hageman, *et al*. 2013). Accordingly, increasing trends in global temperature and change in precipitation causing either extreme wet- or dry weather. These changes will impact the fresh water supply for clean water production (e.g. demi water or drinking water) which is a fundamental concern.

Water companies have to anticipate to these changes to guarantee safe and clean water for domestic and industrial customers. Evides B.V. is one of the Dutch water companies dealing with such problems. Located in Rotterdam, Evides B.V. is responsible for the sewage treatment at Dutch largest sewage treatment plant (SWTP) 'Harnaschpolder'. Furthermore, Evides provides safe and clean water to 2.5 million customers and companies in the Brabantse Wal, province Zeeland and the southwest of the province Zuid-Holland.

A conventional sewage treatment plant (SWTP) exists of three main stages: primary-, secondary- and tertiary treatment (Metcalf & Eddy, 2014). Primary treatment usually physically removes the large substances from the raw sewage, *the influent*. In the secondary treatment biological processes consume or incorporate the bulk sewage parameters: organic matter (COD) and nutrients (N and P). Depending on the receiving water body the secondary treatment product can be discharged to open water, *the effluent*. In case of a high sensitivity of the open water to effluent discharges the water is further treated/polished in tertiary treatment. Conventionally the effluent is discharged on a water body after removal of polluting- and hazardous material (Mo, *et al*. 2013). However, sewage water is one of the most reliable water sources which makes it interesting as source for water reclamation (Ghayeni, *et al*. 1998).

To anticipate to the above mentioned challenges Evides B.V. started a research project in 2015 called 'RINEW' (Innovative Nutrient Energy and Watermanagement in Rotterdam). The goal of the RINEW project is to study ways for resource recovery from sewage in order to directly close the urban water- and resource cycle. In other words, used domestic- and/or industrial water, sewage, is directly treated in order to recover clean water and other valuable substances as nutrients and energy. This thesis is focusses on water recovery from sewage and is performed and written as part of the RINEW project in close collaboration with Evides B.V.

The RINEW project involves a pilot study which is located near the Merwehaven in Rotterdam and treats sewage mainly originating from harbour activities, see red oval in Figure 1-1. Rotterdam municipality attempts to boost the Merwehaven into sustainable living and working communities since harbour activities are moving, increasingly, towards the North Sea, i.e. Maasvlakte I & II (Legierse, 2013). Evides B.V. collaborates with the municipality to realize the sustainable living area.

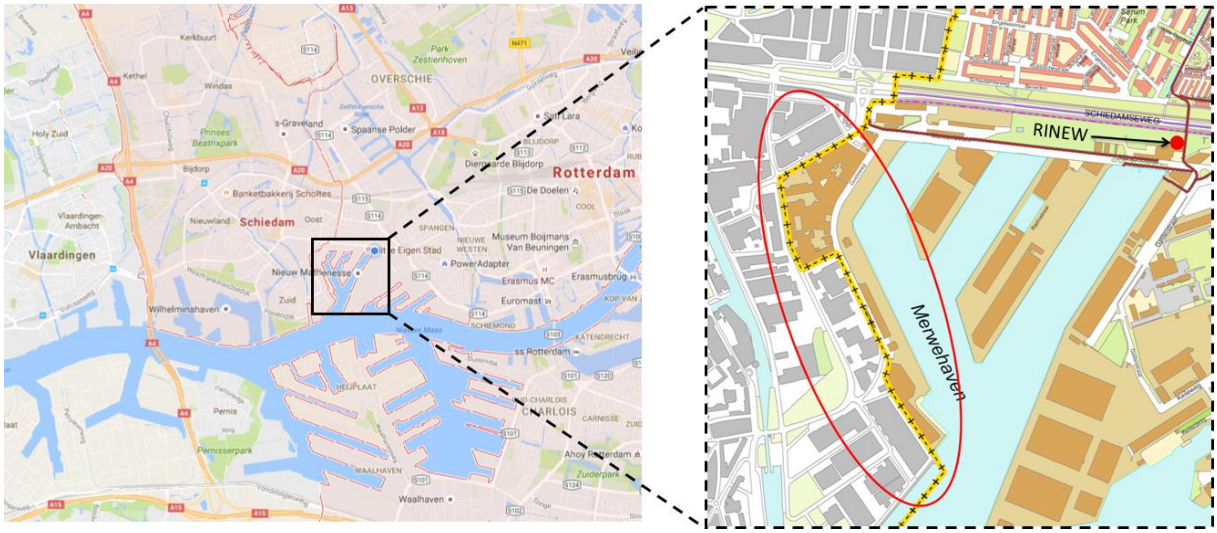

Figure 1-1. The RINEW location in Rotterdam. The red oval represents the origin of the incoming sewage water.

The RINEW pilot is a sewer mining concept where sewage is concentrated and send back into the sewer for further treatment at a central SWTP. While concentrating, clean water and other valuable substances are recovered via physical-chemical treatment processes. The RINEW treatment is novel concept including subsequently coagulation, microscreen, softener and membrane filtration, see Figure 1-2. As membrane filtration the ceramic Microfiltration (cMF) and Reverse Osmosis (RO) are applied. Membranes as dependable barrier in wastewater treatment can increase system reliability as well as lowering the latent riskts due to wastewater reuse (Fane *et al*., 2005). Direct sewage treatment by the cMF is a novel concept which makes it the main topic of this thesis.

Coagulation is a technique where chemical dosing aids in the aggregation of small particles into 'flocs' (Metcalf & Eddy, 2014). The mixing tank provides mixing and contact time for the chemicals to react. The coagulation principle is discussed in more detail in chapter 2.1.1. Coagulation increases the efficiency of the following cMF (Carrol, et al. 1999). The *microscreen* is a rotating micro screen designed to physically remove coarse particles, like hair and sand grains (Ntiako, 2014). The microscreen is used to limit any damage further in following treatment steps. The *cMF* removes the suspended solids and bacteria in order to pre-treat the water for the RO step. The *softener* removes mineral species from the water in order to limit the mineral fouling (scaling) at the RO. The membrane theory is explained in chapter 2.2.3. The final purification step is the RO which is able to produce high quality water.

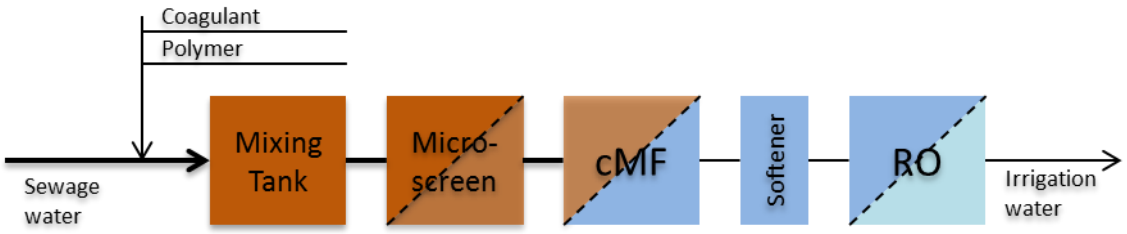

Figure 1-2. General overview of the RINEW plant

In water treatment, the membrane acts as physical barrier to separate specific components from a water flow (Mulder, 1996). Generally, the driving force in membrane filtration is a pressure difference over the membrane, called the 'Transmembrane Pressure' (TMP). Four types of membrane filtration are distinguished: microfiltration (MF), ultrafiltration (UF), nanofiltration (NF) and reverse osmosis (RO), see Figure 1-3. The MF and UF, just like NF and RO, are usually explained in the same way as their removal principles are very similar. Several membrane materials types are available, ceramic or polymeric. Ceramic membranes are emerging in water treatment due to their longer operational life time and higher chemical-, mechanical- and thermal stability (Shang, *et al*. 2015).

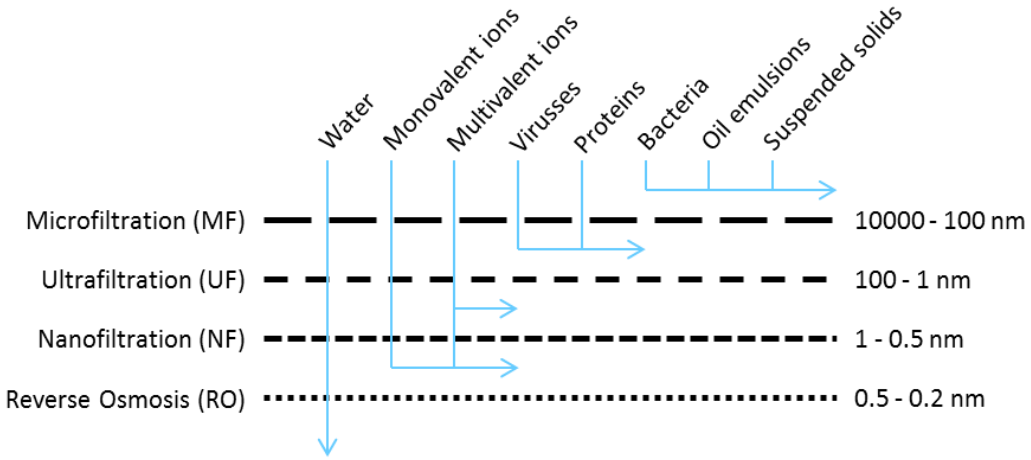

Figure 1-3. Classification of membrane processes with pore size and removable components (adapted from Mulder, 1996)

The major limitation to the application of membrane processes is membrane *fouling*. Fouling are all unwanted deposits on the membrane surface or in membrane pores increasing its resistance. Generally, four types of components foul the membrane simultaneously and may interact with each other (Flemming, *et al*. 1997). These are particle/colloid fouling, inorganic fouling (scaling), organic fouling and microbial fouling (biofouling).

Fouling is also distinguished between hydraulically reversible- and irreversible fouling. The hydraulic reversible fouling is easily removed by physical cleaning (backwash with clean water) where advanced cleaning, generally chemical cleaning, is required to fight irreversible fouling. In membrane processes the irreversible fouling is still a critical aspect increasing the energy consumption and operational costs (Shang, *et al*. 2015). Several lab studies showed that organic matter (or specific organic structures) influence the irreversible fouling at *MF/UF* membranes (Gaulinger, *et al*. 2007).

Generally, a RO step follows a MF/UF pre-treatment. One of the most serious challenges in a RO application is biofouling, i.e. excessive biomass growth (Vrouwenvelder, 2009; Flemming, *et al*. 1997). Biofouling increases the pressure drop across the membrane element resulting in higher operational costs. Depending on the treatment conditions (e.g. temperature, oxygen concentration and pH) different bacteria will grow, resulting in a different biofouling growth rate. The oxygen concentration is a critical condition since aerobic bacteria (heterotrophs) have a higher synthesis yield compared to anaerobic bacteria (autotrophs) (Metcalf & Eddy, 2014). For example, Beyer (2014) studied the fouling assessment of 4 full-scale direct NF installations, treating anoxic groundwater. With oxygen concentration measured below 0.01 mgO_2L^{-1} a stable NF operation could be maintained for one year. In comparison, van Paassen (1998) studied the productivity decline of a NF treating aerated water. Due to significant iron precipitation no stable NF operation could be obtained. In order to deplete the oxygen sodium bisulfite ($NaHSO_3$) is dosed continue causing a stable NF operation for approximately 100 days.

Since the RINEW concept is a sewer mining concept, high quality water is reclaimed at decentralized scale. This is an alternative to conventional water reclamation where secondary effluent is purified at a central SWTP. Generally the treatment includes the MF/UF and RO combination (Metcalf & Eddy, 2014). The additional costs for MF/UF+RO to a conventional SWTP is suggested to be as low as 0.64 $\$m^{-3}$ (Ghayeni, *et al*. 1998). The treatment cost of 0.64 $\$m^{-3}$ will be lower than the decentralized treatment costs since the SWTP acts ass pre-treatment. Also several facilities, like power and space, are already available at a central SWTP. However, central SWTP's are generally at remote locations which results in higher water transport costs. The costs of water transport is often estimated as two third of the total water costs. Thus, the costs and water transport distance can have a significant influence on the feasibility of the RINEW concept as decentralized water reclamation plant.

1.2 Objective and Research Questions

The main goal of this study is "*To gain insight into technical aspects of ceramic Microfiltration (cMF irreversible fouling rate and RO biofouling) and potential financial feasibility of the RINEW concept in the Netherlands.*

To reach the goal three research questions are defined, which are further explained below.

Sewage water arriving at the RINEW pilot plant originates from a relative small industrial area. Therefore, larger and irregular influent concentration peaks are expected, affecting the cMF performance. The cMF performance can be expressed as the irreversible fouling rate which is defined as the change in membrane resistance per hour ($m^{-1}h^{-1}$). Since the incoming water quality affects the irreversible fouling rate the first research question becomes:

1. *Which common digital water quality parameter can be used as irreversible fouling rate indicator for the cMF in decentralized sewage treatment?*

After filtered by the cMF the water is treated by the RO. The water arriving at the RO is fully aerated due to several operational conditions in the RINEW pilot. The high oxygen concentration will enhance fast growing (heterotrophic) bacteria thus a less stable/controlled RO biofouling is expected. Since biofouling is considered the most difficult to control at an RO membrane the second research question becomes:

2. *What is the effect of oxygen in cMF permeate on the biofouling potential in a RO unit?*

Besides the technical feasibility of the RINEW concept, different aspects will determine the realization of RINEW. These aspects can include the costs, location, water source and already realized infrastructure/treatment plants. The effect of costs and location on the potential of the RINEW concept are studied by the following research question:

3. *What is the potential financial feasibility of water reclamation by the RINEW concept compared to water reclamation at a central SWTP?*

1.3 Report outline and working method

To attain the goal and to answer the questions mentioned in the previous section three separate studies are performed.

At first in Chapter 2 the background theory is given of the particle types and all process techniques of importance in present thesis. The theory is followed by a description of site in Chapter 3 of the RINEW pilot in Rotterdam. Here the influent characteristics and the RINEW pilot are discussed

The first research question is described in Chapter 4. Potential relations are studied between different common water quality parameters and irreversible fouling rate at the cMF. The relation is based on digital monitoring results in the RINEW pilot for a period of two months.

The second research question is described in Chapter 5. Possible effects of oxygen in cMF permeate on RO (bio)fouling are discussed. Results are obtained from two runs wherein each two parallel Membrane Fouling Simulators (MFS's) are used. Each time one MFS is fed by present available cMF permeate (aerobic) and one MFS is fed cMF permeate depleted from oxygen.

The third research question is described in Chapter 6. In a concept study costs ($EURm^{-3}$) are calculated for the RINEW concept and conventional water reclamation concept at a central SWTP. The cost difference is expressed as water transport distances, from the central SWTP to the customer/industry. The result is discussed in comparison to the Dutch situation and comparable realized projects in the Netherlands.

Concluding remarks and recommendations are given in Chapter 7.

Chapter 2

Theoretical background

2.1 Sewage composition

Sewage is a complex matrix of *particulates* which individual size range from a few nanometer (macromolecules) to a few milimeters (sand grains), see Figure 2-1 (Ravazzini, 2008). Particulates are typically classified as inorganic (metal ions, clay, phosphorus, etc), organic matter (proteins, polysaccharides, etc.) and living and dead micro-organisms. These different type of particulates are explained in this paragraph.

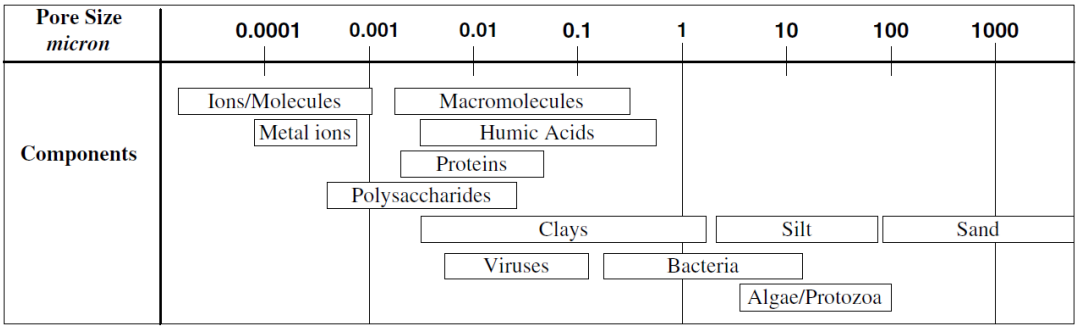

Figure 2-1. Size ranges of organic particles in wastewater

2.1.1 Particulates and particulate destabilization

The form of particulates in water is either soluble (*dissolved substances*) or insoluble (*suspended solids and colloids*). Regarding particle size the forms are ordered as follows: suspended solids > colloids > dissolved substances. Unfortunately, no sharp boundary is known since little information is gained on the nature (size and distribution) of the individual particles.

Total dissolved solids (TDS) are by definition the particulates that pass through a filter with a nominal pore size of 1.2 µm or less (Metcalf & Eddy, 2014). The particulate mass retained on the particular filter is considered the suspended solids (TSS). Yet colloids are present in

wastewater which are typically in range of 0.01 to 1 µm. An additional measurement for suspended solids and colloids is turbidity (NTU) which is the amount of scattered light of a solution containing suspended and colloid particles. However, turbidity is no good measure of total suspended solids since the particle characteristics, regarding light scattering and absorption, will vary per solution.

An important aspect in considering particle sizes below 1 µm *diffusion* becomes important (Ravazzini, 2008). Additionally, *surface interactions* become more relevant than forces like gravity, fluid drag and hydrodynamics. These aspects are typical for colloids, including particulates of organic origin (like macromolecules, proteins and polysaccharides).

Colloidal stability

An important factor which promotes colloidal stability in water is the presence of a surface charge (Metcalf & Eddy, 2014). In sewage, colloids are typically negatively charged. On a charged colloid ions of the opposite charge (counter ions) will attach forming the stern layer, see Figure 2-2. The counter ions attach through electrostatic (repulsion) and van der Waals (attraction) forces. From the stern layer the electrical potential decreases to zero over a length called the 'diffuse layer'. Due to the size of colloids, the stern layer charge is considerably higher than the attractive body forces causing a stable condition.

Generally, the potential of a particle in wastewater is measured by a fixed layer of counter ions at the particle surface, called the shear plane. The corresponding measured potential value is called the 'zeta potential'.

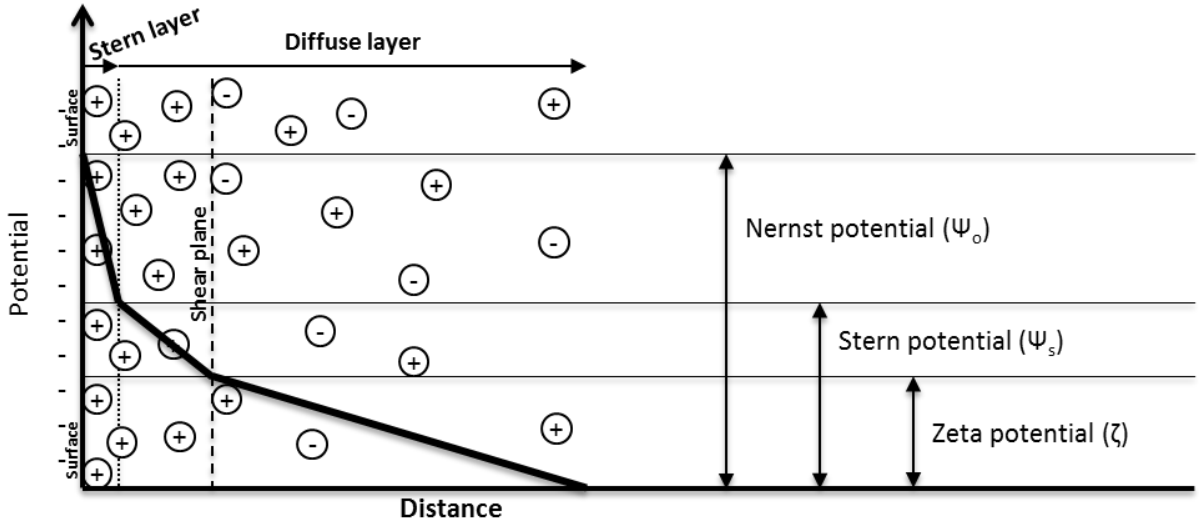

Figure 2-2. Electrical double layer for a flat infinite surface

Colloidal destabilization

In order to destabilize colloidal particles the surface charge needs to be modified. This involves lowering the zeta potential causing a decrease in energy barrier. The zeta potential can be lowered by either the increase of ionic strength (i.e. increasing salt concentration), pH modifications, or by dosing of specific counter ions to be adsorbed at the particle surface. Lowering the zeta potential is usually obtained by chemical dosing, the *coagulant*.

2.1.2 Inorganic components

Inorganic chemical constituents typically include non-metallic constituents, metals and gases (Metcalf & Eddy, 2014). The inorganic non-metallic parameters considered in this section are pH and nutrients. The pH (acidity or basicity) is a measure of the amount of H^+ ions in water which determines the specie concentration of most chemical constituents. Most biological life exist in a pH concentration range of approximately 6 till 9. Nutrients, in most cases nitrogen and phosphorus, are essential to the growth of microorganisms. Besides, they are essential building blocks in the synthesis of protein and will induce algae blooms in open water at significant concentrations.

Important metal constituents in most waters are for example cadmium (Cd), chromium (Cr), copper (Cu), iron (Fe), lead (Pb), and manganese (Mn). Most metals are necessary for growth of biological life, but the same metals will become toxic in excessive quantities.

Common gases in untreated wastewater include nitrogen (N_2), oxygen (O^2), carbon dioxide (CO_2), hydrogen sulphide (H_2S), ammonia (NH_3), and methane (CH_4). The latter three are derived from organic matter decomposition in wastewater. Dissolved oxygen (DO), just like N_2 and CO_2, are common atmospheric gasses and will be found in all waters exposed to air. DO is required for the respiration of aerobic microorganisms. Additionally, the rate of biochemical reactions that use O_2 increases with increasing temperatures.

2.1.3 Organic constituents

Organics include generally a combination of carbon (C), hydrogen (H), oxygen (O) and nitrogen (N) (in some cases). In wastewater these typically consist of proteins (~50%), carbohydrates (~40%) and oils and grease (~10%) (Metcalf & Eddy, 2014) which are discussed below.

Proteins are biomolecules (molecules produced by micro-organisms) which catalyse metabolic reactions, replicate DNA and cell signalling. They mostly consist of linear polymers built from series of up to 20 different amino acids. Carbohydrates are biomolecules consisting of carbon, hydrogen and oxygen atoms. In Biochemistry it is a synonym of ‘saccharide, a group that includes sugars, starch and cellulose. Oil and grease originates mostly from foods and can interfere with biological life and create unsightly films.

Organic structures range from simple to extremely complex, which makes them difficult to quantify. Therefore organic characteristics of interest are classified as aggregates. In wastewater these aggregates include biochemical oxygen demand (BOD) and chemical oxygen demand (COD). For BOD the amount of oxygen is measured used by micro-organisms to oxidize organic matter. And COD measures the oxygen equivalent of the organic material in wastewater that is oxidized chemically using dichromate in an acid solution.

2.1.4 Micro-organisms

Micro-organisms are predominantly present in municipal wastewater. Microbial growth requires a carbon source, energy source and inorganic nutrients (Metcalf & Eddy, 2014):

- The carbon source is used for cell growth and can be either organic matter (heterotrophic growth) or carbon dioxide (autotrophic growth).
- The energy source is needed for cell synthesis and includes light (phototrophic) or a chemical oxidation reaction (chemotrophic). In the chemical oxidation reaction electrons are transferred from an electron donor to an electron acceptor. Both electron donor and -acceptor can be either organic or inorganic constituents. In case the electron acceptor is oxygen (O_2) the organism is called 'aerobic'. In the absence of molecular oxygen, 'anaerobic' organisms are able to grow. The term 'anaerobic' is used when micro-organisms use nitrite (NO_2^-) and nitrate (NO_3^-) as electron acceptor.
- Nutrients, growth factors, are constituents for cell growth which cannot be synthesized by the carbon source.

As the concentration of organic matter and nutrients is elevated at the membrane surface, conditions become favourable for microbial growth. This is called 'biofouling'. Biofouling starts with the attachment of microorganisms to the membrane surface followed by growth and a stationary phase (Vrouwenvelder, 2009). In the latter phase biomass detachment is observed by erosion. In the growth phase micro-organisms start to colonize and are held together by an excreted polymeric matrix of microbial origin called 'extracellular polymeric substances' (EPS). These structures can clog and/or narrow the membrane pores. Bio-fouling is more difficult to control because microorganisms will always invade and colonize the system, even in pure water systems (Mittelman, 1991).

Depending on the oxygen condition (aerobic-, anaerobic- or anaerobic) different bacteria species will grow. Aerobic conditions will enhance heterotrophic bacteria where anaerobic conditions enhance autotrophic bacteria. Bacteria synthesis (reproduction) differs between bacteria that grow in aerobic, anoxic or anaerobic conditions (Metcalf & Eddy, 2014). For aerobic growth conditions the synthesis yield can be up to 0.45 gVSS/gCOD where for anaerobic growth conditions the synthesis yield can be as low as 0.05 gVSS/gCOD. The VSS (volatile suspended solids) represents the newly produced cells.

2.2 RINEW treatment principles

2.2.1 Belt Sieve

The Belt Sieve (Salsnes Filter®) is a rotating micro screen able to either separate solids, thicken sludge or dewater sludge (Ntiako, 2014). At an angle of approximately 45 degrees water is filtered by a 0.35 mm mesh sized filter. Retained solids at the surface will increase the filter resistance and correspondingly the water level. Up till a certain water level the filter starts to rotate in order to clean itself.

2.2.2 Coagulation & Flocculation

The process '*coagulation and flocculation*' involves the destabilization and aggregation of colloidal particles in order to remove them in process such as sedimentation or membrane filtration, like MF (Metcalf & Eddy, 2014). For coagulation is a *hydrolysing metal* is dosed where a *polymer* is dosed to aid the flocculation.

Commonly used hydrolysing metals are the metal salts AlCl or FeCl. The metal salt dissociates and the metal ion hydrolyses to form hydrolysis products: *mononuclear*- or *polynuclear* species. A mononuclear compound is a single metal attached to a group of surrounding molecules or ions called 'ligands'. A polynuclear is an aggregate of multiple mononuclear species. Further aggregation of nuclear species can result is larger structures called 'polymers'. The hydrolysed metal ion species may be responsible for destabilization of colloidal particles. The involved actions can be categorized as:

- *Adsorption and charge neutralization*; involves the adsorption of the mononuclear- or polynuclear species on the colloidal particles;
- *Adsorption and interparticle bridging;* involves the adsorption of polynuclear species or polymer on colloids which will form particle polymer bridges.
- *Enmeshment in sweep floc*; when the formed flocs settle readily they sweep through the water and colloids become enmeshed in the floc.

The coagulation process is time dependent. In order to optimize the effect of a coagulant on colloidal surface charge the formation of mono- and polynuclear species is important. Since coagulants form polymers in a fraction of a second, rapid and intense mixing is required.

Polymers for flocculation are high molecular-weight-substances derived from starch products such as cellulose derivatives and alginates. In water polymers becomes charged which are then called '*polyelectrolytes*'. In sewage colloids are predominantly charged negatively which requires cationic polyelectrolytes (PE). The PE neutralizes or lowers the charge of colloids in wastewater by adsorbing them. In a second step the PE will form bridges between the PE-colloid components increasing the floc size.

In practice the coagulation-flocculation process requires two subsequent mixing tanks. In the first tank the coagulant is dosed in a rapid mixing with a low retention time. Subsequently, a flocculant is dosed in a low mixing tank with a larger retention time.

The coagulation process as pre-treatment is known to reduce the fouling of MF/UF membranes (Carrol, *et al*. 1999; Al-Malack, *et al.* 1996; Jung, *et al.* 2006; Zhang, *et al.* 2016). The produced floc's increase cake permeability or prevent pore blockage, conditioning of the cake by incorporation of fine particles into highly-porous flocs, or precipitation or adsorption of dissolved material into flocs. Coagulation pre-treatment selectively removes certain types of organic matter. Aluminium-based and iron-based coagulants are known to preferentially remove hydrophobic rather than hydrophilic substances, charged rather than neutral substances, and larger-sized rather than smaller-sized substances.

2.2.3 Membrane filtration

A membrane is defined as a selective barrier between two phases (Mulder, 1996). A particular separation is obtained based on the physical and chemical properties of the feed water and the membrane. The membrane rejects specific solutes from the feed water flow (Q_f) into the concentrate flow (Q_c), see Figure 2-3.

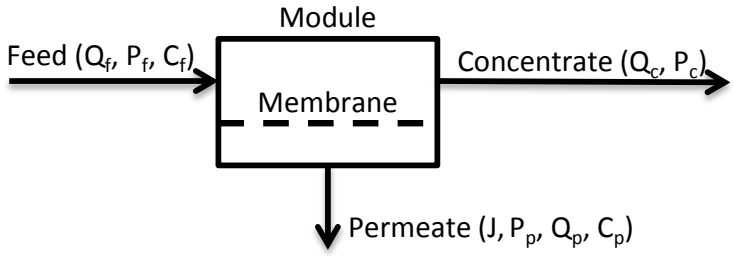

Figure 2-3. Schematic representation of a membrane process.

The driving force is the pressure gradient over the membrane, called the transmembrane pressure (TMP [bar]). The TMP is the average feed pressure (P_f+P_c)/2) minus the permeate pressure (P_p), see Figure 2-3. The produced permeate (J [$Lm^{-2}h^{-1}$]) is expressed as the permeate flux which is the produced liters per square meter membrane per hour, see Equation 2-1.

$$Permeate\ flux = J = \left({}^{L}/_{m^2 * h}\right) = \frac{TMP - \Delta\pi}{\mu * \left(R_m + R_f\right)} \qquad \text{Equation 2-1}$$

As shown in the equation above the driving force TMP opposes a force called 'osmotic pressure' (Δπ [Bar]). The osmotic pressure is a natural driving force which equalizes the concentration of two adjoining solutions separated by a membrane. The solvent, usually H_2O, will flow from the low concentration solution through the membrane to the high concentration solution. Thus, the accumulation of a solution concentration at the feed side is higher will cause an opposing osmotic pressure (Δπ). Additionally, in Equation 2-1, the flux is further influenced by the hydrodynamic membrane (R_m)- and fouling (R_f). The resistance R_m [m^{-1}] is the initially resistance of the membrane and is a constant and does not change due to operational conditions. The fouling resistance (R_f) becomes important when solutes are present in the feed water. Membrane fouling is further explained on page 12. The resistance is multiplied by the factor μ [$kg.m^{-1}s^{-1}$] which is the viscosity of the water. Alternatively the permeate flux can be calculated with Equation 2-2 where the flux is described as permeate flow (Q_p [m^3h^{-1}]) meter divided by the membrane area (A [m^2]).

$$Permeate\ flux = J = \left({}^{L}/_{m^2 * h}\right) = \frac{Q_p * 1000}{A_{membrane}} \qquad \text{Equation 2-2}$$

The TMP drives the membrane process. The TMP can be set e.g. by controlling the feed pump capacity and concentrate flow. Depending on these settings a recovery can be set. The recovery is the percentage of permeate produced from the feed water, see Equation 2-3.

$$Recovery = S\ (\%) = \frac{Q_p}{Q_f} * 100 \qquad \text{Equation 2-3}$$

When the operational parameters are set the selectivity of the membrane can be determined. The selectivity is expresses as the rejection (Rej. [%]) by the membrane for a specific solute from the feed water, see Equation 2-4. In this equation C_f [mgL^{-1}] and C_p [mgL^{-1}] are the solute concentration in the feed and permeate respectively. Thus, the higher the value for Rej. the higher the rejection of the specific solute.

$$Rejection = \ Rej.(\%) = \frac{C_f - C_p}{C_f} * 100$$ Equation 2-4

Often MF and UF are explained in the same way. They are both most often used as pre-treatment to remove suspended solids and bacteria. The dominating separation mechanism of these membranes is 'steric separation'. This mechanism gives the membrane the ability to reject components based on their molecular size. Compared to NF and RO, the MF and UF membranes contain larger pores and therefore operate under lower pressure conditions. Due to the larger pores any solution freely passes the membrane.

Besides, the NF and RO are usually discussed in the same way since their basic principles are the same. They are often used to separate low molecular weight solutes such as inorganic salts or small organic molecules. These solutes accumulate at the membrane surface causing an osmotic backpressure which has to be overcome with a sufficient (high) pressure gradient. This is a solution-diffusion process which separation rate depends on the feed water composition and type of membrane.

Membrane fouling

When components (dissolved or suspended) are present in the feed water the performance of the membrane will change (Mulder, 1996). Depending on the membrane type specific components are retained or partly retained causing a component accumulation near, at or in the membrane. In case of a pressure driven membrane process at constant flux operation a higher operational pressure is required to maintain the constant flux. Thus, *fouling* is defined as the unwanted deposits on or in the membrane, increasing the total membrane resistance. Generally, the increase in operational pressure is caused by concentration polarization, pore blocking, pore narrowing and/or gel layer formation, see Figure 2-4.

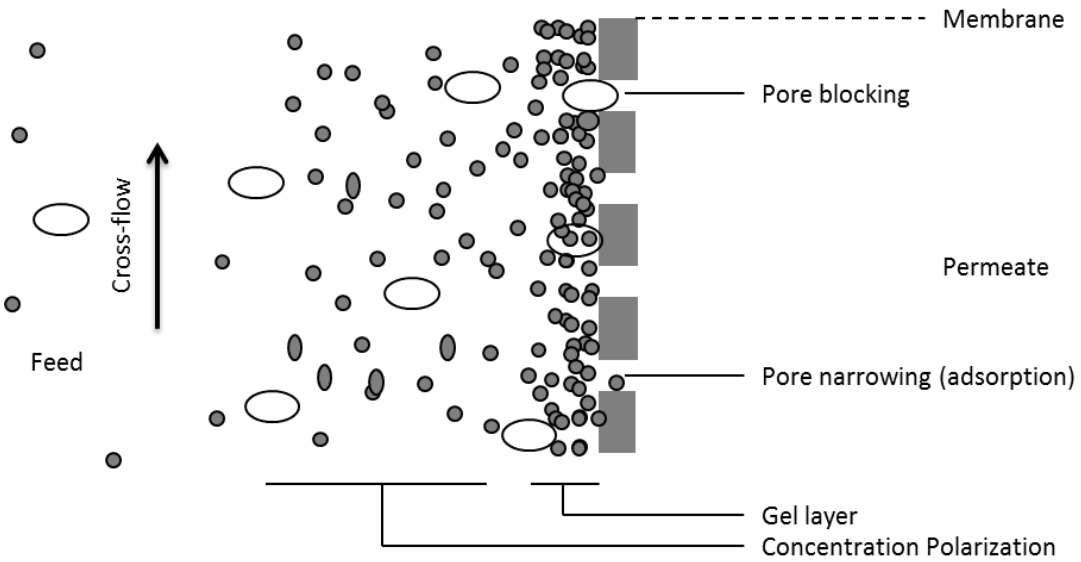

Figure 2-4. Overview of fouling mechanisms

Concentration polarization is the increase in component (dissolved or suspended) concentration towards the membrane surface due to the convective flow towards the

membrane. Normally, concentration polarization is explained with dissolved components (solutes: mainly molecules and ions) which generate an osmotic backpressure over the membrane. This is the case in NF and RO installations and will cause an increase in membrane resistance. However, concentration polarization will not take place in MF and UF membranes since molecules and ions permeate through the membrane. In MF and UF membranes the membrane resistance will increase rather by pore blocking, pore narrowing and gel layer formation (Metcalf & Eddy, 2014). Pore blocking are the large components getting stuck on or in the pores. Pore narrowing occurs when particulates adsorb at the wall of a pore via fouling-membrane interactions. More about fouling-membrane interactions in following section. At last, a gel layer is formed when the particulate concentration at the membrane exceeds high concentrations, due to concentration polarization.

The membrane fouling that can be restored after a physical cleaning is called 'reversible fouling'. Physical cleaning is done usually by reversing of the permeate flow, called 'the backwash'. If not removed by physical cleaning but during rigorous cleaning (e.g. chemical cleaning) the fouling is called 'irreversible fouling'. The cleaning methods are further described in following sections.

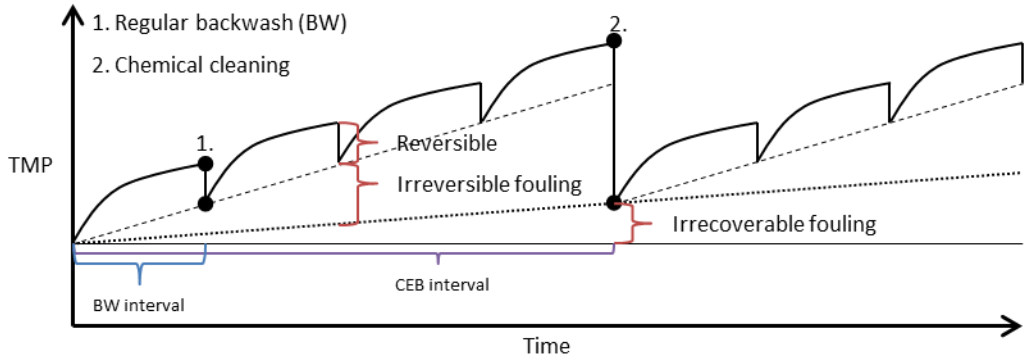

Figure 2-5. Schematical representation of fouling development including the reversible and irreversible fouling.

Fouling-membrane interactions

Components in the water generally foul the membrane by interacting with the membrane surface (Liu, *et al*. 2001). Generally, electrostatic- and hydrophobic interactions are distinguished.

- In electrostatic interactions colloids, particles or dissolved organic matter are repulsed or attracted by the charge of the membrane. A membrane in an electrolyte solution generates a zeta (ξ) potential which defines the effective surface charge of the membrane. The zeta potential depends on the pH and decreases with an increase in electrical conductivity (ionic strength) of the water;
- Hydrophobic attraction results from the van de Waals force (electromagnetic forces) between molecules with similar chemical structures. When the mass/charge ratio ('number of C-atoms'/'charged functional groups') in an organic compound is larger than 12, the energy of hydrophobic attraction exceeds the energy of electrostatic repulsion. This results into a molecule adsorbed onto the membrane. A functional group is an atom or group of atoms in a molecule that is chemically reactive. Important functional groups include alcohols, amines, carboxylic acids, ketones, and ethers. The existence of these functional groups typically increase the hydrophilicity

of natural organic matter by increasing the charge density, and by the formation of hydrogen bonds with water molecules.

As explained, the solute concentration will gradually increase near the membrane surface in case of a NF or RO membrane. When the concentration of the individual inorganic constituents increase beyond their solubility limit, it will precipitate. Precipitates adsorb onto the membrane surface, called 'scaling', increasing the membrane resistance.

Typically various interactions occur between organic foulants, inorganic components and the membrane surface, making it difficult to observe and predict (Huajuan. 2009). Humic acids are negatively charged and can precipitate in contact with the membrane surface. Organic polymers, like proteins and polysaccharides, are sticky and can accumulate on the membrane surface and accelerate fouling by forming stable (in)organic particulate matter. As carbon source, organics play a vital role in biological growth at the membrane surface, see biological constituents.

Reduce fouling

Several approaches to control fouling in the membrane process are (Mulder, 1996):

1. Pre-treatment;
2. Membrane properties;
3. Process conditions;
4. Membrane cleaning.

The first two (no. 1 and 2) are usually determined in the design phase where the last two (no. 3 and 4) can be changed during the membrane operation. Only the last two mentioned will be described below as the design phase has no relevance to this thesis.

Process conditions

The most effective process conditions to reduce fouling is to decrease in permeate flux and to increase the cross-flow. The permeate flux has a direct effect on the amount of components being pulled towards the membrane surface. Lowering the permeate flux will reduce the concentration polarisation. The cross-flow is the flow velocity between the membrane feed and -concentrate. Increasing this flow will induce turbulence across the membrane lowering the concentration polarization.

Membrane cleaning

Membrane cleaning will always be employed in practice. The two main cleaning methods are: hydraulic- and chemical cleaning.

The hydraulic cleaning is usually represented by the term 'back wash'. After a given filtration time, the feed pressure is released and the flow is reversed from the permeate side to the feed side, see Figure 2-6. The hydraulic reversible fouling within the membrane and/or at the membrane is therefore removed. This predominantly maintains the permeate flux without the use of any chemicals.

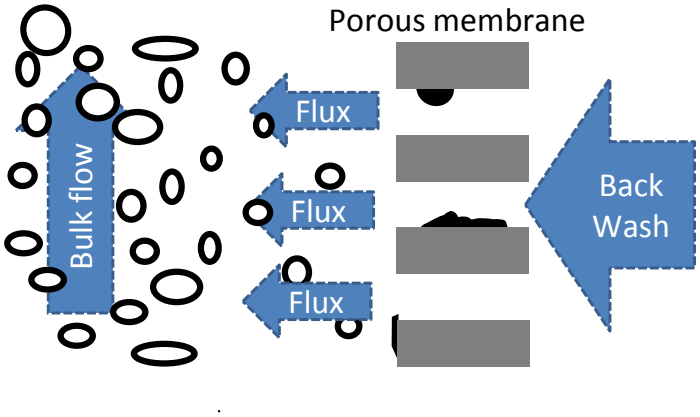

Figure 2-6. The principle of a backwash.

In addition to the hydraulic backwash chemicals can be added which is called a 'chemical enhanced backwash' (CEB). Chemicals are dosed to the back wash flow, followed by a short contact time where after the membrane is further backwashed with clean water. Additionally, a 'cleaning in place' (CIP) can be performed. In this method multiple chemical reagents are subsequently injected into the membrane in normal or reverse filtration. The CIP can take up to 3 hours where a long contact time is provided.

Chemical cleaning principles

Many cleaning chemicals are available which can be characterized by one or more cleaning principles (Liu, *et al*. 2001). Below the cleaning principles are described:

- **Hydrolysis** is the process where a bond in a molecule is broken due to the reaction with water;
- **Solubilisation** is the process where a solute is dissolved in a solvent that has a similar chemical structure to itself. To dissolve a solute both the solute and solution need to be polar or both non-polar. A polar molecule has an imbalance of electrons which results in electrical poles at the molecule ends. At a non-polar molecule the electrons are evenly distributed and cancel each other out.
- **Chelating** is the bonding of a chelating agent with a metallic ion. A chelating agent contains many negatively charged atoms which bound easily to positively charged metallic atoms. This is driven by the fundamental forces that cause surface tension and intermolecular electronic attractions.
- **Oxidation** is the tendency of an atom to lose one or more electrons in a redox reaction. In a redox reaction an oxidizer (electron acceptor) reacts with a reductor (electron donor) generating an electrode potential. Thus, by introduction of a chemical as oxidizer in solution it will take electrons, in reaction, from the fouled species increasing its solubility in water.
- **Chemical disinfection** is obtained by adding chemicals to the water which oxidize (corrode) the cell wall in the cells of microorganisms, or changes in cell permeability, protoplasm or enzyme activity. This process leads to the inactivation of micro-organisms.

Type of cleaning chemicals

In this subsection several available chemicals are described. Generally these chemicals are divided into the following categories (Lui, *et al*. 2008):

- Acidic chemicals;
- Caustic chemicals;
- Oxidants/disinfectants.

Acids are effective in removing inorganic fouling and metal oxides through solubilisation and chelating. Caustics can increase the solubility of solutes by hydrolysis and solubilisation. At last, oxidants/disinfectants oxidize fouling and increase the hydrophilicity by increasing the amount of oxygen containing functional groups. Additionally they can inactivate bio-activity by chemical disinfection.

In Table 2-1 various chemicals are given per category. During a dissociation reaction a molecule is separated into smaller compounds like ions or atoms by hydrolysis. The ratio between the dissociated compounds (ionic products) to the applied chemical is called the dissociation constant (also known as the acidity). This is the pK_a for acidic reactions and pK_b for basic reactions. A $pK_{a/b}$ smaller than -2 is called a strong acid or base where a $pK_{a/b}$ between -2 and 12 is called a weak acid or base. The dissociated products (or chemical itself like ozone) can act as an oxidizer, see the reduction reactions in Table 2-1. Each oxidation reaction has an oxidation potential (E^o) which represents the tendency to acquire electrons and, thereby, will reduce. An oxidizing agent with a high E^o readily accepts electrons from another substance.

Table 2-1. Overview of common used chemicals for membrane cleaning and their dissociation constant and oxidizing potential (E^o).

Chemical		• Dissociation	Diss. constant	E^o
Type	Formula	○ Reduction reaction	($pK_{a/b}$)	(V)
Acid	HCl	• $HCl \rightarrow H^+ + Cl^-$	$pK_a = -5.9(\pm 0.4)$	Nan*
Acid	$NaHSO_3$	• $NaHSO_3 \rightarrow H^+ + NaSO_3^-$	$pK_a = 6.97$	
		○ $4NaHSO_3 + O_2 \rightarrow 2Na_2SO_4 + 2SO_2 + 2H_2O$		Nan*
Caustic	NaOH	• $NaOH \rightarrow Na^+ + OH^-$	$pK_b = 0.2$	No
Caustic	NaOCl	• $NaOCl + H_2O \rightarrow HOCl + Na^+ + OH^-$	$pK_b = 7.53$	
		○ $HClO_2 + 2H^+ + e^- \rightarrow HClO + H_2O$		+ 1.67
		○ $ClO_3^- + H^+ + e^- \rightarrow ClO_2 + H_2O$		+ 1.18
Oxidant	O_3	• $O_3 + 2H^+ + 2e^- \rightarrow O_2 + H_2O$	Nan*	+ 2.07
Oxidant	H_2O_2	• $H_2O_2 \rightarrow H_2O + O_2$	$pK_a = 11.75$	
		○ $H_2O_2 + 2H^+ + e^- \rightarrow 2H_2O$ (acidic)		+ 1.78
		○ $H_2O_2 + OOH^- + 2e^- \rightarrow 3OH^-$ (alkaline)		+ 0.88

*NAN = Not a number

Ceramic Microfiltration

Multiple synthetic materials are available for MF, the process principle of cMF are discussed in chapter 2.2.3, which are classified as polymeric (organic) or ceramic (inorganic) (Mulder, 1996). Polymers are high molecular weight components built from monomers where ceramics are formed by the combination of a metal with a non-metal in the form of an oxide. Examples of ceramic materials are alumina (g-Al2O3 and a-Al2O3), zirconia (ZrO2) and titania (TiO2). Ceramic membranes, compared to polymeric membranes, have a higher thermal- and chemical resistance. Also ceramic membranes are expected to have higher fluxes compared to organic membranes, due to their higher porosity.

Besides the high thermal- and chemical resistance another important aspects are the high porosity and hydrophilic surface (de Paula Santos, *et al*. 2003). Hydrophilic means the membrane surface has the ability to form hydrogen-bonds with water creating a water film or coating on the surfaces (Gaulinger, *et al*. 2007). In contrast, hydrophobic materials have little or no tendency to adsorb water, which tends to form “beads” on their surface. Hydrophobicity and hydrophilicity of the surface of membranes strongly influence fouling (Jung *et al*., 2006). Jung (2006) observed a greater adsorption ratio for the hydrophobic membrane compared to the hydrophilic membrane, regardless of the kind of organic fractions.

Chapter 3

Description of Site

3.1 Influent characteristics

The RINEW pilot is located near the Merwehaven in Rotterdam, the Netherlands. The influent originates from activities near the Merwehaven at the border of Schiedam and Rotterdam, see oval in Figure 3-1. The area size is approximately 50 hectares and includes mainly office- and industrial activities.

The industries with most tap water consumption are a steam laundry (no1), a glass manufacturer (no.2) and distillery (no.3). However, only the steam laundry discharges their ‘used’ water into the sewer. Besides offices and the steam laundry, multiple automobile services may influence the influent composition.

The different industries that discharge on the sewer are studied further in this section. The sewage is collected in a combined sewer system and flows in northern direction towards the pumping station. At irregular interval sewage water is pumped at the pumping station into the buffer tank at the RINEW location.

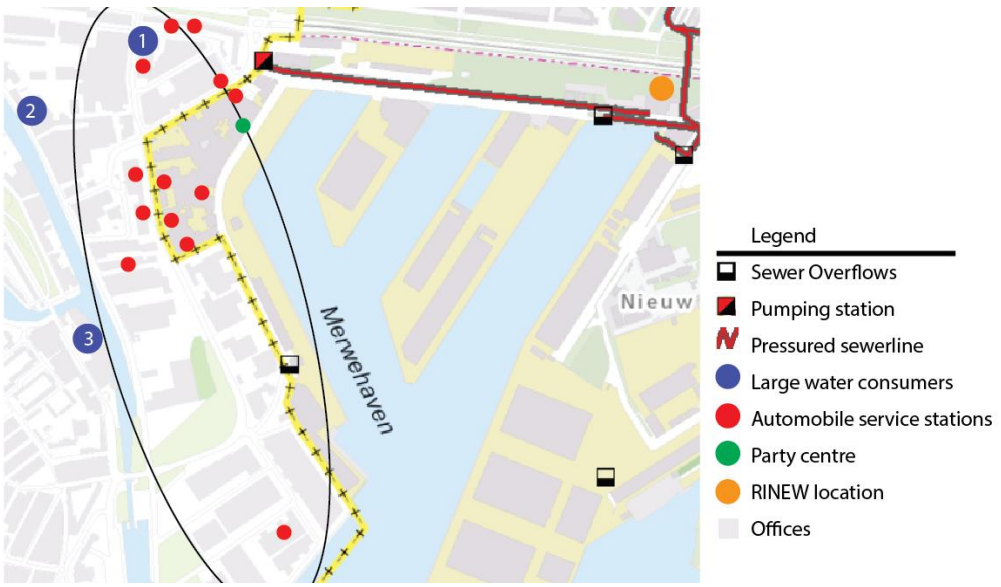

Figure 3-1. Overview sewage water origin and the transport to RINEW project.

Steam laundry wastewater

The steam laundry, as large tap water consumer, has an annual tap water consumption of 11.166 m^3 (Ref. Evides Customer Contact). Brage et al. (2014) monitored laundry wastewater for 30 days on nitrogen, phosphate, heavy metals, linear alkylbenzene sulphonate (LAS) and volatile organic acids (VOA). LAS being *colourless salts* with properties as *surfactants* and are major components in laundry detergents. Together with the VOA's and alcohols is LAS organic of nature. Notable high averages and –variances were observed for phosphate (94.6 ± 75.3 $mgP.L^{-1}$) and COD (1710 ± 968 $mgCOD.L^{-1}$). Similar values have been found in a study by Envirochemie (2006) which additionally measured a conductivity of approximately 3000 $\mu S.cm^{-1}$.

Automobile service station wastewater

Automobile service stations range from authorised service centres to small scale service station which undertake repair, washing and servicing of vehicles take place (Asha, *et al*. 2016). Wastewater is produced from car-, floor-, and equipment cleaning and typically includes oil and grease, detergents, phosphates, hydrofluoric acid, ammonium bifluoride products (ABF) and heavy metals. Joseph (1997) studied 40 samples from 10 automobile service stations and found TSS, BOD_5, COD and oil and grease concentration in the range of 610 – 4950 mgL^{-1}, 75 – 570 mgL^{-1}, 270 – 1640 mgL^{-1} and 14 – 420 mgL^{-1} respectively.

Office wastewater

As assumption, average Dutch sewage quality is expected from all office activities. This includes the average concentrations of 550 $mgCOD.L^{-1}$, 275 $mgTSS.L^{-1}$, 40 $mgTN.L^{-1}$, and 10 $mgTP.L^{-1}$ (Afvalwater, 2017).

RINEW influent

As the RINEW influent is buffered before treatment always a continue flow is provided. Therefore only variations are expected in influent composition and concentration. As the area of sewage origin is relatively small relative high concentration peaks are expected (Metcalf & Eddy, 2014). In order to get insight into the RINEW influent sewage composition 24 hour mix samples are taken from the influent flow. These are tested daily on multiple water quality parameters, see Table 3-1. In the same table the above discussed industrial water quality data is added.

Table 3-1. RINEW influent characteristics compared with literature data

		RINEW infl.	Steam laundry	Auto mob. station	Office wastewater
Parameter1	Unit	Average(σ)	Average(σ)	Range	Range
COD	mgL^{-1}	169(116)	1710(968)	270-1640	450-650
Turbidity	NTU	60(39)	-	-	-
TSS	mgL^{-1}	-	80(60)	610-4950	250-300
Total-N	mgL^{-1}	32(15)	-	-	30-45
NH4	mgL^{-1}	18(13)	7(10.8)	-	-
Total-P	mgL^{-1}	4(4)	94.6(75.4)	-	7-12
Ortho-P	mgL^{-1}	2(2)	-	-	-
pH	-	7(1)	5.6(0.9)	-	6.7-7.5
Conductivity	μScm^{-1}	1891(968)	-	-	-
Hardness[2]	dH^o	19(9)	-	-	-

[1]24 hour mix samples are measured each day in the period from 1-10-2016 to 31-01-2017.
[2]Hardness measurements started from the 30th of December

Table 3-1 shows that the RINEW influent composition has no high resemblance with typical sewage characteristics which indicates significant influence of industrial activities, like the steam laundry or automobile service stations. The variation of industrial wastewater composition is high which compares to the variation in RINEW influent composition. However, mostly low average RINEW influent concentrations are observed except for conductivity and hardness.

3.2 The RINEW pilot

During the day sewage is pumped at irregular interval from a pumping station into the RINEW influent buffer, see Figure 3-1. The pumping station switches on when filled till a certain limit. An example of the pump frequency at the pumping station is given in Figure 3-2.

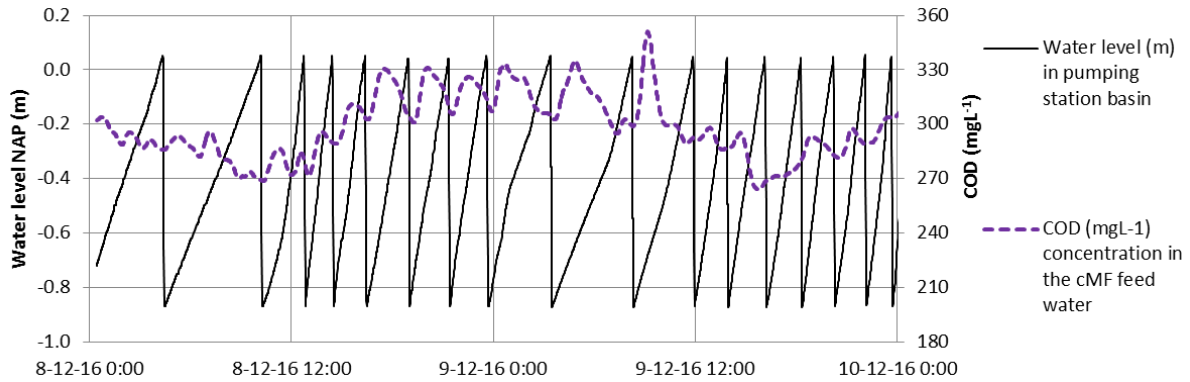

Figure 3-2. Example of the pump frequency at the pumping station. Date: 18-04-2017.

In Figure 3-2 the water level (m) in the pumping station basin is given at the left y-axis. The COD concentration (mgL^{-1}) is given at the right y-axis. The COD data originates from time series Dec 7-10, see Appendix A on page 62. The fluctuating water level indicates the pump frequency since the pumping start when the basin is filled till a maximum water level. Generally, a relation is observed between the pumping frequency and monitored COD concentration in the cMF feed water. After pumping, the sewage transport time, influent buffering and cMF pre-treatment cause a delay in COD concentration increase. The sewage is circulated inside the RINEW pilot, see Figure 3-3. Bacteria degrade organic matter over time, causing the COD to drop. The COD peaks therefore better represent the actual COD concentration of the raw/fresh sewage originating from the Merwehaven.

From the influent buffer sewage is pumped into the RINEW pilot, see Figure 3-3. At first, a coagulant and cationic polymer is added to the flow (~2 m^3h^{-1}). The coagulant $AlCl_3$ (PAX 14, 38%) is used and dosed with a flow of 0.05 Lh^{-1}. This results in an effective alumina dosage of 4.6 $mgAl.L^{-1}$. Since the coagulation optimization had no part in present thesis study the applied Al dosage is discussed regarding corresponding literature. Carrol (1999) obtained an optimum aluminium dose of 3.2 $mgAl.L^{-1}$ with surface water. Al-Malack (1996) found that above 13 $mgAl.L^{-1}$ no further increase in flux occurred at a MF fed by secondary effluent. This effective Al dose in present research of 4.6 mgL^{-1} is in range of the discussed Al dosages from literature. A contact time of approximately 5 minutes is provided in a mixing

tank for the chemicals to react. The contact time is considered too low since generally a contact time of 20 minutes is applied (Metcalf & Eddy, 2014).

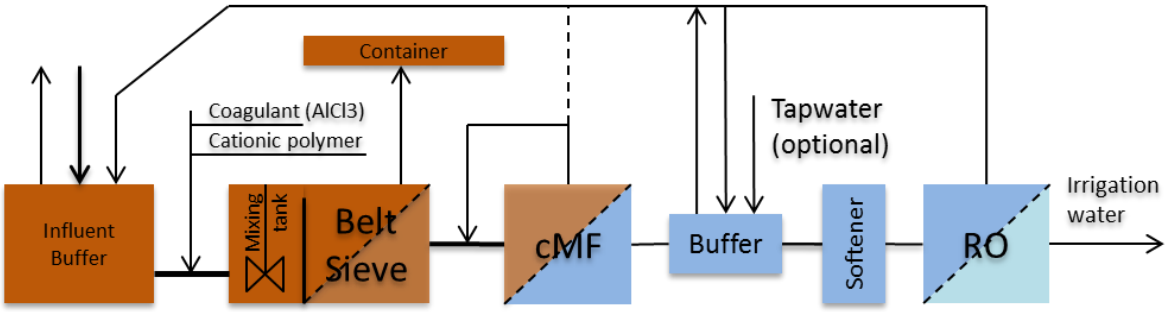

Figure 3-3. Operational scheme of the RINEW pilot. The colours indicate the quality level of the water going from brown (sewage water) to RO permeate (light blue).

The water subsequently flows by gravity over into the Belt Sieve. Particulates retained by the belt sieve (screenings) are mechanically removed and collected in a container. In present study, the removal efficiency of the Belt Sieve (0.35 mm) is studied for COD and turbidity (NTU). For both parameters 5 water samples are taken in duplicate before and after the Belt Sieve. The average removal efficiency was found to be 21.4% and 30.1% for COD and turbidity respectively. In comparison, Reijken (2014) found removal efficiencies of approximately 25% for suspended solids and 35% for COD. Removal efficiencies increase when a 'filter mat' or 'filter cake' develops (Jonas, 2014). In Jonas's study a removal efficiency of < 20% is expected, based on the feed water particle size distribution. However, higher removal efficiencies (SS = 48% and COD = 47%) were observed due to the occurrence of a filter mat at the filter surface. It was found that the 0.35 mm microscreen with a filter mat behaves as a 0.25 mm microscreen.

Following the Belt Sieve, the water is filtered by the cMF. The cMF concentrate is circulated back into the Belt Sieve product or back into the influent buffer. In present research the cMF concentrate was recirculated mostly into the Belt Sieve product. Resulting 'dirty' water from backwashes and chemical cleanings is send back into the sewer system.

According the supplier, the average pore size of the cMF membrane is 0.2 µm. This is also tested in practice at the RINEW location with two different methods (particle solutions and SEM-EDX analysis).

1. Janse (2016) studied the pore size using the solutions PES100 and PES20. Both are concentrated particle solutions with a particle size of 100 nm and 200 nm respectively. In a single batch each solution is filtered by the cMF. Samples of the feed, concentrate and permeate are measured on particle count. Via extrapolation towards 90% pore size the average membrane resulted at 0.06 µm.
2. The surface of a new cMF membrane is observed in a SEM-EDX analysis, see Figure 3-4. A rough estimate on average pore size can be made by determining the distance between particles. In Figure 3-4 three black circles are drawn which represent a typical diameter of the aluminium molecules. The white circle in between represents a typical pore at the cMF membrane. The diameter of the white circle is 0.1 µm.

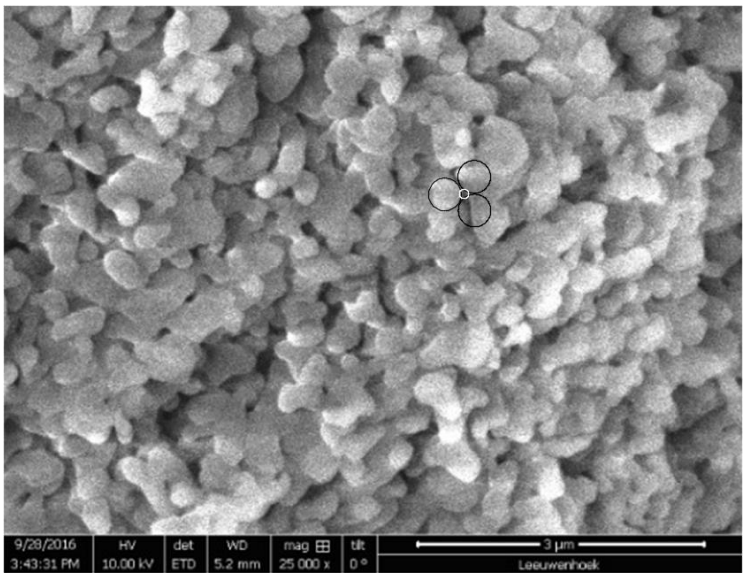

Figure 3-4. SEM-EDX image of a new cMF membrane surface

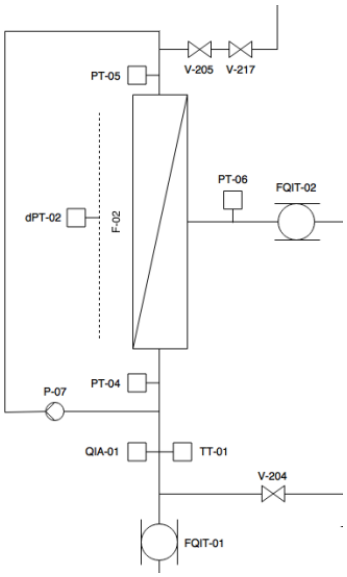

Figure 3-5. Operational scheme cMF

The cMF module contains 37 uncoated Al_2O_3 MF elements. Each element has 4 channels with a length and channel diameter of 1.2 m and 7 mm, respectively. Therefore, the total effective filtration area is 3.93 m^2. It operates in cross-flow mode, see Figure 3-5. The feed pump (FQIT-01) provides sewage and assist to obtain the required pressure. The feed pump frequency and concentrate valve (V-217) set the operational pressure which predominantly controls the permeate flux. The cross-flow pump (P-07) creates a flow across the membrane, called 'cross-flow', substantially removing the cake layer. The cross-flow pump can be set from 20 to 50 hertz which produces a cross-flow velocity of 1.8 – 4.8 $m.s^{-1}$ (corresponding to a Reynolds number of 9979 to 25735). Gan (1999) found that a variation in cross flow velocity between 2-4 ms^{-1} had only limited effect on the permeate flux. Therefore, the cross-flow pump is set to 20 hertz in order to limit the operational costs. Additionally, the removal efficiency is tested for ATP and Total Direct Cell Count (TDC) in triplicate. The log removal resulted in the range of 2.6-4.3 for ATP and 3.6-5 for TDC. These results are in range of common log removal efficiencies between 2 and 5 for different bacteria types (Metcalf & Eddy, 2014)

The cMF permeate is buffered and subsequently treated by a softener and RO unit. However, during the experimental period the cMF permeate production was too low for the softener and RO to operate properly. Therefore the treatment scheme after the cMF is not further discussed.

Chapter 4

Digital quality monitoring as fouling indicator for Microfiltration

4.1 Introduction

Fouling on ceramic membranes, especially irreversible fouling, will increase operational costs and energy consumption (Shang, *et al*. 2015). Irreversible fouling are unwanted deposits on or in the membrane that cannot by hydraulically removed. In order to get insight into the irreversible fouling rate at the ceramic Microfiltration (cMF), online water quality monitoring of the cMF feed water is required.

Microfiltration (MF) in sewage treatment is a barrier for suspended solids (Metcalf & Eddy, 2014) and is predominantly fouled by organic matter (Lateef, *et al*. 2013; Shang, *et al*. 2015). In chapter 2.1 it is discussed that suspended solids are measured by the parameters TSS and organic matter by the parameter COD and BOD.

However, in urban drainage applications, TSS and soluble COD are measured directly by spectrometers which are, nevertheless, expensive and require expertise and time investment (Schilperoort, *et al*. 2011). Therefore the parameters Turbidity (NTU) and Electrical Conductivity $mScm^{-1}$), and its product called ‘surrogate Event Mean Concentration’ (sEMC), are monitored and studied in a combined sewer overflow (van Daal-Rombouts, 2013). Turbidity and conductivity are measured by robust sensors which are relatively easy to calibrate. The sEMC represents the relative pollution, e.g. relative particle concentration, of sewage in a combined sewer. The Turbidity represents the suspended solids concentration where Electrical Conductivity (dissolved ions concentration) represents the dilution by rain.

As introduced: the water quality parameters of interest are the parameters: COD, BOD, TSS, Turbidity and Electrical Conductivity. The research question therefore becomes:

1. Which common digital water quality parameter can be used as irreversible fouling rate indicator for the cMF in decentralized sewage treatment?

4.2 Microfiltration operation

Starting a filtration, the cMF is cleaned by a manual caustic (NaOH, pH ~12.5) backwash for ~20 minutes. A backwash solution with a pH of ~12.5 was found to restore the membrane resistance significantly. Following, a regular (manual) backwash is performed for ~20 minutes in order to flush the caustic solution. A manual cleaning was necessary since the programmed Cleaning In Place (CIP) method was found to be ineffective.

As discussed, the cMF operates in cross-flow mode with a cross-flow (v_{cf}) of approximately 1.8 $m.s^{-1}$. Starting, a flux of 58 $Lm^{-2}h^{-1}$ and recovery of 50 % are set since previous small tests showed less stable operation at higher values. For the regular backwash a backwash time of 1 minute is set. Following, backwash intervals of 15 and 30 minutes are tested. The backwash interval of 15 minutes is chosen since it resulted in a significant more stable operation of the cMF.

Every 7th backwash an automatic chemical enhanced backwash (CEB) is performed. Starting the CEB, a 1 min backwash is performed including 1 min of caustic dosing (NaOH) and 30 sec of sodium hypochlorite (NaOCl) dosing. Following a contact time of 5 minutes is provided for the chemical solution to react. At last, an automatic backwash is performed of 5 minutes in order to flush the chemical solution. The backwash water is cMF permeate which originates from the permeate tank. The caustic dosing time of 1 minute in the CEB is chosen since the permeate tank volume limits the available water to flush the chemical solution. Via testing, pH of ~12.5 was achieved in the backwash flow after 2 minutes of caustic (NaOH) dosing (28 Lh^{-1}). However, the cMF containing such a solution required a too large water volume in order to flush the caustic solution. Therefore the caustic dosing time was to one minute. A typical cMF start-up is shown in Figure 4-1.

When the TMP exceeds the limit of 5 bar the cMF operation stops and a manual caustic cleaning is performed.

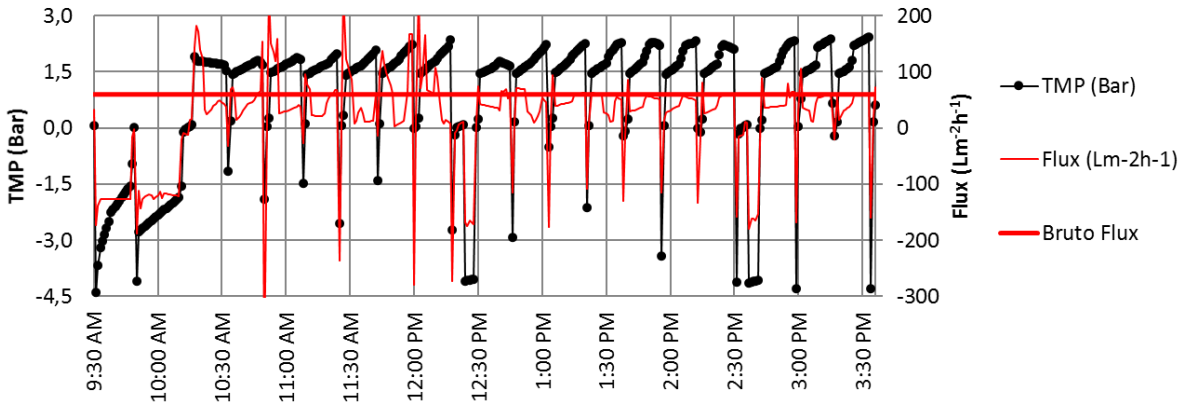

Figure 4-1. Typical TMP and Qp development during the start-up of the cMF. Data originates from the JAN 6-9 time series.

In Figure 4-1 the raw TMP (Bar) and permeate flux ($Lm^{-2}h^{-1}$) data is shown during a typical start of a cMF run. In the first 45 minutes, between 9:30 and 10:15 AM, the membrane gets a manual caustic backwash followed by a regular (manual) backwash to flush the caustic solution. During this chemical cleaning, already an improvement in TMP, going from -4.5 to -1.5 bar, can be observed.

At the start of the filtration run, from 10:15, the TMP is relatively stable around +1.5 bar, 1.5 bar being the clean membrane resistance. Following, the TMP development changes from straight lines to a more S-form, between 3:00 and 3:30 PM. The so called 'S-form' can be explained by the slow start-up of both the feed- and cross-flow pump. The slow start-up restrict too high changes in operational pressure over time which is a safety measure to prevent any membrane breakages. Due to the slow build-up the set flux of 58 is achieved approximately halfway each regular backwash interval. Parallel to the flux stabilization the TMP stabilizes resulting in a more or less S-form in between the regular backwashes. However, Figure 4-1 shows already the discontinuity in the flux development which will be a point of discussion in present chapter.

4.3 Quality monitoring

4.3.1 Sensors, calibration and validation

In the cMF feed tank multiple sensors are installed to measure the parameters of interest with a measurement interval of 5 minutes. Below, the sensor types, measurement principles and calibration methods are described:

COD, BOD and TSS
These quality parameters are monitored by the *Spectro::lyzer™ UV-Vis probe*, provided by Qsenz B.V. This probe is operated with use of a con::nect (controller) and the process software ANA::PRO, installed on a commercial laptop. Besides the operation, the con::nect provides power and compressed air (cleaning) to the spectro::lyzer™.

As example the measurement principle for COD is explained. In the UV-Vis spectrometer a water sample is irradiated with UV light, wave length from 200 to 400 nm, and visible light, wave length from 400 to 800 nm (Website). A detector measures the amount of absorbed radiance by the components in the water sample over a specific measurement path length. COD is measured at various wave lengths in UV spectrum. For example a wave length of 222 nm is maximal absorbed by 'isoprene', a common organic compound.

Calibration curves are made for TSS, COD and BOD, see Figure 4-2. These curves are logged into the ANA::PRO software as local calibration point enabling the sensor to directly correct measurements based on the calibration data. In Figure 4-2 the calibration curves are shown for TSS, COD and BOD. The degree of correlation is categorised as good (>0.8), moderate (0.7 - 0.8) and weak (<0.7).

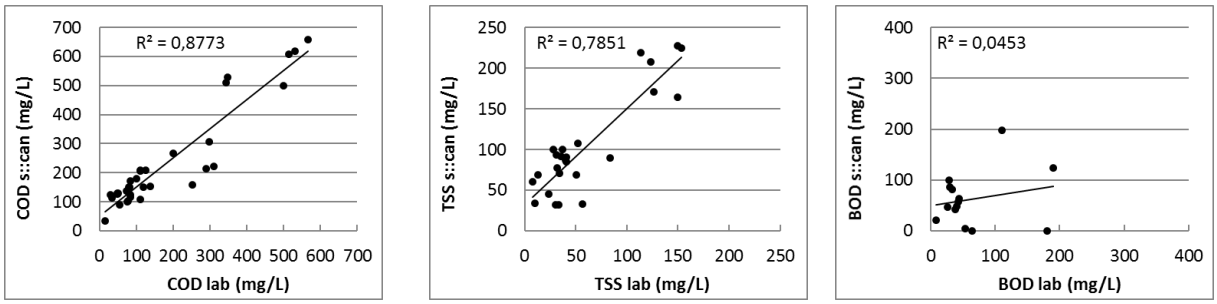

Figure 4-2. Calibration curves for COD (R^2 = 0.88), TSS (R^2 = 0.78) and BOD (R^2 = 0.045)

For COD a good and for TSS moderate squared correlation value (R^2) is calculated. Unfortunately, the calibration points do not cover the complete concentration 'spectrum', e.g. missing points in the 'middle' part of the TSS calibration. The calibration samples were picked up always before 11 in the morning which limits the available water present quality for lab analysis. Also the average influent concentrations were low and concentration peaks occurred sporadically, see Table 3-1.

Regarding the BOD concentration, in case of a steep COD concentration peak the BOD concentration tend to decrease or even became zero. This is shown in the BOD calibration curve in Figure 4-2 where the sensor measures zero contrary the BOD measured in the lab. Therefore, unfortunately, the BOD results are disregarded.

Turbidity

Turbidity is measured by a *Hach® SOLITAX sc Turbidity Analyzer*. The sensor is a photometer which is factory calibrated in conformity with ISO 7027 (Turbidity, 2017). This standard design requires a monochromatic light source (visible light with a narrow band of wavelengths) at a wavelength of 860 nm. The scattered light is detected at an angle of 90 degrees which is converted to a turbidity value. The sensor includes a one-point calibration. For the calibration a *Hach® 2100Q Portable Turbidimeter* is used which itself is calibrated and validated by *Hach®* standard solutions.

Electrical Conductivity

Conductivity is measured by the *Hach® 3400 sc Digital Conductivity Analysis Sensor*. The sensor quantifies the amount of traveling atomic species (ions), each carrying an electrical charge, in a liquid (Wiki, EC). Conductivity is a general principal method of measuring total dissolved solids like nutrients, salts and other impurities. It is calibrated via a zero- and one-point calibration. For this calibration the *Hach HQ30d Portable meter* is used which itself is calibrated via a one-point calibration with a 1000 μScm^{-1} solution.

4.4 Time series analysis

A common method to define membrane fouling is by analysis of the hydraulic filtration resistance, (van der Marel, 2009), see Equation 4-1. The resistance is calculated by Darcy's law in which R is the total hydraulic resistance (m^{-1}), TMP the transmembrane pressure (Pa), η is the dynamic viscosity of the permeate (Pa*s) and J is the flux ($m^3\ m^{-2}\ s^{-1}$). The dynamic viscosity is in this thesis corrected for temperature using the formula: $\eta = 0.497*(T+42.5)^{-1.5}$ in which T is the temperature in °C.

$$Hydraulic\ membrane\ resistance = R = \frac{TMP}{\eta * J} \qquad \text{Equation 4-1}$$

The dynamic viscosity and flux can be seen as corrections for the TMP in order to normalize the TMP. The cross-flow cMF in present study is operated with constant permeate flux of 58 $Lm^{-2}h^{-1}$. Therefore, the permeate flux should not have any influence on the membrane resistance, in optimal operation conditions. However, looking at the obtained TMP and flux data, see Figure 4-3, no optimal operation is observed.

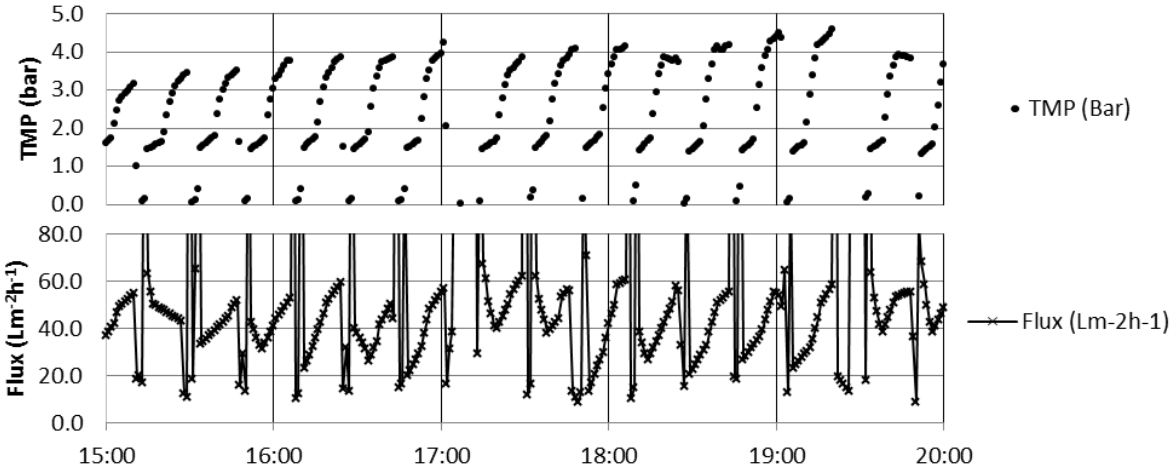

Figure 4-3. Example of typical raw data, obtained at Jan 24.

Figure 4-3 shows typical 1-minute TMP- and permeate flux data of two CEB intervals, 15:00 to 17:00 and 17:15 to 19:30. The flux results show no continuous stable flux around 58. As discussed in chapter 4.2, a slow build-up of the permeate flow occurs after each regular backwash. Following the slow build-up a more or less stable permeate flux of ~58 is achieved in the last minutes which varies each filtration. The TMP data shows approximate similar behaviour to flux data. The first step in present analysis is selecting the data corresponding to the last minutes, the absolute TMP and flux values, see Figure 4-4.

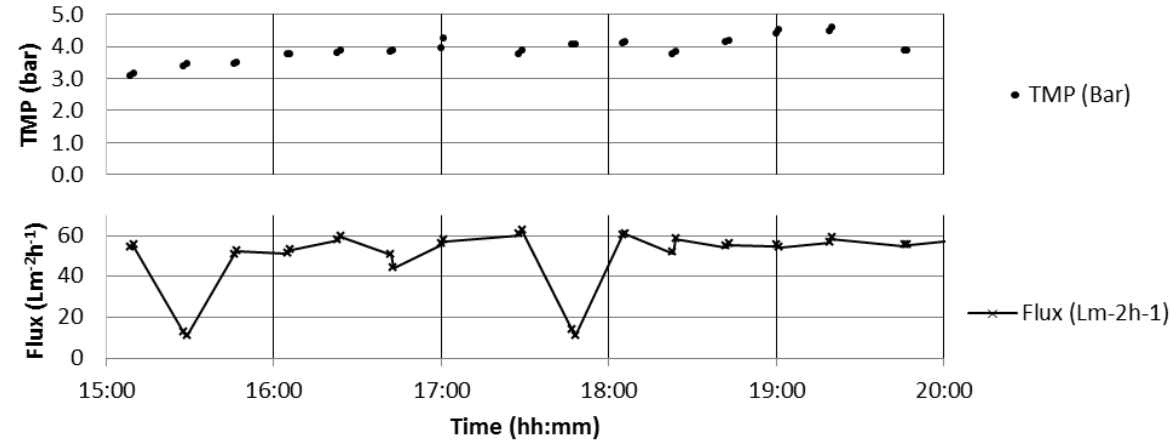

Figure 4-4. Compressed TMP- and flux data, Jan 24.

Figure 4-4 shows the compressed TMP- and flux data. Still, multiple flux data point are too low or too high, in this case only too low. Right before each second backwash, at 15:30 and 17:45, the flux decreases too early during filtration. This is a repeating phenomenon and may be explained by an error is the operational software or flow sensor.

Since the cMF is operated at constant flux, too low or too high permeate flux data points are considered not reliable due to the deviant operational conditions. The TMP and flux data is therefore further compressed for further analysis. TMP data and corresponding flux data is disregarded outside the range of 58 $Lm^{-2}h^{-1}$ ±10%. With the obtained 'final' data the hydraulic membrane resistance (10^8 m^{-1}) is calculated, see Figure 4-5.

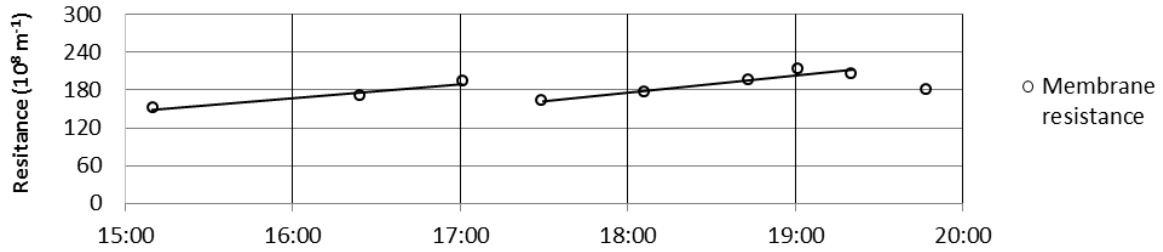

Figure 4-5. Representation of the irreversible fouling rate (10^8 $m^{-1}h^{-1}$), based on calculated resistance values (10^8 m^{-1}) from the compressed data. Data obtained from Jan 24

As discussed in chapter 2.2.3, irreversible fouling is the membrane resistance which is not recovered by physical cleaning, e.g. backwashing. When latter mentioned is applied to present data, as shown in Figure 4-5, the irreversible fouling can be determined by drawing a line through the resistance results in between two CEB's. Therefore, the irreversible fouling rate is defined as the increase in membrane resistance per hour ($m^{-1}h^{-1}$) in between two CEB's.

Additionally to the analysis, the start-up per time series is taken into account. The water quality in this period characterizes a certain stable pressure drop over the membrane. Thus, until the first moment of stable operation the increase in TMP is irrelative according the present water quality. This is nicely shown in Figure 4-6. The COD, NTU and EC are plotted to show a low change in concentration over time. Meanwhile the TMP increases from the start till stabilization at around 4 bar. Therefore in the time series, all data from the start-up till 23-12-'16 7:30 are rejected.

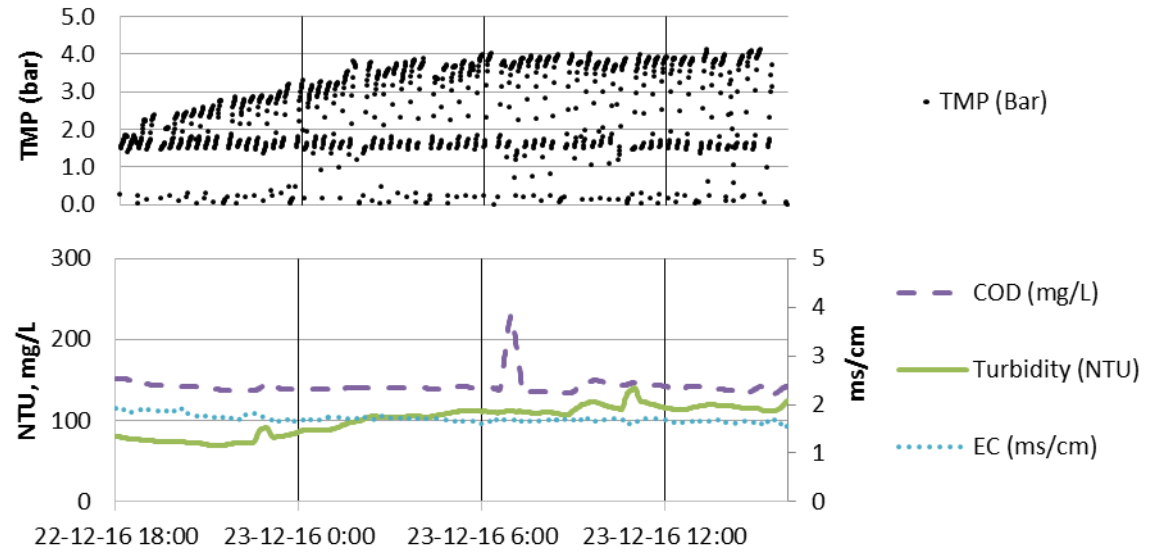

Figure 4-6. The effect of initial water quality on the TMP development in time series 'Dec 22-23'

4.5 Results and discussion

4.5.1 General results

In two months of experimental monitoring 15 time series are obtained with a duration of 1.9 days. An overview of the results per time series are added in the appendix, see Appendix A. Table 4-1 shows per time series the average values (AVG.) with corresponding standard deviation (SD) for COD, turbidity and conductivity.

Table 4-1. Monitoring results in the cMF feed per time series for COD, Turb., and EC.

		COD		Turbidity		Conductivity (EC)	
		AVG.	SD.	AVG.	SD.	AVG.	SD.
Run	T (days)	mgL^{-1}	σ	NTU	σ	$mScm^{-1}$	σ
DEC 7-10	3.2	293	20	60	16	1.7	0.2
DEC 14-16	2.1	186	19	31	8	1.3	0.4
DEC 17-19	2.3	254	114	31	9	1.5	0.1
DEC 22-23	0.9	143	11	101	18	1.7	0.1
DEC 23-25	1.5	200	59	154	24	1.7	0.1
DEC 28-29	0.7	367	53	260	45	2.7	0.3
DEC 30-31	0.8	226	56	204	97	2.5	0.3
DEC 31-1	0.9	276	25	309	65	2.5	0.3
JAN 2-4	1.9	143	32	73	33	2.0	0.3
JAN 6-9	3.5	185	82	113	69	1.7	0.2
JAN 11-13	2.1	98	40	45	23	0.9	0.1
JAN 16-19	3.8	88	47	60	34	0.8	0.1
JAN 20-22	1.5	199	15	112	15	0.8	0.1
JAN 24-26	2.0	219	53	125	27	1.8	0.4
JAN 26-28	1.1	100	5	36	7	4.0	1.6
DEC 7-JAN 30	1.9 (AVG.)	222	103	94	75	1.6	1.0

In Table 4-1 it can be seen that over the total period, DEC 7-JAN 30, the concentration values for COD, turbidity and conductivity are 222(103) mgL^{-1}, 94(75) NTU, 1.6(1) $mScm^{-1}$, respectively. In order to check whether the results corresponds to the influent characteristics, see Table 3-1, the average are determined. The results are comparable to the influent characteristics except for turbidity which is a factor ~1.5 higher. The higher turbidity may be explained by a change in sewage composition, weather conditions or pilot setup. As the area of sewage origin is relatively small a large variance in sewage composition is expected. Regarding weather conditions, less rainfall should increase the concentrations in case of a combined sewer system. At last, the coagulation dosing + flocculation tank were installed at the beginning of December. The effectiveness of the installed coagulation process may have altered the suspended solids and coagulants concentration.

4.5.2 Correlation analysis

In order to understand if an increase in concentration of a particular parameter causes an increase in TMP, the squared correlation (R^2) is calculated per parameter per time series. In time series 'Dec 28-29' too few data points were collected for the R^2 calculation. The time series 'Jan 6-9' is divided into two smaller time series. A concentration peak occurred halfway the time series which increased the irreversible fouling suddenly. The fouling could not be recovered by the CEB's and subsequent TMP development became irrelative to the corresponding COD concentration regarding the previous COD concentration. This interrupts a proper R^2 calculation of the total Jan 6-9 time series.

A positive R^2 indicates, within a single time series, that a relative high membrane resistance (R) value corresponds to a relative high COD concentration and that a relative R value corresponds with a relative low COD concentration. And a negative R^2 indicates that a higher concentration does not correspond to a relative high TMP value. In other words, a high positive R^2 value defines a good correlation between an increase in membrane resistance corresponding an increase in the concentration. The results are shown in Figure 4-7.

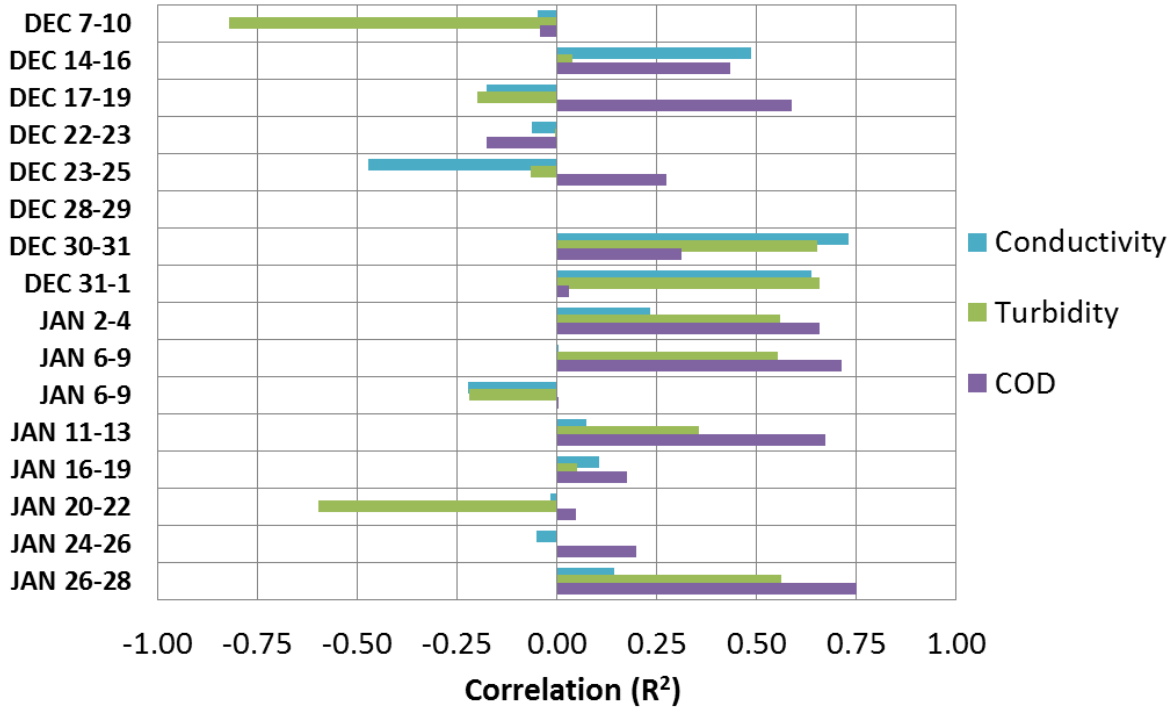

Figure 4-7. Squared correlation between the hydraulic membrane resistance (m^{-1}) and concentration load ($conc.m^{-2}h^{-1}$) of COD, NTU and EC per time series.

In Figure 4-7 the highest consistency for positive correlations is observed for COD. As discussed in chapter 2.1.3, COD is a surrogate measurement for organic matter, including proteins, polysaccharides and humic substances which are mainly bio-macromolecules. Biopolymers (bio-macromolecules > 100 kDa), except for proteins and humic acids, contain gelling properties enhancing the formation of a gel layer on the membrane surface (Zhou, *et al*. 2016). Hydrophilic and/or hydrophobic interactions between gelling biopolymers and the membrane can be an important contributor to membrane fouling. Yamamura et al (2014) demonstrated that despite identical total organic carbon (TOC), fouling development trends

were significantly different between hydrophilic and hydrophobic fractions. The hydrophobic fractions did not increase membrane resistance, while the hydrophilic fractions caused severe loss of membrane permeability. The largest difference in NOM characteristics was a significant higher presence of biopolymers in hydrophilic factions which are likely responsible for fouling due to their larger size. In contrast, Xiao (2014) showed that hydrophobic organics adsorbed more quickly than hydrophilic organics on a UF membrane. In this case the hydrophobic organics are thought to cause higher pore blocking and gel layer resistance due to their smaller size and higher presence of carboxylic complexing groups. Thus, fouling results based on hydrophobic and –philic organic characterization will differ depending on the water source and type of organic characterization.

Several membrane studies support the COD-fouling correlation. Kumar (2015) studied the correlation of turbidity and different types organic components with dead-end MF fouling treating secondary effluent (Kumar, 2015). Protein and carbohydrates resulted in good correlations with reversible fouling which was mainly attributed to size exclusion and the resulting cake layer. Only protein showed a moderate correlation with irreversible fouling due to its relative small particle size. Kumar (2015) also found a weak correlation for turbidity with membrane fouling since particulate matter forms a loosely bound layer on the membrane surface. However, depending on the interactions between the particulate matter and present organics a different correlation can occur. Shang (2015) characterized the organic matter in hydraulically irreversible fouling of a dead-end ceramic MF membranes of a natural surface water treatment. Humic substances and biopolymers were concluded as main fractions of the irreversible foulants.

Dissolved solids are defined as particulates that pass a filter with a mesh size of 1.2 µm, generally 0.45 µm. Since the cMF contained an average pore size of ~0.15 µm TDS will predominately penetrate through the MF pores. Therefore conductivity shows a low correlation with the membrane resistance.

4.5.3 Irreversible fouling rate

The collected time series include more than 40.000 1-minute data points. From the data 203 irreversible fouling rates ($m^{-1}h^{-1}$) are obtained. Figure 4-8 shows the irreversible fouling rate values plotted against the corresponding parameter concentrations per time series.

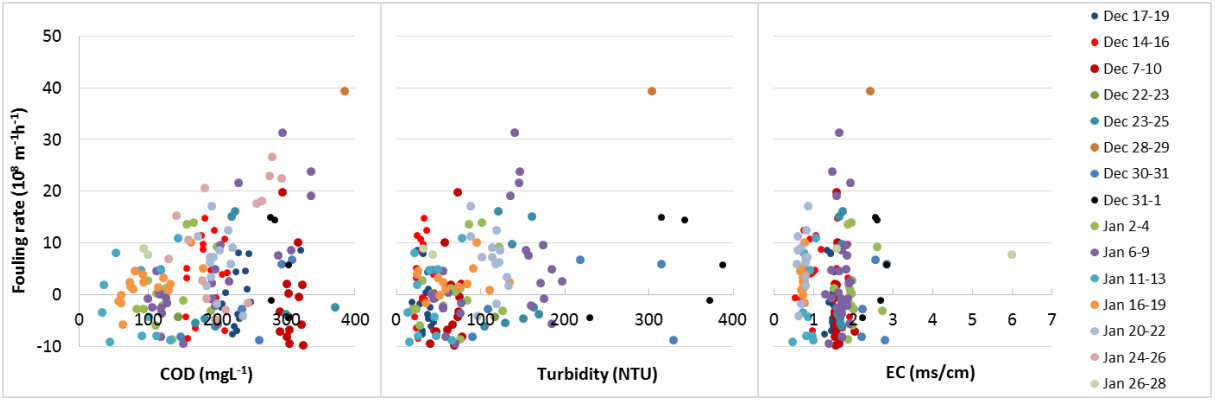

Figure 4-8. Per parameter the irreversible fouling rate (10^8 $m^{-1}h^{-1}$) values are plotted against the particular parameter concentrations per time series.

The COD results in Figure 4-8 illustrates that at higher COD concentrations the possibility to a higher irreversible fouling rate increases. For turbidity and conductivity there is no such trend. This corresponds to the concentration-fouling correlation analysis where COD was found the best correlating parameter. Therefore, for further analysis, only the COD parameter is considered.

The irreversible fouling rate results for COD are elaborated in Figure 4-9. In the figure three time series are highlighted, Jan 6-9 (red O's), Dec 7-10 (green X's) and Dec 14-16 (purple Δ's). In addition, the trend in increasing fouling rate values at increasing COD concentration is determined which is represented by the black line.

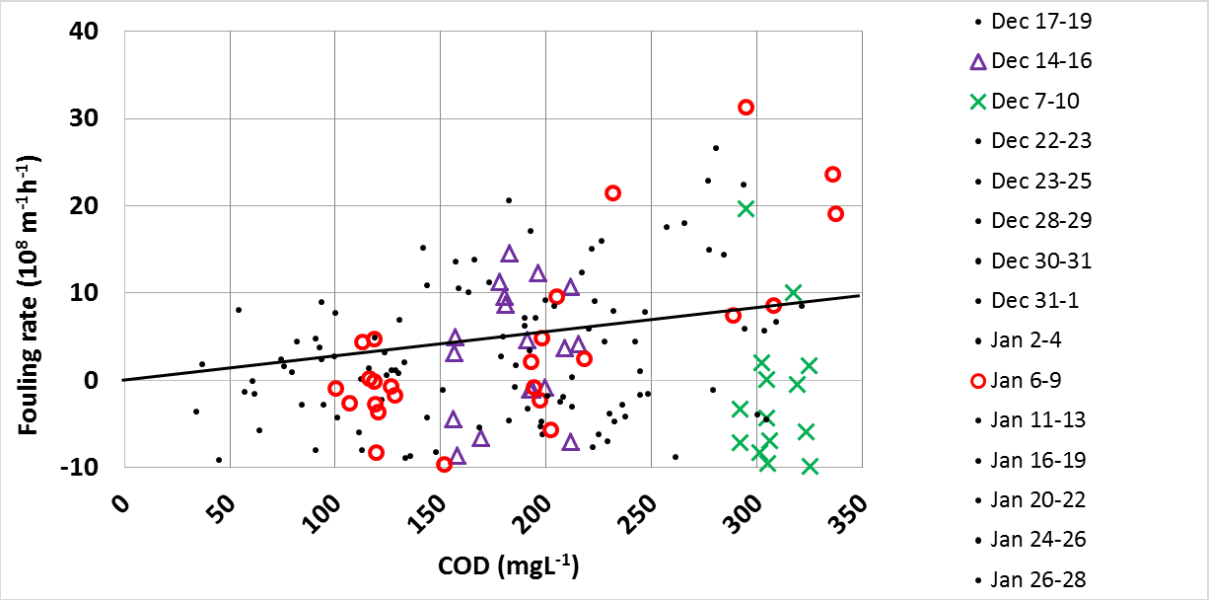

Figure 4-9. The irreversible fouling rate versus the COD concentration included

At first, the time series Jan 6-9 is discussed to distinguish between stable and instable cMF operation. In this way the approximate breakeven COD concentration can be determined. The time series 'JAN 6-9', see Figure 4-10 (and Appendix 7-10 on page 71), shows the data on membrane resistance (m^{-1}) and COD concentration (mgL^{-1}) on the left hand side. On the right hand side the corresponding irreversible fouling rates are given.

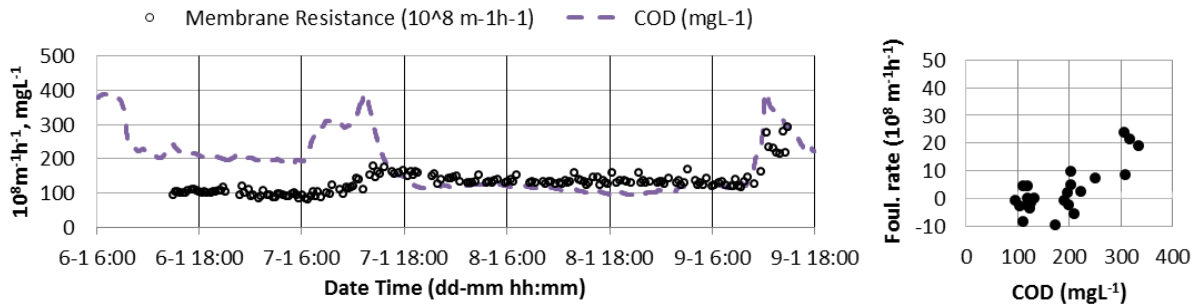

Figure 4-10. COD (mgL^{-1}) and R (m^{-1}) development on the left and corresponding irreversible fouling rates (10^8 $m^{-1}h^{-1}$) on the right, from time series 'JAN 6-9'.

The time frame of the time series Jan 6-9 is more than two days. The COD concentration was around 200 and 100 mgL^{-1} and irregular COD peaks can be seen. After the first COD peak, at 7-1 12:00, the membrane resistance increased and could not be fully recovered by the CEB's. Then during the following COD peak, almost similar to the first COD peak, the membrane resistance strongly increased. Probably the irreversible fouling content at the membrane was higher during the second peak making it more susceptible to concentration peaks. On the right-hand side in Figure 4-10 the irreversible fouling rates are shown. Higher fouling rates are observed at COD concentrations around 300 mgL^{-1} which were the COD peaks. During the second COD peak the operation pressure of 5 bars was achieved and the filtration stopped. Therefore, the COD concentration of 300 mgL^{-1} is considered to cause an unstable cMF operation. Similar observation are made in the time series 'Jan 24-26', see Appendix 7-14 on page 75. In the time series there is an initial high COD concentration, causing high starting irreversible fouling rates. From the start the COD concentration gradually decreases where at approximately 260 mgCODL-1 a significant stable cMF operation occurs.

Looking back at Figure 4-9, the low irreversible fouling rates at relative high COD concentrations, between 250 and 300 mgL^{-1}, are considered remarkable. The remaining two highlighted time series in Figure 4-9 are discussed below. These are the time series Dec 14-16 (purple Δ's) and Dec 7-10 (green X's). The discussion aims to show the restrictions of the cMF operation influencing the fouling rate results.

At first, the time series Dec 7-10 is discussed which is shown in Figure 4-11. On the left hand side the COD concentration, TMP, Flux, and membrane resistance are presented. On the right hand side the corresponding irreversible fouling rates are given. The time series duration is over 3 days which makes the cMF operation considerably stable. The data in Figure 4-11 is only one day in order to make the data presentable. The COD concentration during the total time series was approximately continue 300 mgL^{-1}. Remarkably, relatively low- or even negative irreversible fouling rates are observed.

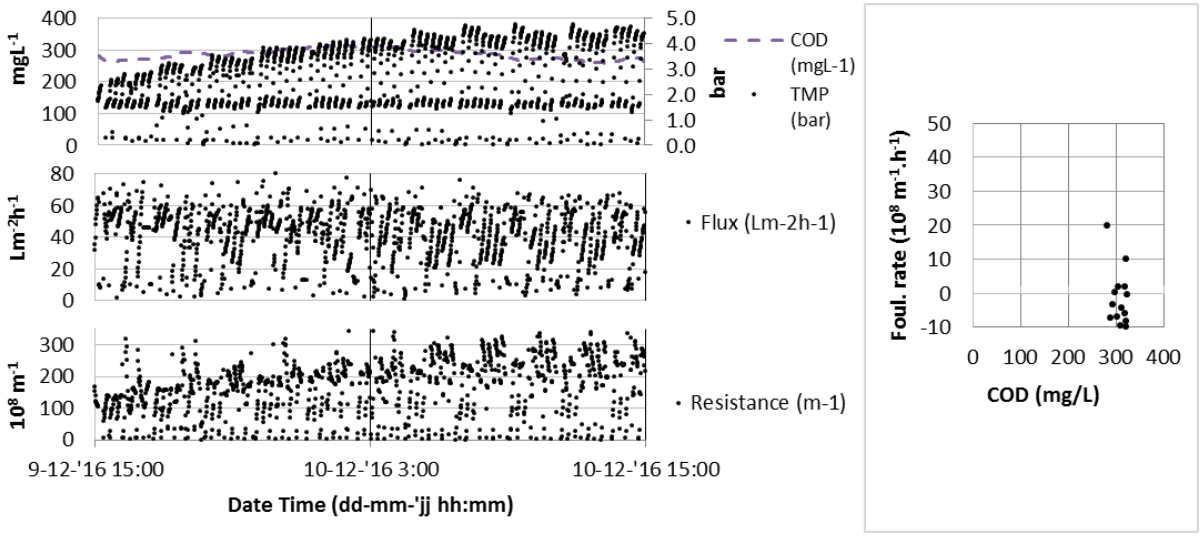

Figure 4-11. COD, TMP, Flux and membrane Resistance results on the left and corresponding irreversible fouling rates (10^8 $m^{-1}h^{-1}$) on the right, from time series 'Dec 7-10'.

The COD composition may have changed which increased the coagulation effectiveness. As discussed in chapter 2.2.2, aluminium-based coagulants are known to preferentially remove

hydrophobic rather than hydrophilic (organic) substances. Large particles/flocs are formed increasing the reversible fouling and subsequently decreasing the irreversible fouling.

However, a more reasonable discussion is obtained when looking at the raw flux data in Figure 4-11. The cMF should operate at a constant flux of 58 $Lm^{-2}h^{-1}$. Instead, many flux data points fall between the flux of 20 and 58, especially in the second half (between 10-12 3:00 and 10-12 15:00). The net flux is significantly lower than the set 58 Lm-2h-1 causing considerably stable operation at relative high COD concentrations. Looking closely at the flux data, the decreasing TMP trends is determined by a decreasing trend in the permeate flux. Generally, the first two 15 min of filtration start at relative high permeate fluxes. Following filtrations, the permeate flux significantly decreases causing the TMP to drop within a single CEB interval. The unstable permeate flux may be explained by the fact that the installed pump capacity is designed for a ceramic Nanofiltration (cNF) installation. The feed pump is considered over dimensioned for a MF.

Secondly, the time series 'Dec 14-16' is discussed, see Appendix 7-2 on page 63. The COD concentration during the complete time series was approximately 200 mgL^{-1}. The time series duration is over 2 days from which the last day is shown in Figure 4-12. At the left hand side the COD concentration, TMP, flux and membrane resistance data is shown. At the right hand side presents the irreversible fouling rates.

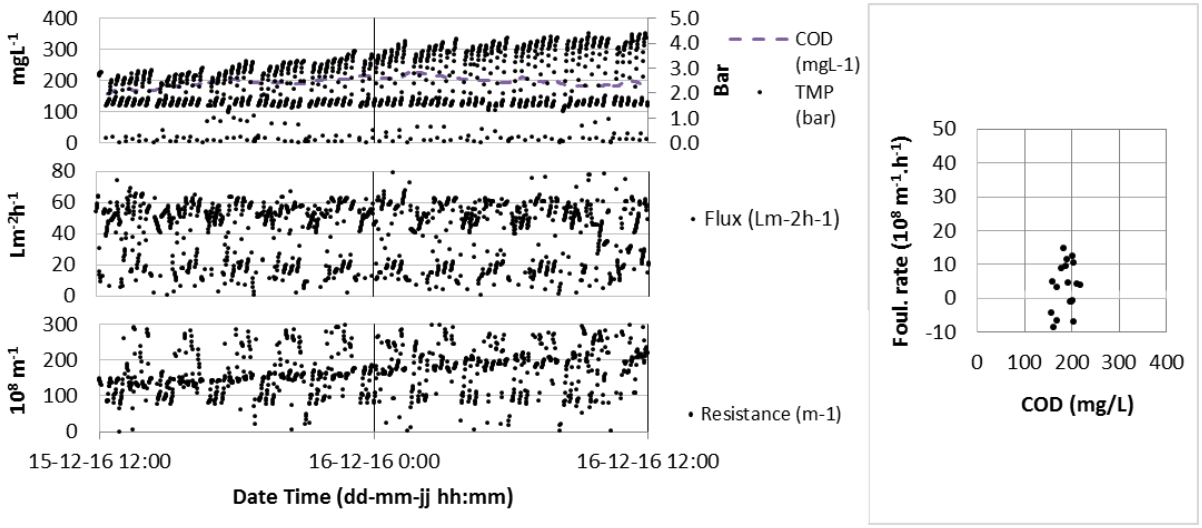

Figure 4-12. COD, TMP, Flux and membrane Resistance results on the left and corresponding irreversible fouling rates (10^8 $m^{-1}h^{-1}$) on the right, from time series 'Dec 14-16'.

The permeate flux data in Figure 4-12, compared to the flux data in Figure 4-11, is relatively more consistent around the flux of 58 $Lm^{-2}h^{-1}$. The cMF operation in present example therefore is considered relatively good. The net flux will be therefore closer to 58 compared to the net flux in Figure 4-11. The TMP- and flux data show similar trends in the development over time. Therefore, the membrane resistance increases at a lower rate compared to the TMP.

The major components influencing the flux are: the feed pump, cross-flow pump and the flow controlling valve in the concentrate stream. The obtained concentrate flow velocity data shows a high stability around the set flow velocity, see Figure 4-13, indicating a proper performing flow controlling valve. Considering the pumps, the NF membranes have been replaced by MF membranes. The imperfect cMF operation may be explained by the feed-

and/or cross-flow pump being over-designed. For as well the NF as the MF, the cross-flow pump is operated at minimum capacity. Together by the fact the MF operates at lower operational pressures (~3 bars instead of the ~6 bars for NF), the feed pump is considered as major contributor to the instable flux operation.

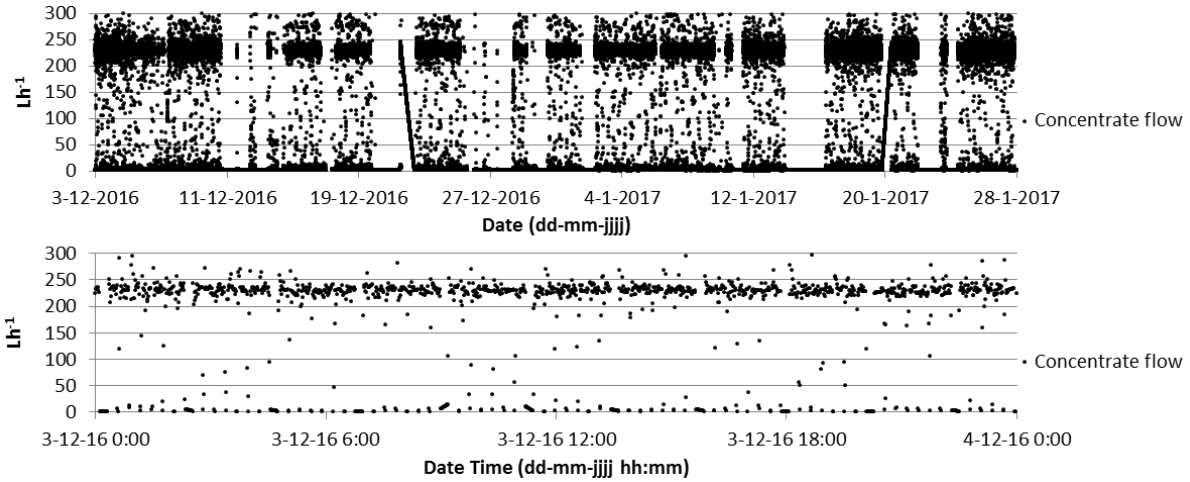

Figure 4-13. Upper graph: complete concentrate flow velocity data set. Lower graph: concentrate flow velocity data of 3-12-‘16.

Chapter 5

Effect of oxygen on Reverse Osmosis biofouling

5.1 Introduction

Arriving at the RO, the sewage water is strongly aerated due to several operational conditions in the RINEW pilot plant. Due to the higher synthesis yield for aerobic bacteria, a faster biofouling development is expected in a RO filtration. The research question therefore becomes:

2. *What is the effect of oxygen in cMF permeate on the biofouling potential in a RO unit?*

To simulate the (bio)fouling development in a RO filtration the Membrane Fouling Simulator (MFS), is used.

5.2 Membrane Fouling Simulator (MFS)

Conventional studies on biofouling in spiral wound RO elements were predominantly based on parameters such as pressure drop and on a destructive membrane study afterwards. Generally, a spiral wound element is a rolled up RO membrane with a feed- and permeate spacer at both sides. The feed spacer guides the feed water to the membrane while enhancing the turbidity. Micro-organisms predominantly grow in the low velocity areas in the feed spacer increasing the pressure drop from the feed side towards the concentrate side. To measure the biofouling potential in spiral wound elements the Membrane Fouling Simulator (MFS) was developed) which is proven to be able to measure biofouling in RO-membranes (Vrouwenvelder, 2009; Valladares Linares, 2016). The MFS is a small element containing a RO membrane and –feed spacer, see Figure 5-1. Since biofouling only affects the pressure drop from the feed to the concentrate side no permeate is produced by the MFS. Besides pressure drop monitoring, the fouling at the spacer side can be visually observed through a transparent glass at the top side, spacer side, of the MFS.

Following a MFS run an autopsy is performed which characterizes the accumulated fouling. In a membrane autopsy 4 cm^2 sections of the membrane and feed spacers are taken. These are placed in capped tubes filled with sterile water. The tubes are placed in an ultrasonic bath (2 min) followed by mixing on a Vortex (few seconds). The biomass-water suspension from tubes is used to determine the adenosinetriphosphate (ATP) which is a suitable indicator of biofouling (Vrouwenvelder, 2009). ATP is measured with a portable luminometer. With a honey-comb shaped dipper a particular volume of biomass-water suspension is taken. Added to an enzyme solution the ATP is released from the bacterial cells and light is produced. The produced light is measured by the luminometer in relative light units (RLU).

Figure 5-1. Installation for operation of the MFS. The feed flow enters the MFS scheme at (A) and is regulated with a flow controller at point (B). The pressure drop over the MFS is measured with the differential pressure transmitter (dP) (Endress+Hauser Deltabar S: PMD70).

5.3 Research approach

To study the effect of oxygen on RO biofouling two parallel MFS setups are installed. One setup is fed with oxygen rich water where the other is fed by anaerobic water.

Since the cMF permeate production is too unstable the MFS runs are done in batch form, see Figure 5-2. cMF permeate is collected and stored in two separate buffer tanks, both filled up to 100 L. Starting, the water in buffer 2 is made anaerobic by dosing the strong oxygen scavenger $NaHSO_3$ (aq), approximately 100 mL per 100 L. The dosing ensures the dissolved oxygen (DO) concentration to stay below 0.15 mgL^{-1}. Present study is performed in winter period. Therefore the water temperature (T) in both buffer tanks were heated by a pond heater. The heater kept the water temperature between 14 and 19 degrees, depending on the outside air temperature. Each morning, if the cMF is in operation, both buffers are emptied and rinsed with tap water, fresh cMF permeate is collected, etc.

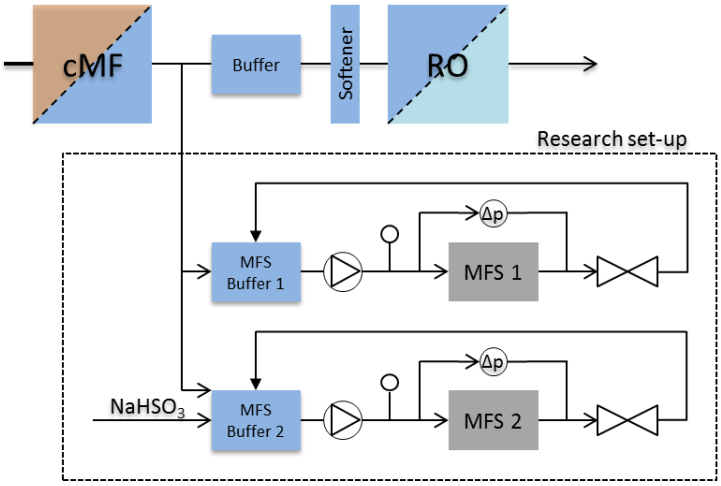

Figure 5-2. Schematic overview of the MFS research setup in the treatment line.

With use of a peristaltic pump the water is circulated over both the MFS setups. The pulsation effect from the peristaltic pump is significantly reduced by dead-end t-joints in between the pump and the MFS. These t-joints function as expansion vessels. The flow is kept constant at 16 Lh^{-1} in order to supply a sufficient load for biofouling to develop. In each MFS a polyamide NF membrane + feed spacer (spacer thickness: 0.787 mm = 32 mil) is installed. Both MFS's are equipped with a transparent window for direct fouling observation. During the experiment, the pressure drop increase over the MFS is measured with the differential pressure transmitter 'Deltabar S'. In order to get insight into the MFS feed water quality the following parameters are measured at the start and end of each water batch within one MFS run: ATP ($ng.mL^{-1}$), T (^oC), DO (mgL^{-1}), pH (-) and EC (μScm^{-1}).

5.4 Results and discussion

To investigate the effect of oxygen in cMF permeate on RO biofouling the research, as discussed in paragraph 5.3, is performed twice. One run is done is December and one run is done in January. The results are discussed below.

5.4.1 MFS Run December

The first MFS run is performed in December for ~7 days, see Figure 5-3. The corresponding data is added in Appendix B. The water is refreshed two times, on 19-12 and 21-12. The temperature in the anaerobic setup was approximately 14.3 degrees and in the aerobic MFS around 22.5 degrees. Due to a malfunctioning water heater the aerobic water was heated till too high temperatures.

Temperature is a determining variable for microbial growth and thus for biofouling of the RO unit. This is confirmed by Farhat (2016) who investigated the pressure drop development in a MFS fed by filtered tap water for three different feed water temperatures. The results showed a running time, till a pressure drop of 800 mbar, of two days for 30 °C, five days for 20 °C and 18 days for 10 °C. This signifies a faster biofouling development occurrence at higher water temperatures, especially from 10 °C to 20 °C. Thus, the aerobic- and anaerobic MFS

results are discussed separately making a membrane autopsy unnecessary. All aerobic- and anaerobic MFS results are shown below in order to indicate certain behaviours.

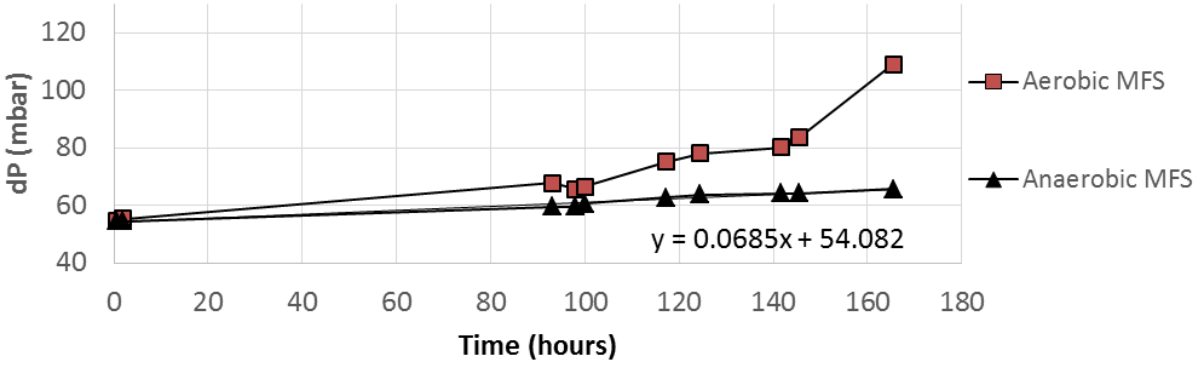

Figure 5-3. Pressure drop development in the first MFS run.

In Figure 5-3 the pressure drop (dP) development over time is shown for both MFS's. A linear trend line is drawn through the anaerobic dP results. The corresponding formula (y=0.0685x+54.082) is given in the graph. The observed dP trends in both MFS's are discussed below.

Anaerobic fouling rate

In Figure 5-3, a gradually pressure drop increase over time is observed in the anaerobic MFS. Looking at the linear trend line formula the pressure drop increases at a rate of approximately 0.07 $mbarh^{-1}$. The result compares to conclusions drawn in similar studies:

- Kramer et al. (2015) studied the biofouling potential of ceramic NF permeate. The water, pre-treated by a microscreen, was kept anaerobic throughout the treatment process. A duplicate experiment, a 7 days- and a 14 days run, resulted in an anaerobic fouling rate of approximately 0.07 and 0.08 $mbarh^{-1}$ respectively.
- Vrouwenvelder (2009) studied the effect of nutrients on RO biofouling using MFS installations. Parallel MFS installations were fed by Dutch tap water where additional nutrients were added to one MFS. Looking at the biofouling rate in the MFS installation fed by tap water (13 ^{o}C), feed flow of 16 Lh^{-1}, a fouling rate of approximately 0.09 $mbarh^{-1}$ was determined.

Aerobic fouling rate

In present MFS run, direct in-situ camera observation are made of both MFS's at the end of the run, on 23-12-2016, see image A and B in Figure 5-4. The water flow direction is from bottom to top. The direct in-situ camera observations are made of the bottom first cm. A denser fouled spacer is observed in the aerobic MFS (B) compared to the spacer in the anaerobic MFS (A). In both MFS's the fouling predominantly occurred at the inlet of the MFS. A brownish filamentous growth is observed which mainly attaches to the spacer crossings.

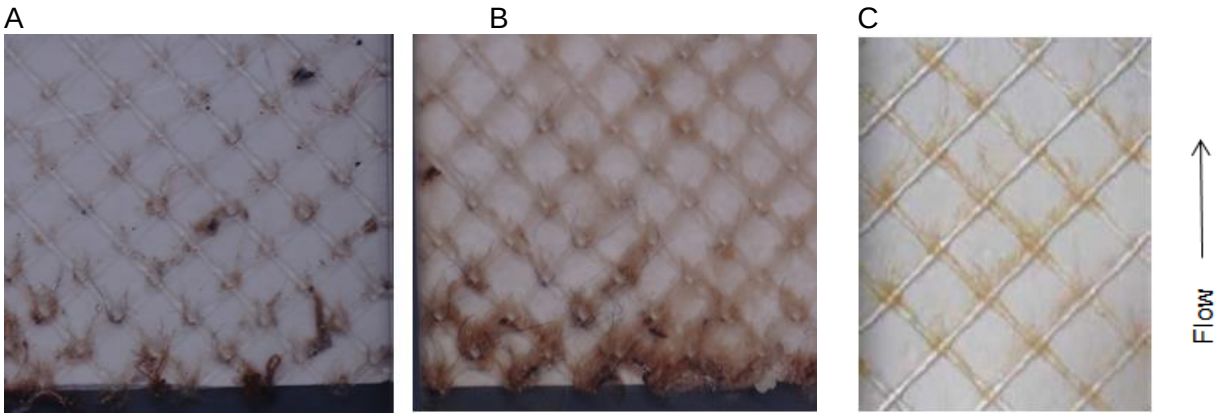

Figure 5-4. Direct in-situ camera inspections. The anaerobic MFS (**A**) and aerobic MFS (**B**) are shown at the 23-12-2016. A visual reference regarding biofouling (**C**) (Vrouwenvelder, et al. 2009)

Comparing to a similar study: Vrouwenvelder (2009) created a controlled biofouling in a similar MFS set up in order study the validation of a biofouling model (Vrouwenvelder 2009). At a rate of 16 Lh^{-1} tap water, mixed with a compound containing substrate, was fed to the MFS setup for 5 days. The analysis of the accumulated material confirmed biomass accumulation, see image C in Figure 5-4. Additionally, the following observations have been done:

1. Biomass growth is predominantly at the inlet side of the spacer;
2. Biomass attaches predominantly at positions with low shear;
3. Filamentous biofilm structures are observed and attach mainly to the spacer crosses.

The observations in present MFS study and Vrouwenvelder's biofouling experiment show multiple similarities like the bio growth positioning and -structures. Therefore the occurrence of bacterial growth is considered in present MFS results. Many scientists conclude that transparent exopolymer particles (TEP) may be a substance that has the most impact on membrane biofouling (Rachman, *et al*. 2015; Kennedy, *et al*. 2009). TEP is an abundant form of the sticky extracellular polymeric substances (EPC) which is an excreted polymeric matrix of microbial origin. EPC has a major role in microbial growth and aggregation of the membrane surface.

5.4.2 MFS Run January

The second MFS run is performed MFS for 11 days, see Figure 5-5. The corresponding background data is added in Appendix C. The water heaters in both MFS setups kept the water temperature at a similar level. The temperature was generally between 15 and 19 degrees, depending on the outside air temperature. Figure 5-5 shows the pressure drop (dP) development per MFS installation. Linear trend lines are drawn through the dP results per MFS from which formula is given in the figure. Between the 150th and 230th hour aerobic MFS results could not be used due a necessary tube replacement in the peristaltic pump. Between the 150th and 230th hour the aerobic pressure drop measurements became irrelative to the pressure drop results before the replacement. The problem was solved at the 230th hour and proper pressure drop results were obtained again.

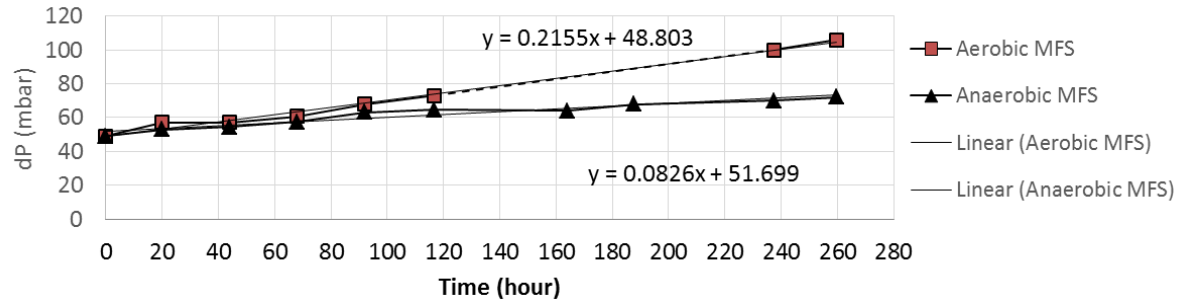

Figure 5-5. Pressure drop development in the second MFS run.

Fouling rate

In Figure 5-5 the pressure drop results are shown. Gradual increases in pressure drop over time are observed for the aerobic- and anaerobic MFS. The fouling rates for the aerobic- and anaerobic MFS resulted in ~0.22 mbar.h^{-1} ~0.08 mbar.h^{-1} respectively. As discussed in chapter 5.4.1, anaerobic cNF permeate (Kramer, *et al*. 2014) and Dutch tap water (Vrouwenvelder, 2009) resulted in MFS fouling rates of ~0.075 and 0.09 mbar.h^{-1} respectively. These results are in line with the obtained anaerobic pressure drop increase of 0.08 mbarh^{-1} in this MFS run.

Iron deposits (20 hours)

Direct in-situ camera inspections are given in Figure 5-6, see anaerobic MFS (A1) and aerobic MFS (A2). A red/brown colour fouling is observed in the aerobic MFS after 20 hours. The red/brown colour indicates the deposits of iron oxides (Beyer, *et al*. 2014; Hiemstra, *et al*. 1999). Iron oxides are formed when soluble iron (II), in anoxic conditions (like raw sewage water), is brought into contact with oxygen (Iron Oxide, WIKI). The iron oxides have a low solubility and can clog or adsorb onto a specific surface. As discussed in chapter 2.1 the influent composition varies over time. Possibly, an industry (maybe auto service station) discharged a specific waste into the sewer which caused a temporary increase in soluble iron which subsequently oxidized and precipitated in the aerobic MFS.

A1 A2

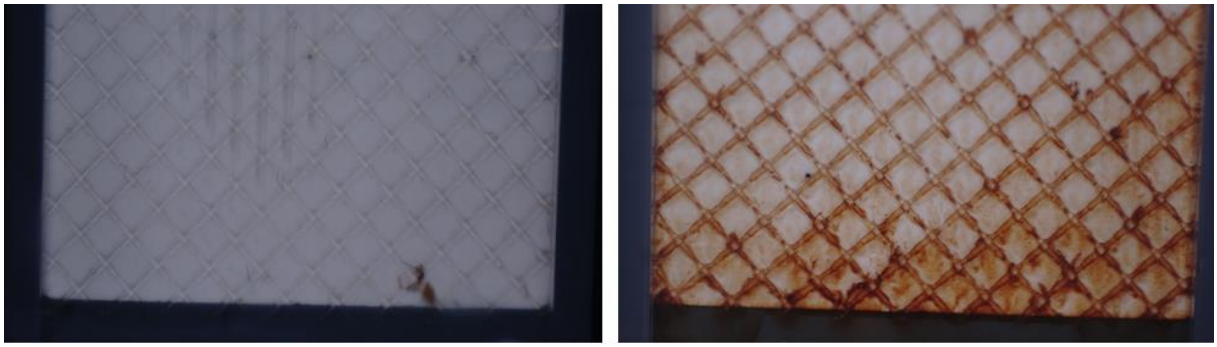

Figure 5-6. Direct in-situ camera inspection taken after 20 hours (**A1** = anaerobic and **A2** = aerobic)

Membrane autopsy (260 hours)

At the end of the run, after 260 hours, a significant higher dP occurred in the aerobic MFS see Figure 5-5. Figure 5-7 shows the in-situ camera inspections at that moment. In the anaerobic MFS (B1) black accumulation is observed. In the aerobic MFS (B2) a thick white precipitation replaced the initial red/brown colour. The white precipitation may indicate a heavy Calcium precipitation. As discussed in chapter 3.1 the sewage Hardness (Calcium + Magnesium concentration) can be very high.

In order to characterize the accumulation at the end of the run a membrane autopsy was performed. The autopsy resulted in RLU values of 4824 and 13085 (top and bottom respectively) in the anaerobic MFS and RLU values of 73 and 392 in the aerobic MFS. The result contradicts the hypothesis that aerobic conditions enhance the development of biofouling in a RO installation. Possibly, the iron deposits or heavy calcium precipitation inhibited proper bio growth in the aerobic MFS.

B1 B2

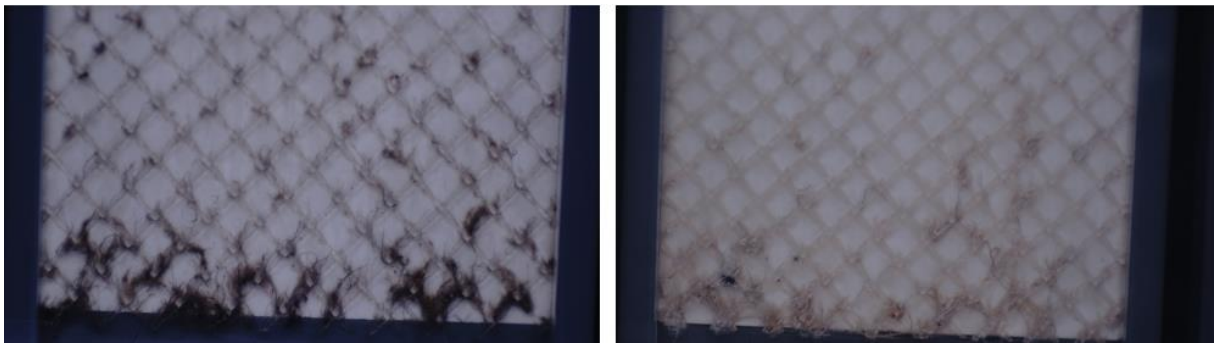

Figure 5-7. Direct in-situ camera inspection taken and after 260 hours (**B1** = anaerobic and **B2** = aerobic)

In chapter 2.1 already a large variety in water composition is observed. Together with the MFS study results it is concluded that there are too much variables for proper biofouling research with use of the MFS. Recommendations regarding on how to study the effect of oxygen on RO biofouling is given in Chapter 7.

Chapter 6

Potential financial feasibility of the RINEW concept

6.1 Introduction

Conventionally, sewage is transported via sewer network to a central and remote SWTP. There the suspended solids, organic substances and nutrients are removed by either physical sedimentation or biological sludge treatment. The average estimated costs of conventional treatment are ~0.31 EURm^{-3}, see cost calculation in Appendix D. The treatment involves predominantly big concrete tanks causing a relative large geographic footprint. The sewage is treated till a required water quality ready to be discharged to open water.

However, sewage water is one of the most reliable water sources which makes it interesting for water reclamation (Ghayeni, *et al*. 1998). High quality water (e.g. demiwater) can be reclaimed by tertiary treatment, which generally includes MF/UF and RO (Metcalf & Eddy, 2014). The additional costs for centralized MF/UF+RO is suggested to be as low as 0.64 $m^{-3}.

An alternative to water reclamation at a central SWTP is the concept of decentralized treatment at upstream locations (Metcalf & Eddy, 2014). Decentralized water reclamation at upstream locations safes the infrastructure costs of storing and transporting the reclaimed water. Since the infrastructure costs can be up to 2/3 of the total costs, decentralized water reclamation can be economical feasible. Therefore the research question becomes:

3. *What is the potential financial feasibility of water reclamation by the RINEW concept compared to water reclamation at a central SWTP?*

6.2 Research approach

In order to answer the research question a cost analysis is performed on a concept study. Figure 6-1 schematically represents the concept study where the sewage of multiple cities is treated at a central Sewage Treatment Plant (SWTP). A new industrial area is built near City A which demands a specific flow of demi water for industrial purposes. Due to the arid climate sewage water is considered the most suitable water source for the industrial demand.

High quality water can be produced either decentralized (**Concept 1**) or centralized (**Concept 2**). In concept 1 the industrial water demand is provided by the RINEW concept where the rest of the sewage is treated at the SWTP. In concept 2 all sewage is treated at the SWTP where the industrial demand is produced by the additional MF/UF+RO from secondary effluent. The specific costs ($EURm^{-3}$) for both concepts are calculated for various industrial demands. The most important variable between the two concepts is the transport distance between the SWTP and industry. In this research the breakeven distance will be calculated which is the distance where both concepts equally in price. The water transport distance in the RINEW concept is assumed to be negligible.

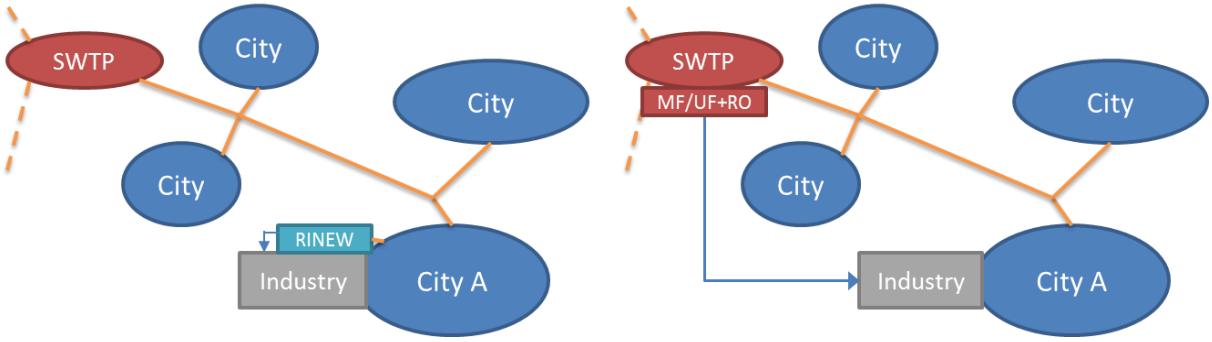

Figure 6-1. Schematic representation of concept 1 (left) and concept 2 (right)

In concept 1 a small amount of water will be reclaimed relative to the total amount of treated sewage at the SWTP. Thus, the sewer system and SWTP size in both concepts is considered equal and is therefore left out of the cost analysis. However, a cost calculation is made for the SWTP with the 'Afvalwatercalculator (Sewage calculator) by Padmos (2012) which is added in Appendix D.

The treatment costs are calculated for different industrial demands. In order to estimate costs the tool 'RHDHV Drinkwater Kostenstandaard (Drinking water cost standard)' is used. Since the tool is based on full-scale plants no cost-results can be obtained directly at low flows (decentralized flows). The costs for low design-flow are therefore extrapolated and assessed from accurate cost results from the cost tool. The cost tool and input characteristics are explained further in the section below.

6.2.1 Input 'Drinkwater Kostenstandaard'

Since the involved treatment techniques are widely applied in drinking water applications the tool 'RHDHV Drinkwater Kostenstandaard (Drinking water cost standard)' is used. Royal HaskoningDHV developed the tool in corporation with the Dutch water companies. The tool presents investments based on Standaard Systemeatiek Kostenraming (SSK). It calculates the specific cost ($EURm^{-3}$) regarding three cost components: the *construction-, total investment-* and *operational costs*:

- The construction costs are based on post calculations of civil-, electro-, and mechanical engineering costs of realized projects, literature data and available detail estimations. The construction costs include the categories water winning, treatment, wash water- and sludge treatment, storage, transport and distribution;

- The total investment costs are the construction costs plus surcharges, called ‘overhead’. These are for example: general facilities, installation costs, security costs, and interest. The costs for process and automation (PA) are project-/ and industry dependent. These are therefore calculated based on the amount of I/O’s per process part. An I/O stands for Input/Output which is a single communication line between a system and a computer. The amount of I/O’s per process step is multiplied by a ken-figure for PA (€ per I/O). The ken-figures are given in the operational costs;
- Operational costs are based on the NEN 2632 which is a standard providing operational costs estimates for buildings including process installations. Included are the cost components: fixed costs (depreciation, interest, levies), energy costs, maintenance, administration management costs (staff costs), and specific control costs.

Further in this chapter all used process steps are described. Per process step the following is discussed:

1. Its relevance;
2. Technical design parameters;
3. The uncertainty in cost estimates at a design flow of 100 m^3h^{-1}. Per treatment process an accuracy of 25% is achieved for cost estimates resulting from a certain range parameter input. Since the cost tool is based on realised full scale plants the minimal design-flows are relatively high. Therefore the costs per process step are extrapolated till a design flow of 100 m^3h^{-1} which is considered the lower limit of the cost tool;
4. Important cost-determining parameters with a corresponding sensitivity analysis, if necessary.

Influent buffer and -pump

An *influent buffer* is required to equalize a fluctuating influent flow. Depending on the area size, discharging the sewage, a different daily flow peak factor is expected (Metcalf & Eddy, 2014). The smaller the area the larger the peak factor, see Figure 6-2. For treatment efficiency purposes a continuous influent flow is required. The design- and cost-determining parameter is ‘volume’ (m^3) which is expressed as a percentage of the average daily flow (generally between 15 and 25%).

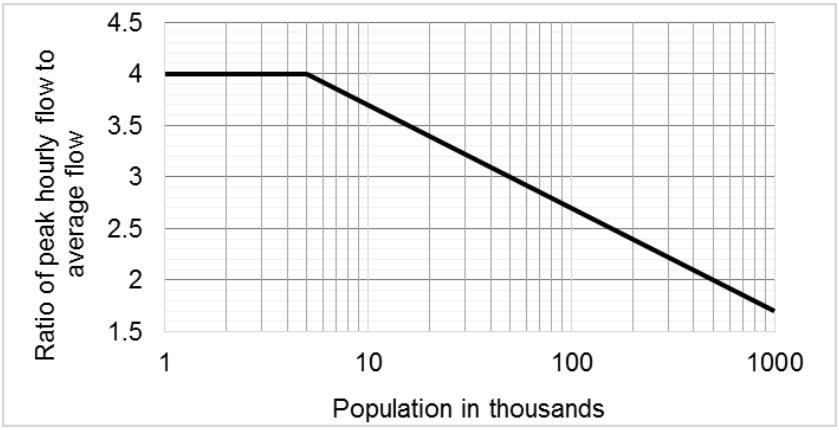

Figure 6-2. Ratio peak hourly flow to the average flow regarding the population.

The *influent pump* takes sewage from the influent buffer and exerts pressure for transport towards the treatment facility. The design parameter is the flow in m^3h^{-1}. An accuracy of 40% in cost estimation is obtained with a design flow between 1,300 to 15,000 m^3h^{-1}. The extrapolation line, see Appendix E, shows a relative small uncertainty in specific costs (~1 EURct.m^{-3}) at 100 m^3h^{-1}. The additional cost-determining parameter is the pump pressure which is set as 100 kPa (default).

Microscreen

By microscreening, the larger components, like grains and hair, are removed in order prevent any damage further in the treatment. Additionally it partly removes suspended solids and COD. The design parameter 'load' (default = 30 mh^{-1}) determines the screening surface in m^2. At the interval 5 to 500 m^2, corresponds to a design flow of 150 and 15,000 m^3h^{-1}, an accuracy of 25% in cost estimation is obtained. The extrapolation line, see Appendix E, shows a small uncertainty in specific costs (~0.1 EURct.m^{-3}) at 100 m^3h^{-1}.

Coagulation

As explained in chapter 2.2.2, coagulation reduces the fouling rate at a MF. The design parameter is the water residence time (default = 20 min) in the flocculation tank. An accuracy of 25% in cost estimation is obtained at the tank volume between 240 and 3720 m^3. This corresponds with a design flow of 720 and 11160 m^3h^{-1}. The extrapolation line, see Appendix E, shows no uncertainty in the specific costs at 100 m^3h^{-1}. Together with the design flow a tank volume is calculated, which is the cost-determining parameter. Additional cost-determining parameters are the power consumption (default = 20 Wh.m^{-3}) and coagulant dosing (default = 20 gr.m^{-3}).

Micro-/Ultrafiltration (MF/UF)

In sewage water treatment MF/UF is used as pre-treatment in order to remove bacteria and suspended solids. The most important design parameter is the flux ($Lm^{-2}h^{-1}$) which is generally 60 $Lm^{-2}h^{-1}$ for feed waters with a high fouling potential. An accuracy of 25% in cost estimation is obtained for design flows between 100 and 3040 m^3h^{-1}. The cost tool does not discriminate between either MF and UF or cross-flow and dead-end. In the RINEW concept ceramic MF is applied instead of the conventional 'polymeric' material. Default settings for polymeric membranes are a life time of 5 years and membrane costs of 80 $EURm^{-2}$. Ceramic membrane are assumed to have a life time of 10 years. However, the membrane costs [$EURm^{-2}$] are considered uncertain, ranging from 80 to 500 $EURm^{-2}$. In order to discuss the membrane cost input for concept 1, the effect of membrane costs [$EURm^{-2}$] and –life time [year] are analysed on the specific treatment costs (EURct.m^{-3}), see Table 6-1.

Table 6-1. Sensitivity of membrane costs and -life time on treatment costs

		Q_{feed}					
		100 m^3h^{-1}			2500 m^3h^{-1}		
	$EURm^{-2}$	80	300	500	80	300	500
5 year	EURct.m^{-3}	40,6	46,8	52,4	15,5	21,7	27,4
10 year	EURct.m^{-3}	38,7	39,8	40,8	13,7	14,7	15,7

In Table 6-1 shows that a membrane life time of 10 years results in lower treatment costs [EURct.m^{-3}] compared to a membrane life time of 5 years. Both design flows result in similar conclusions. Based on the above analysis it is decided to change the default membrane cost setting in concept 1 to 300 EURm^{-2}. Besides the membrane costs [EURm^{-2}] cost-determining parameters in the MF/UF process are the pump pressure (set to 350 kPA) and chemical dosages (default: HCL = 100 gr.m^{-3}, antiscalant = 5 gr.m^{-3} and NaOH 10 gr.m^{-3}).

Softening

In decentralized treatment the influent composition can differ to a great extend depending on the connected household- and/or industrial activities. Besides biofouling is 'scaling' the difficult to control in a RO treatment step. Therefore a preceding softening step is applied to increase the RO efficiency. The design parameter is the flow velocity (default = 100 mh^{-1}). In the cost tool results an accuracy of 25% is achieved at a feed flow between 200 and 7200 m^3h^{-1}. The extrapolation line, see Appendix E, shows a relative small uncertainty (1 EURct.m^{-3}) in the specific costs at 100 m^3h^{-1}. Besides the flow velocity, cost-determining parameters are the pump pressure (default = 100 kPA) and chemical dosing (default: NaOH = 40 gr.m^{-3}).

Reverse Osmosis (RO)

The RO is used as final step the demi water reclamation from sewage. The RO produces demi water by removing ions to a great extent. The most important design parameter, just as MF, is the flux (default = 30 $Lm^{-2}h^{-1}$). An accuracy of 25% in cost estimation is achieved at a feed flow from 340 to 2800 m^3h^{-1}. The extrapolation line, see Appendix E, shows an uncertainty of approximately 3 EURct.m^{-3} in the specific treatment costs at 100 m^3h^{-1}. The important cost-determining parameters are the membrane costs (default = 15 EURm^{-2}), pump pressure (default = 1300 kPA), membrane life time (default = 5 years) and chemical dosing (default: H_2SO_4 = 36 gr.m^{-3}, HCl = 27 gr.m^{-3}, antiscalant = 5 gr.m^{-3}).

Clean water buffer and –pump

A clean water buffer is a storage for the produced high quality water. The buffer is able to deliver a varying flow to the industry, depending on the industrial demand during the day. Assumed is a buffer volume of 25% of the daily average flow. An accuracy of 25% in cost estimation is achieved at a buffer volume between 880 and 12000 m^3. The extrapolation line, see Appendix E, shows no uncertainty in the specific treatment costs at a design flow of 100 m^3h^{-1}.

Subsequently, water is pumped from the buffer into a transport pipe. For the clean water pump an accuracy of 25% is achieved at a flow input between 600 and 7700 m^3h^{-1}. The extrapolation line, see Appendix E, shows an uncertainty of ~1 EURct.m^{-3} for the clean water buffer and clean water pump respectively at a design flow of 100 m^3h^{-1}.

Transport line

In order to provide demi water to the industry a transport line is required. An accuracy of 30% in cost estimation is obtained at pipe diameters between 200 and 1600 mm. The most important design parameter is the maximum flow velocity of 1 $m.s^{-1}$. The cost calculation includes general construction aspects like pipe costs, digging and filling. However, additional aspect like the official land ownership, governmental fees and temporary facilities etc. are not included. Therefore, the transport cost are expected to be underestimated.

Besides the uncertainty in the transport costs, there are various important cost-determining parameters to adjust. These are the pipe diameter (mm), area type (rural or urban), pipe material (PVC, HDPE, steel, concrete, etc.) and number of parallel transport lines (No.). A

pipe line construction in urban areas is generally 1.4x more expensive compared to rural areas. In present concept study demi water is transported which can cause pipe leaching for improper pipe material. For demi water applications polypropylene (PP) is used which is not available in the cost tool. However, HDPE is similar in price and used for drinking water purposes and thus available in the cost tool (DeArmit, 2017). Regarding the number of parallel pipelines, usually a double pipeline is constructed. The demi water delivery is more reliable in case of pipe leakages or breakages. Additionally, for maintenance works the demi water delivery can continue due to the second pipe line.

In order to analyse the effect of pipe diameter, area type and number of transport lines on the specific costs ($EURm^{-3}km^{-1}$) the following graphs are constructed, see Figure 6-3. The lower limit for HDPE pipe diameter is 315 mm which corresponds to the smallest industrial demand shown in the graphs below. In both graphs extrapolation lines are drawn which are used to calculate the breakeven distance in which both concepts are equally expensive.

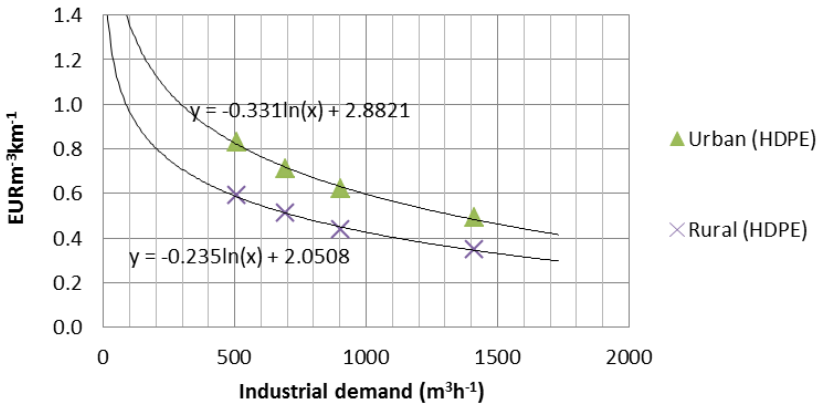

Figure 6-3. The transport costs per km for a double pipe line.

6.3 Results and discussion

As indicated before: concept 1 (decentralized system) includes all discussed process step except the transport line where concept 2 (centralized system) includes only the MF/UF and RO with the transport line. The MF/UF in concept 1 includes the more expensive ceramic membranes with a longer lifetime where the MF/UF in concept 2 includes the cheaper polymeric membranes with a shorter life-time. The specific treatment costs per concept are shown in Figure 6-4 for different industrial demands. These flows are assumed to represent design-flows for a decentralized sewage treatment plant.

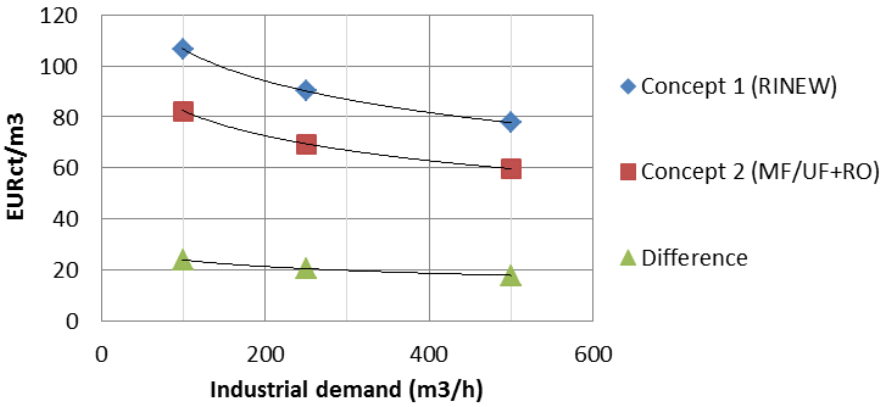

Figure 6-4. The specific cost and extrapolation lines per concept.

Figure 6-4 shows a higher treatment price for concept 1 compared to concept 2. The difference (~20 EURct.m^{-3}) is generally the additional process steps in concept 1 like the microscreen, coagulation and softener. Both extrapolation lines are nearly parallel to each other since the membrane technologies dominate the cost. In chapter 6.2.1 it is discussed that there is a limited price difference between ceramic and polymeric membranes. The higher membrane price for ceramics is cancelled out by the longer expected life time of ceramics. Both extrapolation lines are drawn back until 100 m^{3}h^{-1} which is considered the lower limit of the cost tool.

The cost difference between the two concepts in Figure 6-4 is used to calculate the breakeven distance. This is done for the transport line cost functions given in Figure 6-3. The lines shown in Figure 6-5 are the breakeven distances where both concepts are equally expensive. Above the line concept 1 is more feasible than concept 2 and below the lines concept 2 is more feasibly than concept 1.

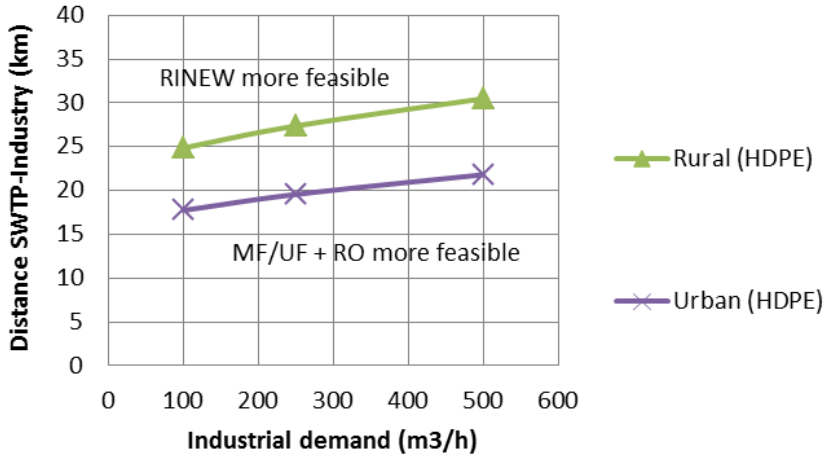

Figure 6-5. Resulting breakeven distance from the cost difference between the two concepts.

Figure 6-5 shows the breakeven distances at different industrial water demands regarding rural and urban environments. Concept 1 becomes less feasible at larger industrial demands since the water transport costs per m^3 are significantly higher at 100 m^{3}h^{-1} than at 500 m^{3}h^{-1}, see Figure 6-3. The breakeven distance in rural and urban areas is on average 27.5 and 20

km, respectively. Regarding an industrial demand of 100 m^3h^{-1} a population size of around 28.000 is expected, assuming a drinking water consumption of 130 $Lp^{-1}d^{-1}$ and a RINEW recovery rate of 66% (influent flow of 150 m^3h^{-1}). A rural area is a geographic area located outside towns and cities. Therefore it is highly unlikely to apply present cost analysis to rural areas. To get a sufficient treatment flow there will be always a rural area involved.

Potential financial feasibility in the Netherlands

In order to discuss how the resulting breakeven distances apply to the Netherlands Figure 6-6 is constructed. A part of the Netherlands is shown together with all existing SWTP's. A black circle is drawn with a radius of 20 km which represents the breakeven distance for urban areas, most expensive scenario. The SWTP density in the Netherlands is 118 km^2 per SWTP. Approaching the density as circles the average diameter becomes approximately 12 km which is significantly shorter than the estimated 20-27.5 km in present study. This suggests that water reclamation in a RINEW concept is not feasible, compared to centralized treatment, in the Netherlands.

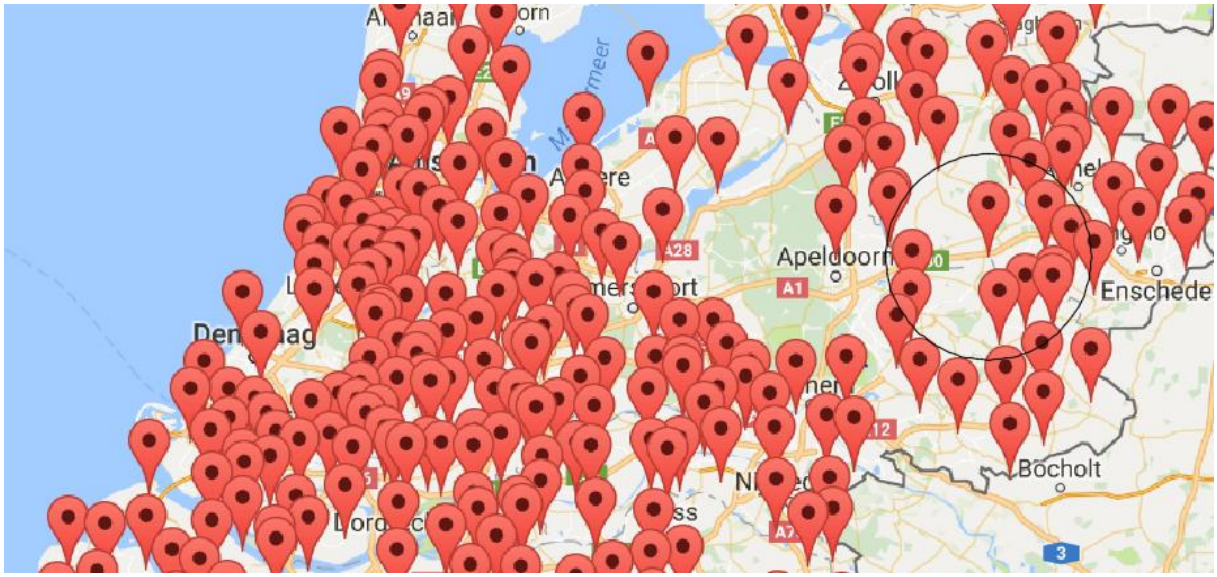

Figure 6-6. Potential financial feasibility of the RINEW concept in the Netherlands.

Since present research method excludes other water sources, existing facilities and areal limitations the results are considered hypothetical. In order to discuss the general feasibility of the RINEW project two realized projects are described. Information is gathered on the World Wide Web, and by semi structured interviews by phone and email conversations with senior engineers from Evides and WLN.

Demiwater Plant (DWP)

From the seventies Evides produced distilled water at the Botlek location to the Rotterdam harbour, from refinery no.2 towards the east, see Figure 6-7. Upgrading its product quality Evides started to produce demi water (1400 m^3h^{-1}) from the start of 2010. At the Botlek two water sources are used: surface water from the Brielse meer and drinking water from the drinking water production plant 'The Beerenplaat' near Spijkernisse. Then, the construction of the industrial harbour area '2e Maasvlakte', west side of refinery no.1, finished in 2013. Evides performed a scenario study in 2014 and concluded that the demi water demand

would increase in the future. Also the Botlek demi water production capacity got to its maximum.

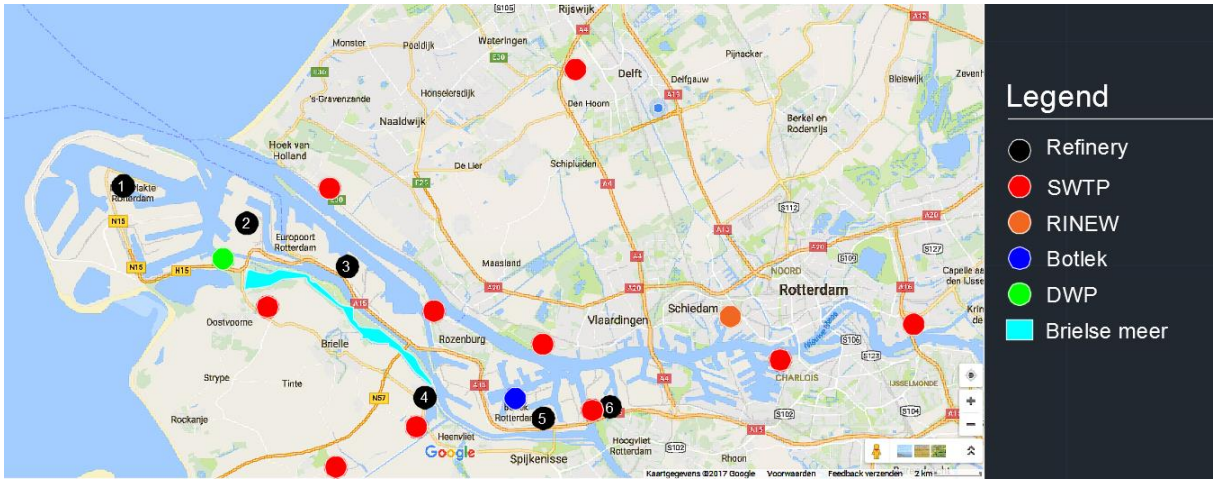

Figure 6-7. Potential financial feasibility discussion regarding the Demi water plant

At the Botlek site the lack of space forced Evides to find a different production location. The following water sources were considered: SWTP effluent, surface water (Brielse meer) and drinking water. Taking into account an increasing demi water demand, the DWP design capacity is pushed to ~800 m^3h^{-1} since larger treatment plants result in lower treatment costs. This is also observed in Figure 6-4 where the specific RINEW treatment costs are estimated for different demi water demands. Due to the existing water transport lines from the Botlek to the Maasvlakte the new production location should be somewhere at the south side of the canal. Evides B.V. already has the expertise in demi water production (from surface- and drinking water) and the nearby SWTP's only treat low flows (Dry weather flows between 150 to 500 m^3h^{-1}). Therefore the DemiWaterPlant (DWP) is realized at the Maasvlakte, see Figure 6-7. The intake water is, just like the Botlek plant, Brielse meer- and drinking water.

The above described project development shows that besides the water transport costs, the water source and existing facilities are important factors in the decision making. This is probably because the Maasvlakte is constructed in multiple stages over the years.

Puurwaterfabriek (Pure water factory)

At Schoonebeekerveld, see purple dot in Figure 6-8, petroleum is mined since 1947. Due to the high viscosity of the petroleum the mining stopped in 1996. However, by steam infiltration petroleum mining became feasible again. For steam ultrapure water is recommended which limits scaling problems in the corresponding systems.

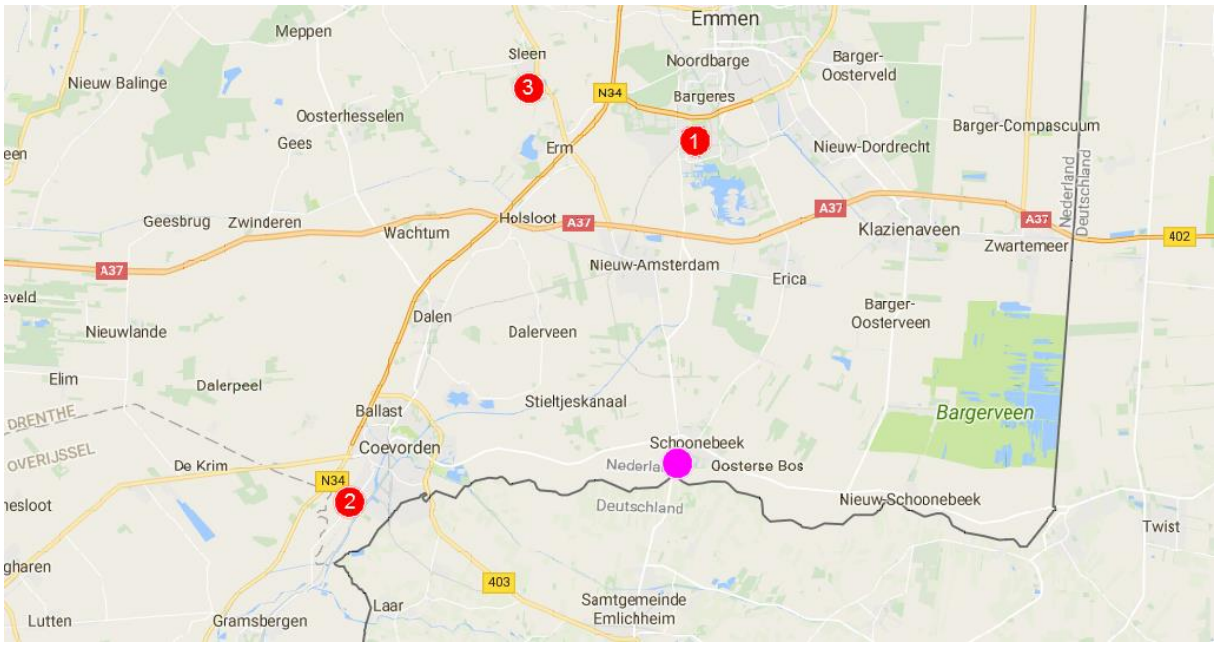

Figure 6-8. Potential financial feasibility discussion regarding the Ultra-pure water factory

The available water sources for the production of ultra-pure water include ground-, surface- and SWTP effluent. However, in the province Drenthe groundwater is destined for drinking water production and there is a lack of surface water. In the area multiple SWTP's are located from which SWTP Emmen, see red dot no.1 in Figure 6-8, has the most water available. Therefore, in 2010 the Pure water factory opened at the SWTP Emmen. The effluent is treated till ultra-pure water with use of subsequent microcreens, UF, biological activated carbon, RO and electro deionisation at a rate of approximately 400 m^3h^{-1}. Over a distance of approximately 8 kilometers the ultra-pure water is transported towards the petroleum mining location near Schoonebeek.

The area between Emmen and Schoonebeek is considered as rural. Looking at Figure 6-5 at a transport distance of 8 km, 400 m^3h^{-1} in rural environments decentralized (RINEW concept) will not be feasible. The village 'Schoonebeek' includes approximately 5000 capita. Assuming a daily water consumption of 130 liters per person a sewage flow of 650 is expected. Thus a sufficient sewage flow will be available for decentralized treatment. However, since the SWTP Emmen is too close the RINEW not financially feasible.

Chapter 7

Conclusions and recommendations

7.1 Irreversible fouling indicator

1. *Which common online water quality parameter can be used as irreversible fouling rate indicator for the cMF in sewage water treatment?*

Conclusions
The pilot influent originates from a small area including mainly offices, a few automobile service stations and a large steam laundry. Due to the small area high concentration peaks were expected and observed in the monitoring results. The irregularity and magnitude of the concentration peaks points out to a significant influence of industrial activities. The high average influent Conductivity may originate from the steam laundry using colourless salts with properties as surfactants. The average influent COD concentration is low compared to ordinary sewage. This indicates a significant industrial influence and/or a circulation of clean water over the pumping station or influent buffer.

In order to answer the research question sewage water is treated by a coagulant dosing, Belt Sieve and ceramic Microfiltration (cMF) over a period of 2 months. Over the period the operational parameters (like TMP, temp, Q_p, Q_c, Q_f) are digitally monitored. Simultaneously, cMF feed water quality is digitally monitored and characterized by COD (mgL^{-1}), Turbidity (NTU) and Conductivity ($mS.cm^{-1}$).

The quality monitoring results ($mgCODL^{-1}$, NTU and $mS.cm^{-1}$) are correlated with the membrane resistance (m^{-1}) of the cMF. The parameter 'COD' correlates the best with the membrane resistance. COD is considered the most suitable as fouling indicator due to the relative large particle size and sticky properties of biopolymers. Turbidity and Conductivity barely correlate with the membrane resistance since turbidity forms a loosely layer on the membrane surface which is hydraulically removed. Conductivity is a measurement for the traveling ions in water which readily penetrate through a MF membrane.

At CEB interval, each two hours, the irreversible fouling rate is determined which is the increase in membrane resistance per hour ($m^{-1}h^{-1}$). When plotted against the corresponding COD concentration an increasing trend is observed in higher fouling rates ($m^{-1}h^{-1}$) at higher COD concentrations. Above the COD concentration of approximately 250 mgL^{-1} fouling rates above 20.10^8 $m^{-1}h^{-1}$ occur causing significant unstable cMF operation.

Recommendation
Present research indicates a potential in feed water quality monitoring for operation optimization of a MF. However, several encountered challenges limited proper cMF operation and sensor calibration:

- Regarding cMF operation, the stability in flux operation is low which is mostly influenced by the feed pump (designed for the cNF application). It is recommended to use a feed pump able to accurately operate a MF installation. Additionally, the Cleaning In Place programme, designed for the cNF, ineffectively restored the cMF membrane resistance. In the RINEW context a manual caustic backwashe (pH of 12) was found to effectively restore the membrane resistance.
- The lack in expertise limited proper sensor calibration. Due to the varying influent composition the measured BOD concentration could drop to zero which very unlikely in sewage water applications. To investigate the abnormal BOD behaviour the fingerprints needed to be saved. A Spectro::lyser fingerprint is a single measurement presenting a graph in which the absorbed radiance is plotted against the wave length (200 - 800 nm). However, in present research the fingerprints were not saved as the importance of the fingerprints was unknown. For future research it is recommended to maintain a close relation with the sensor supplier for optimal sensor performance. Ask In any case, the significant variety in influent composition is a major challenge since optimal sensor calibration is obtained with a stable water quality.

In order to test the potential of digital water quality monitoring in MF operation/optimization it is recommended to perform a similar study at a central treatment plant. With a proper MF system design and low variety in feed water composition better correlation results are expected.

7.2 Effect of oxygen on RO (bio)fouling development

Research question
2. *What is the effect of oxygen in cMF permeate on the biofouling potential at a RO membrane?*

Conclusions
In the RINEW context, the effect of oxygen in cMF permeate is studied on the (bio)fouling development on spiral wound Reverse Osmosis (RO). The study is done in duplicate using two parallel Membrane Fouling Simulator's (MFSs) which are fed by cMF permeate. The cMF permeate is highly aerated due to several operational conditions in the RINEW pilot. In one MFS setup the feed water is depleted from oxygen by adding Sodium Bisulfite ($NaHSO_3$).

The aerobic MFS indicated a faster development of biofouling in the form of filamentous growth attached in the low shear areas. Additionally, in the aerobic MFS a heavy inorganic fouling is observed, possibly, in the form of brown/red iron oxides and calcium precipitates. Therefore, the pressure drop results show significant unstable fouling rates in the aerobic MFS's compared to MFS's where the oxygen is depleted. Parallel to the aerobic fouling rate a significant lower fouling rate was observed at the oxygen depleted MFS's. However, the variety in sewage composition over time inhibited a controlled biofouling development.

Therefore no decisive conclusion can be made based on the difference in synthesis yield between aerobic and aerobic bacteria.

The obtained fouling rates in the MFS's, fed by oxygen depleted water, compare to fouling rate results from a MFS fed by anaerobic cNF permeate and Dutch tap water. It can be concluded that the cMF permeate treatment with NaHSO3 causes a significant more stable MFS fouling rate. This indicates the potential for a stable RO operation in sewage treatment with preceding $NaHSO_3$ treatment.

Recommendation
In order to study the effect of oxygen on biofouling in more detail, lab experiments are required. At first, tap water will be used as experimental feed water. The experiment can be performed manually or automated. If manually, the experiment is performed as described in chapter 5.3. If automated, flow controlling valves feed two parallel buffer tanks from nearby drinking water taps. In one buffer tank a continuous $NaHSO_3$ dosing is applied in order to deplete the oxygen concentration. Each buffer tanks feeds a single MFS setup. In the automated performed experiment a once flow-through system is applied which predominantly limits any unwanted additional bio growth (e.g. in the buffer tank).

In a second lab experiment the manual experiment, as described in chapter 5.3, can be performed with artificial sewage. The artificial sewage includes substrate- (including organic matter) and nutrient concentration representing MF/UF permeate levels.

At last, the experiment can be performed in practice to study the economic feasibility of making RO feed water anaerobically. The automated experiment, as described above, is recommended to perform at a central SWTP where a MF is installed to purify the secondary effluent. At a central SWTP the variation in influent composition will be limited enabling proper biofouling experiments.

7.3 Potential financial feasibility of the RINEW concept

Research question
3. What is the potential financial feasibility of demi water reclamation from sewage at decentralized scale (RINEW concept) in the Netherlands?

Conclusions
The potential financial feasibility of decentralized water reclamation (concept 1 'RINEW') is studied in the Netherlands. Concept 1 is compared to water reclamation at central SWTP from secondary effluent (concept 2), tertiary treatment. In concept 2 the produced water is transported over a significant longer distance towards the customer. For both concepts the investment- operational- and specific treatment costs are estimated with the online cost estimate application 'the RHDHV Kostenstandaard'.

Depending on the specific water transport price ($EURm^{-3}km^{-1}$) in concept 2 a certain distance (breakeven distance) is calculated where both concepts are equal in specific price ($EURm^{-3}$). Depending on the production flow and environment (rural or urban), indicative breakeven distances between 18 km and 30 km are presented. Production flows between 100 and 500 m^3h^{-1} result in a breakeven distance of approximately 20 km in urban area. Thus, for

distances shorter than the distance of 20 km it is financial more feasible to produce high quality water at a central SWTP from secondary effluent (concept 2). The density of SWTP's in the Netherlands is approximately one SWTP per 118 km^2. This compares to a square of 11 by 11 km or circle with a range of 12.4 km. Both being significantly lower than the calculated breakeven distance of 20 km. This suggests that the RINEW concept, as sewer mining concept, will not be financial feasible in the Netherlands.

To further discuss the potential feasibility of the RINEW concept in the Netherlands the development of two comparable and realized treatment plants are described. In the first case a treatment plant (800 m^3h^{-1}) is constructed at the Maasvlakte producing demi water from surface- and drinking water. This case indicates that besides the transport distance the water source, existing facilities (e.g. underground infrastructure) and available space were more important in the decision making. In the second case ultra-pure water is produced (400 m^3h^{-1}) from SWTP effluent and transported (~8 km) towards an industry. The case description showed that at least one SWTP's, in a range of 20 km from the industry, is able to provide a sufficient effluent flow for water reclamation.

Bibliography

Afvalwater: Wat is dat? (2017). Retrieved from http://saniwijzer.nl/content/content.asp?menu=1000_000010

Al-Malack, M.H., Anderson, G.K. (1999). Coagulation-crossflow microfiltration of domestic wastewater. *Journal of Membrane Science, 121*, 59-70.

Asha, M.N., Chandan, K.S., Harish, H. P., NikhileswarReddy, S., Sharath, K. S. and Mini Liza, G. (2016). Recycling Of Waste Water Collected From Automobile Service Station. *Procedia Environmental Sciences, 35*, 289–297.

Beyer, F., Rietman, B.M., Zwijnenburg, A., van den Brink, P., Vrouwenvelder, J.S., Jarzembowska, M., Laurinonyte, J., Stams, A.J.M., Plugge C.M. (2014). Long-term performance and fouling analysis of full-scale direct nanofiltration (NF) installations treating anoxic groundwater. *Journal of Membrane Science, 468*, 339-348.

Carrol, T., King, S., Gray S.R., Bolto, B.A., Booker, N.A. (1999). The fouling of a microfiltration membranes by NOM after coagulation treatment. *Water Research, 34*(11), 2861-2000.

De Paula Santos, F., de Campos, E., Costa, M., Melo, F.C.L., Honda, R.Y., Mota, R.P. (2003). Superficial Modifications in TiO_2 and Al_2O_3 Ceramics. Materials Research, 6(3), 353-367.

DeArmitt, C. (2017, April). Plastics & composites Performance: Cost. Retrieved from http://phantomplastics.com/wp-content/uploads/2013/08/High-Performance-Fillers-2005-BASF.pdf

Envirochemie. (2006). Ideal treatment of laundry wastewater with ultrafiltration installations. WRP, 07-08.

Fane, A.G., Fane, S.A. (2005). The role of membrane technology in sustainable decentralized water systems. *Water Science & Technology, 51*(10), 317-325.

Farhat, N.M., Vrouwenvelder, J.S., Van Loosdrecht, M.C.M., Bucs, Sz.S., Staal, M. (2016). Effect of water temperature on biofouling development in reverse osmosis membrane systems. *Water Research, 103*, 149-159.

Flemming, H. (1997). Reverse Osmosis Membrane Biofouling. *Experimental Thermal and Fluid Science, 14*, 382-391.

Gan, Q., Allen, S.J. (1999). Crossflow microfiltration of a primary sewage effluent–solids retention efficiency and flux enhancement. *Journal of Chemical Technology and Biotechnology, 74*, 693-699.

Gaulinger, S. Heijman, B. (2007). TECHNEAU: Coagulation Pre-Treatment for Microfiltration with Ceramic Membranes. Retrieved from https://www.techneau.org/index.php?id=122

Ghayeni, S.B.S., Beatson, P.J., Schneider, R.P., Fane, A.G. (1998). Water reclamation from municipal wastewater using combined microfiltration-reverse osmosis (ME-RO):

Preliminary performance data and microbiological aspects of system operation. *Desalintation, 116*, 65-80.

Hagemann, S., Chen, C., Clark, D.B., Folwell, S., Gosling, S.N., Haddeland, I., Hanasaki, N., Heinke, J., Ludwig, F., Voss, F., Wiltshire, A.J. (2013). Climate change impact on available water resources obtained using multiple global climate and hydrology models. Earth System Dynamics, 4, 129-144.

Hiemstra, P., van Paasen, J., Rietman, B., Verdouw, Jil. (1999). Aerobic versus anaerobic nanofiltration: Fouling of membranes. Proceedings AWWA Membrane Technology Conference, Long Beach Californië.

Huajuan, M. (2009). A Study on Organic Fouling of Reverse Osmosis Membrane (PhD thesis), National Universtity of Singapore, Singapore.

Janse, B.J. (2016). Operational applicability of ceramic nano- and microfiltration for municipal wastewater reuse (Thesis). HZ University of Applied Sciences.

Joseph, K., Natarajan, K. (1997). Studies on wastewater automobile service station. *Indian Journal of Environmental Health, 39*(1), 37-43.

Jung, C., Son, H., Kang, L. (2006). Effects of membrane material and pretreatment coagulation on membrane fouling: fouling mechanism and NOM removal. *Desalination, 197*, 154-164.

Kennedy, M.D., Munoz Tobar, F.P., Amy, G., Schippers, J.C. (2009). Transparent exopolymer particle (TEP) fouling of ultrafiltration membrane systems. *Desalination and Water Treatment, 6*, 169-176.

Kramer, F.C., Shang, S.G.J., Scherrenberg, S.M., van Lier, J.B., Rietveld, L.C. (2015). Direct water reclamation from sewage using ceramic tight ultra- and nanofiltration. *Separation and Purification Technology, 147*, 329-336.

Lateef, S.K., Soh, B.Z., Kimura, K. (2013). Direct membrane filtration of municipal wastewater with chemically enhanced backwash for recovery of organic matter. *Bioresource Technology, 150*, 149-155.

Liu, C., Caothien, S., Hayes, J., Caothuy, T., Otoyo, T., Ogawa, T. (2001). Membrane Chemical Cleaning: From Art to Science. in: Proceedings of 2001 Membrane Technology Conference, American Water Works Association, AWWA.

Metcalf & Eddy, Inc. (2014). Wastewater engineering: treatment and reuse. Boston :McGraw-Hill,

Mittelman, M.W. (1991). Bacterial Growth and Biofouling Control in Purified Water Systems. *Biofouling and biocorrosion in Industrial Water Systems*, 133-154.

Mo, W., Zhang, Q. (2013). Energy-nutrients-water nexus: Integrated resource recovery in municipal wastewater treatment plants. Journal of Environmental Management, 127, 255-267.

Mulder, M. (1996). Basic Principles of Membrane Technology – Second Edition. Dordrecht, The Netherlands.

Ntiako, J. (2014). Pilot Scale Testing of Salsnes Filter (SF500) for Biofilm Solids Removal from a Full Scale Wastewater Treatment Plant (master's thesis). University of Stavanger, Stavanger, Norway.

Rachman, R., Dehwah, A.H.A., Li, S., Winters, H., Al-Mashharawi, S., Missimer, T.M. (2015). Effects of Well Intake Systems on Removal of Algae, Bacteria, and Natural Organic Matter. *Environmental Science and Engineering*, 163-193.

Ravazzini, A.M. (2008). Crossflow Ultrafiltration of Raw Municipal Wastewater. Technical University Delft, Delft, The Netherlands.

Reijken, C. (2014). STOWA 2014-W01 report: Praktijkresultaten Influent Fijnzeef RWZI Blaricum. Retrieved from http://www.stowa.nl/publicaties/publicaties/

Schilperoort, R.P.S. (2011). Monitoring as a tool for the assessment of wastewater quality dynamics (PhD thesis). Tehcnical Universitiy Delft, Delft, The Netherlands.

Shang, R., Vuong, F., Hu, J., Li, S., Kemperman, A.J.B., Nijmeijer, K., Cornelissen, E.R.C., Heijman, S.G.J., Rietveld, L.C. (2015). Hydraulically irreversible fouling on ceramic MF/UF membranes: Comparison of fouling indices, foulant composition and irreversible pore narrowing. *Separation and Purification Technology, 147*, 313-310.

Turbidity and Total Suspended Solids Measurement Methods. (2017). Retrieved from: http://www.fondriest.com/environmental-measurements/equipment/measuring-water-quality/turbidity-sensors-meters-and-methods/#TurbidMM1

Van Paassen, J.A.M., Kruithof, J.C., Bakker, B.M., Kegel, F.S. (1998). Integrated multi-objective membrane systems for surface water treatment: pre-treatment of nanofiltration by riverbank filtration and conventional ground water treatment. *Desalination, 118*, 239-248

Vrouwenvelder, J.S. (2009). Biofouling in spiral wound membrane systems (PhD thesis). Delft University of Tehcnology, Delft, The Netherlands.

Xiao, K., Shen, Y., Liang, S., Liang, P., Want, X., Huang, X. (2014). A systematic analysis of fouling evolution and irreversibility behaviors of MBR supernatant hydrophilic/hydrophobic fractions during microfiltration. *Journal of Membrane Science, 467*, 206-216.

Yamamura, H., Okimoto, K., Kimura, K., Watanabe, Y. (2014). Hydrophilic fraction of natural organic matter causing irreversible fouling of microfiltration and ultrafiltration membranes. Water Research, 54, 123-136.

Zhang, X., Catriona, Devanadera, M.C.E., Roddick, F.A., Fan, L., Dalida, M.L.P. (2016). Impact of algal organic matter released from Microcystis aeruginosa and Chlorella sp. on the fouling of a ceramic microfiltration membrane. *Water Research, 103*, 139-400.

Zhou, Z., He, X., Zhou, M., and Meng, F. (2017). Chemically induced alterations in the characteristics of fouling-causing bio-macromolecules - Implications for the chemical cleaning of fouled membranes. *Water Research, 108,* 115-123.

Van der Marel, P. (2009). Influence of membrane properties on fouling in MBRs (PhD Thesis). University of Twente, Enschede, The Netherlands.

Abstract

RINEW	Rotterdam Innovative Nutrients and Energy Watermanagement
EUR	Euro
SWTP	Sewage Treatment Plant
MF	Microfiltration
cMF	Ceramic Microfiltration
UF	Ultrafiltration
NF	Nanofiltration
cNF	Ceramic Nanofiltration
RO	Reverse Osmosis
TMP	Trans Membrane Pressure
BW	Backwash
CEB	Chemical Enhanced Backwash
CIP	Cleaning In Place
Q	Flow [m^3h^{-1}]
J	Flux [$Lm^{-2}h^{-1}$]
R	Membrane resistance [m^{-1}]
BOD	Biochemical Oxygen Demand
COD	Chemical Oxygen Demand
ATP	Adenosinetriphosphate
TSS	Total Suspended Solids
TDS	Total Dissolved Solids
NTU	Turbidity
EC	Electrical Conducitivy
sEMC	Surrogate Event Mean Concentration

Appendix A Time series

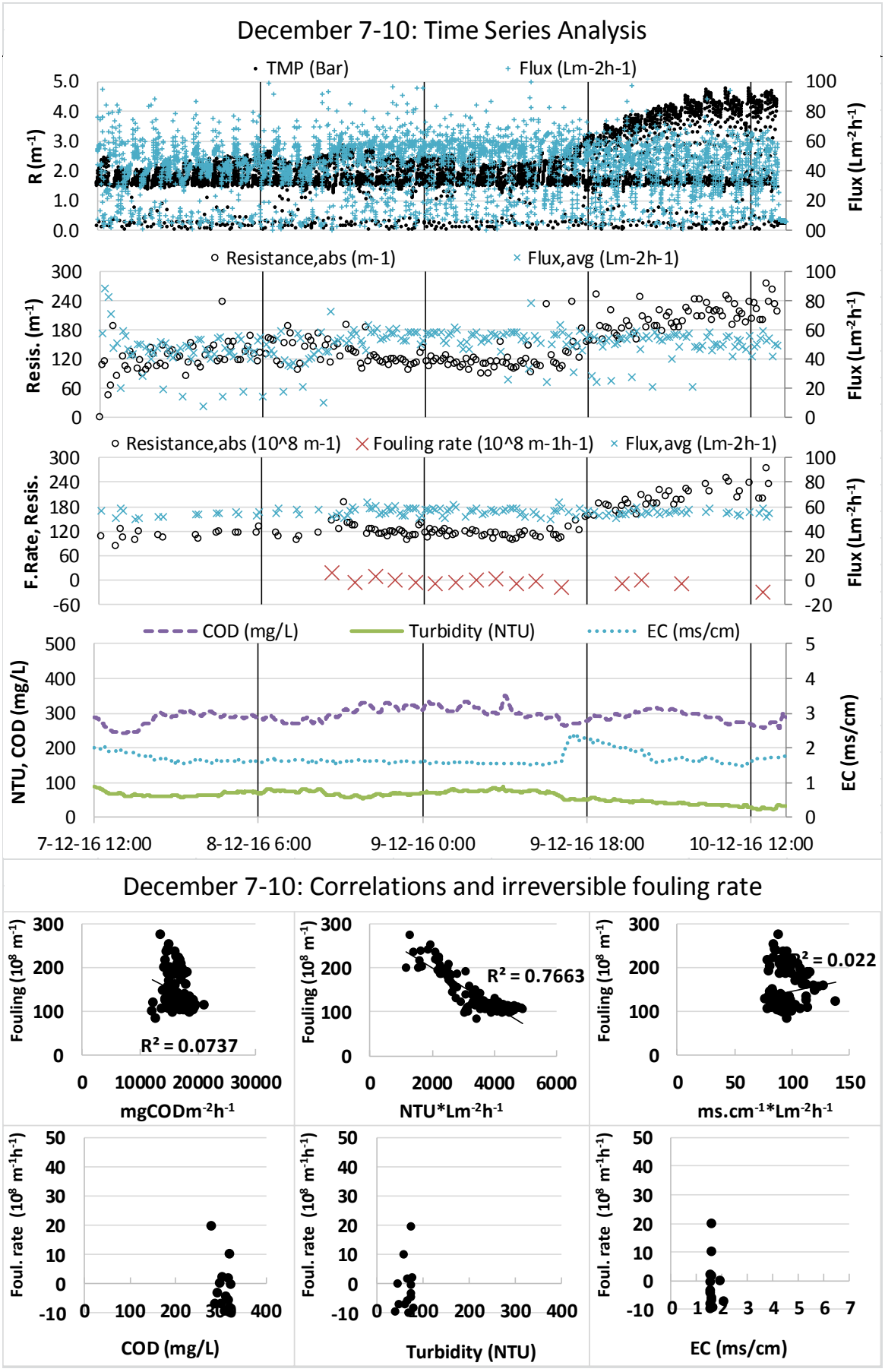

Appendix 7-1. Time series Dec 7-10

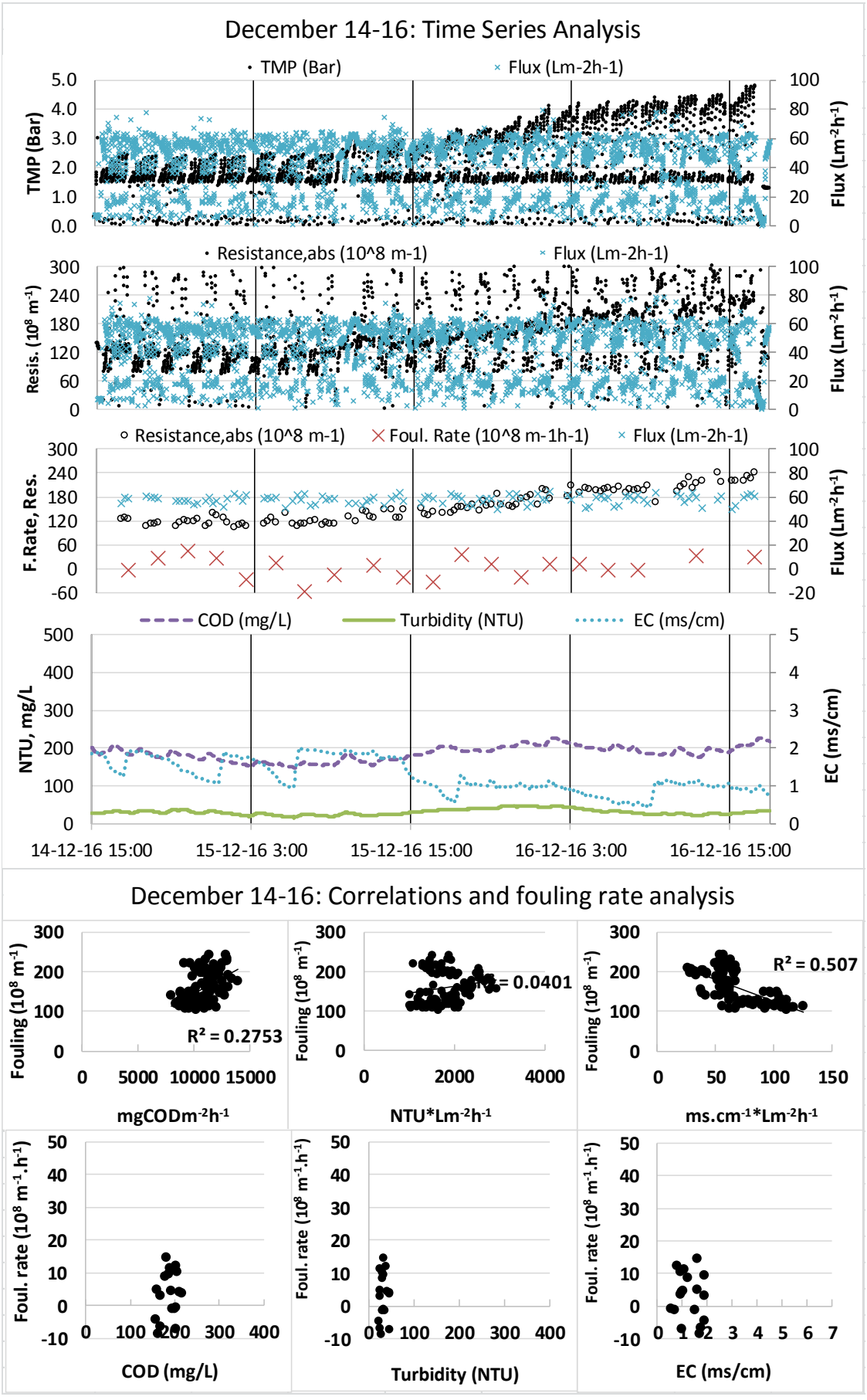

Appendix 7-2. Time series Dec 14-16

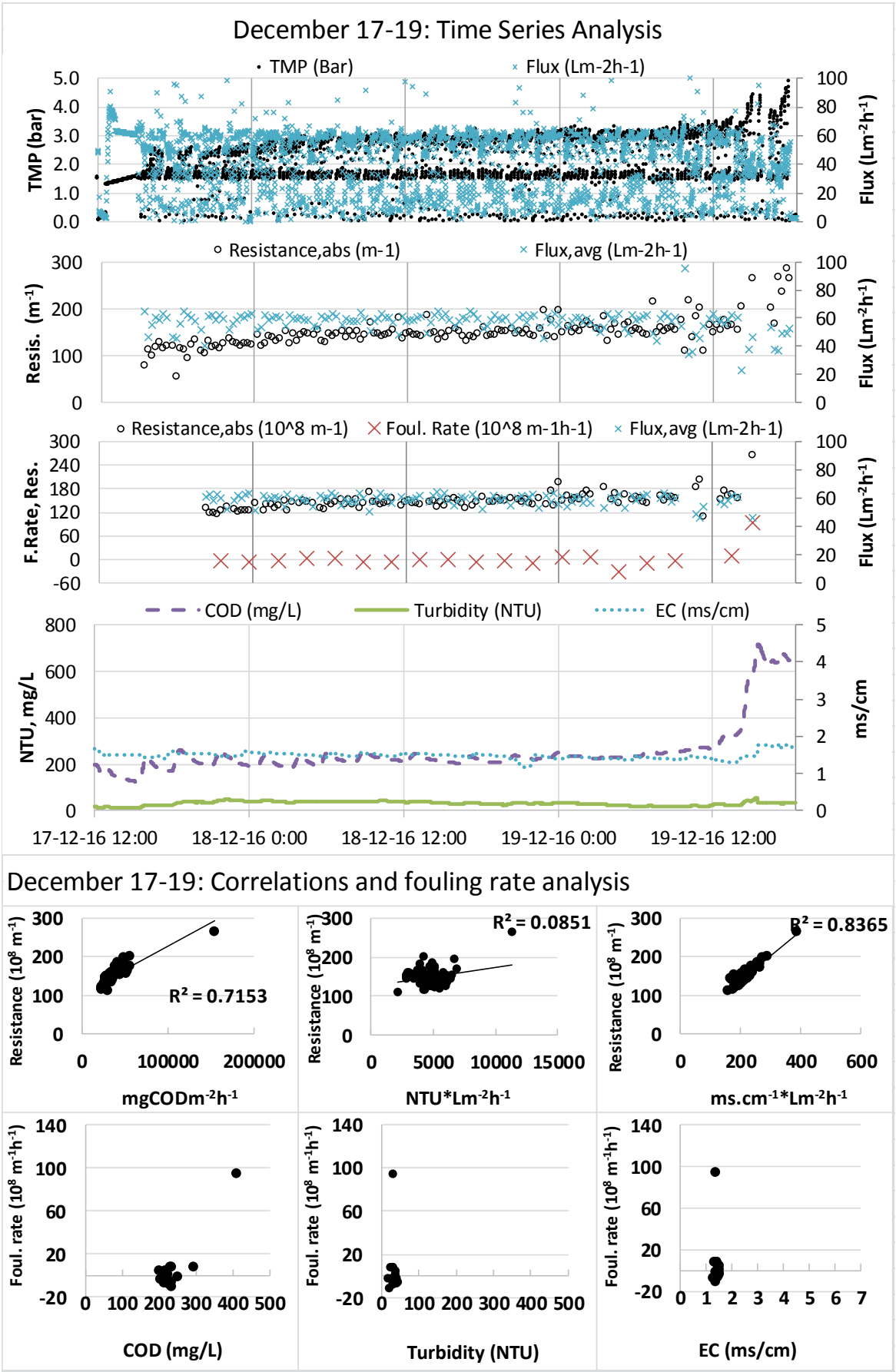

Appendix 7-3. Time series Dec 17-19

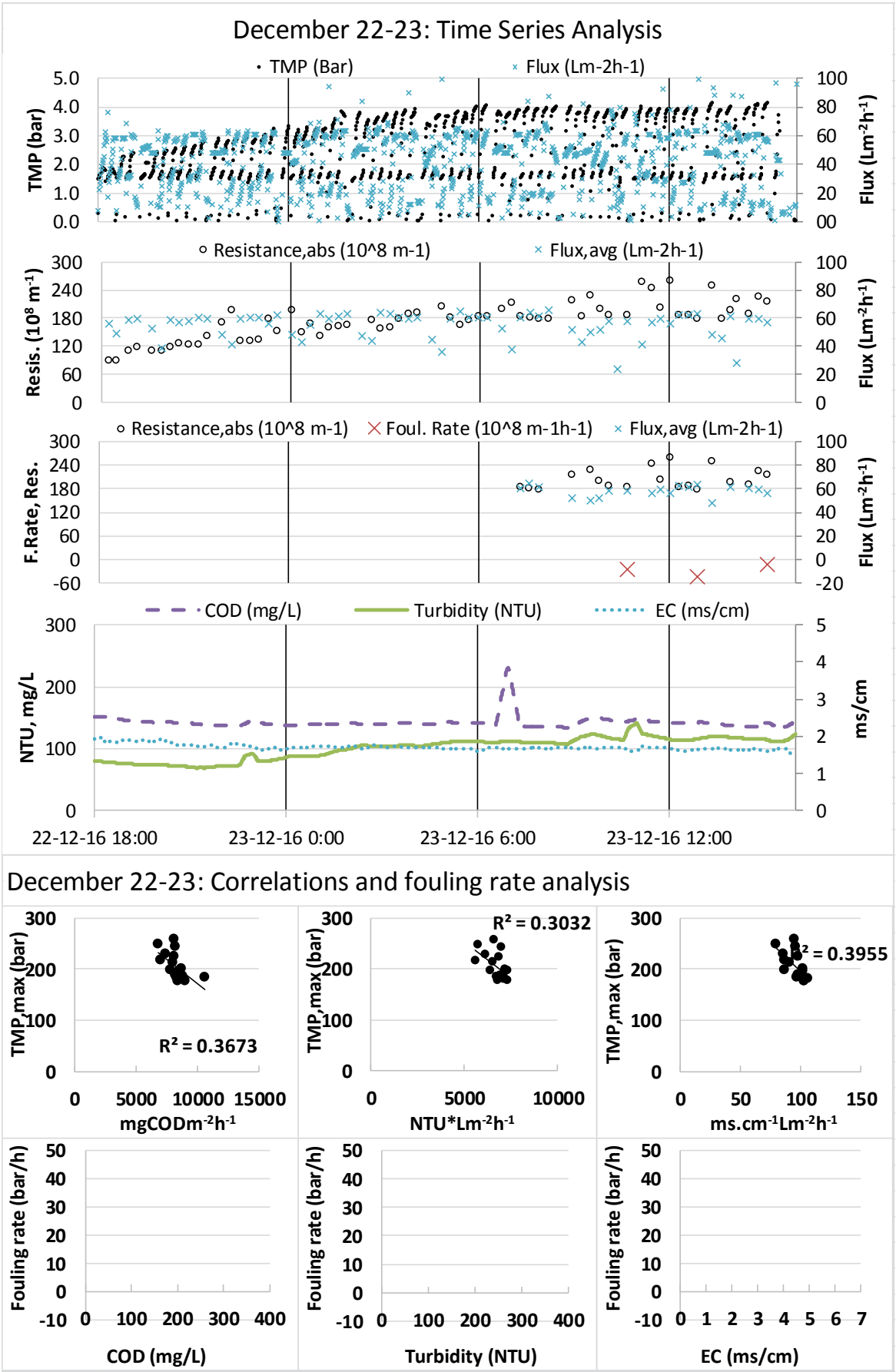

Appendix 7-4. Time series Dec 22-23

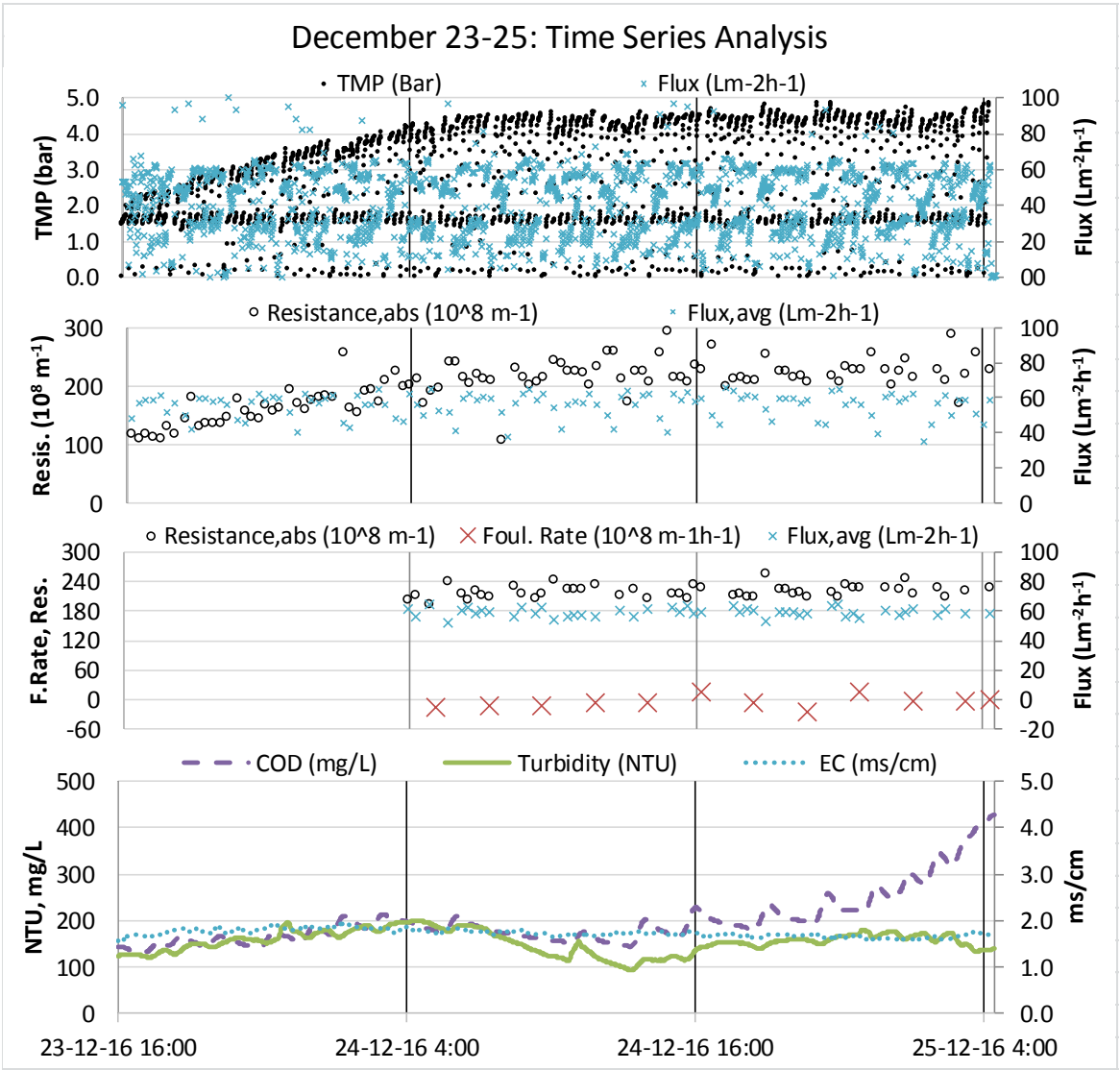

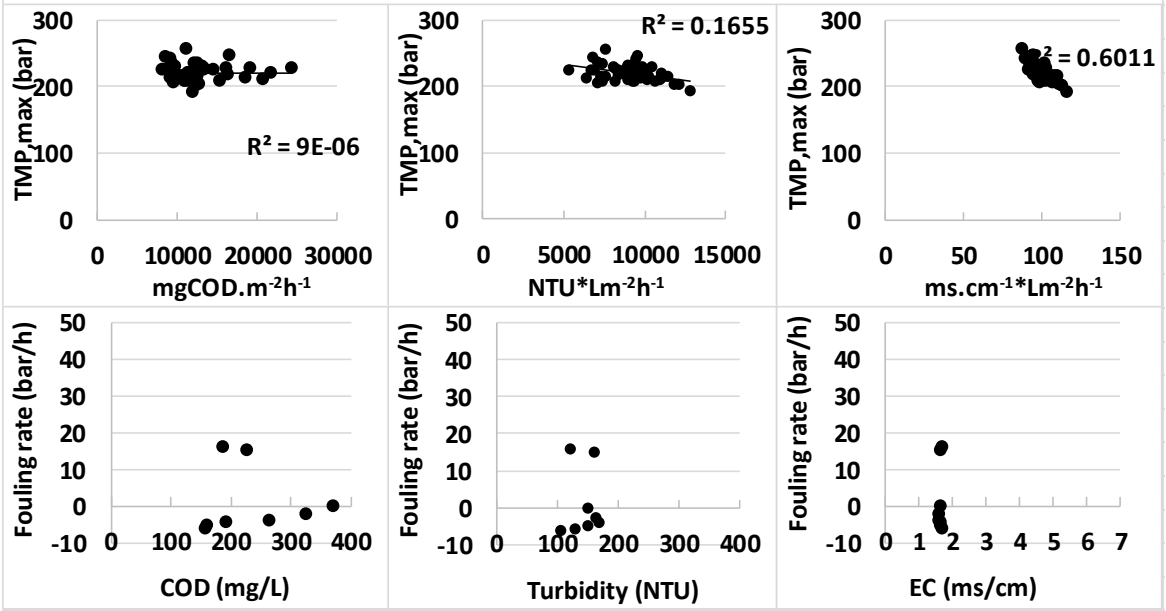

Appendix 7-5. Time series Dec 23-25

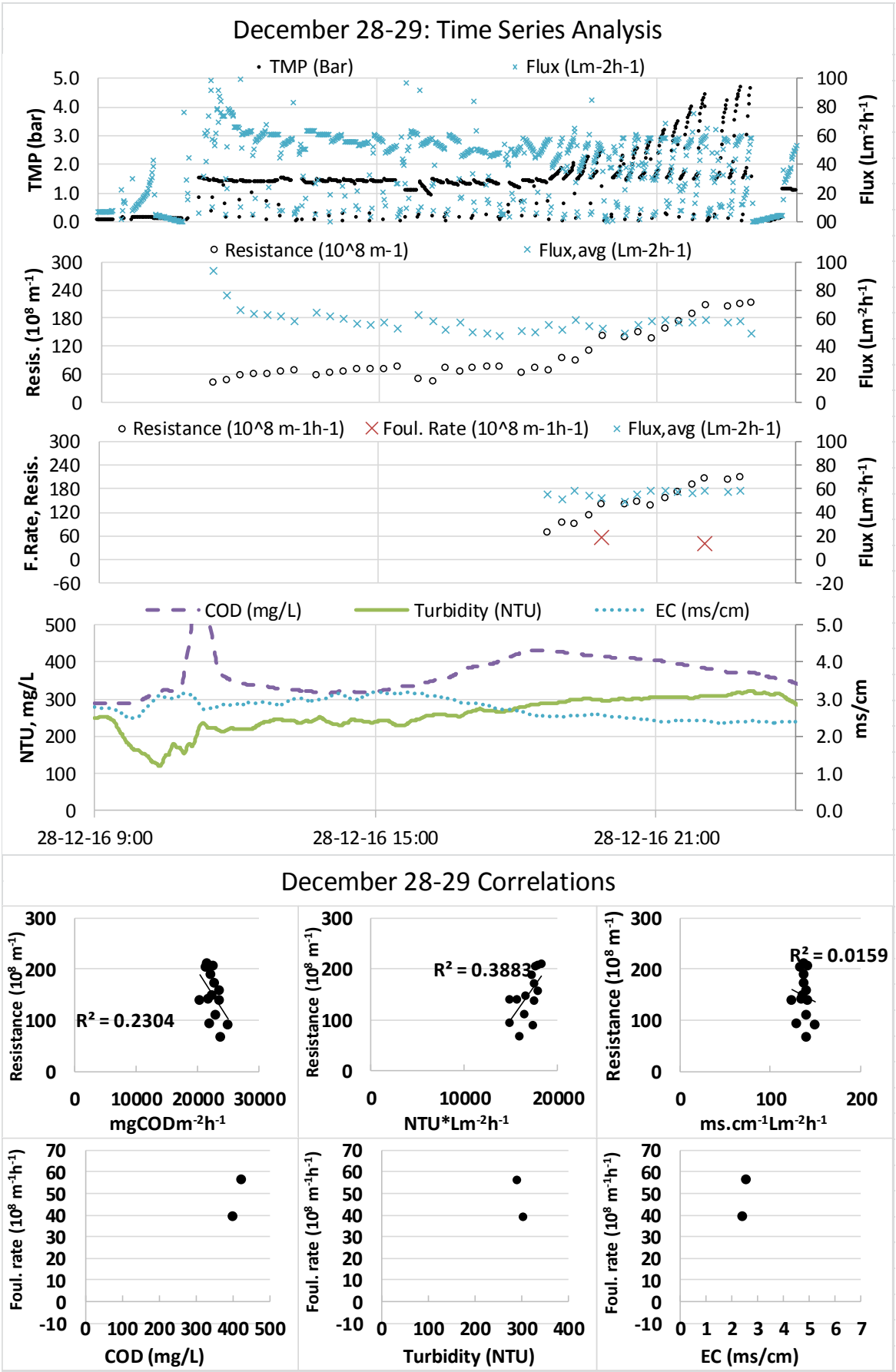

Appendix 7-6. Time series Dec 28-29

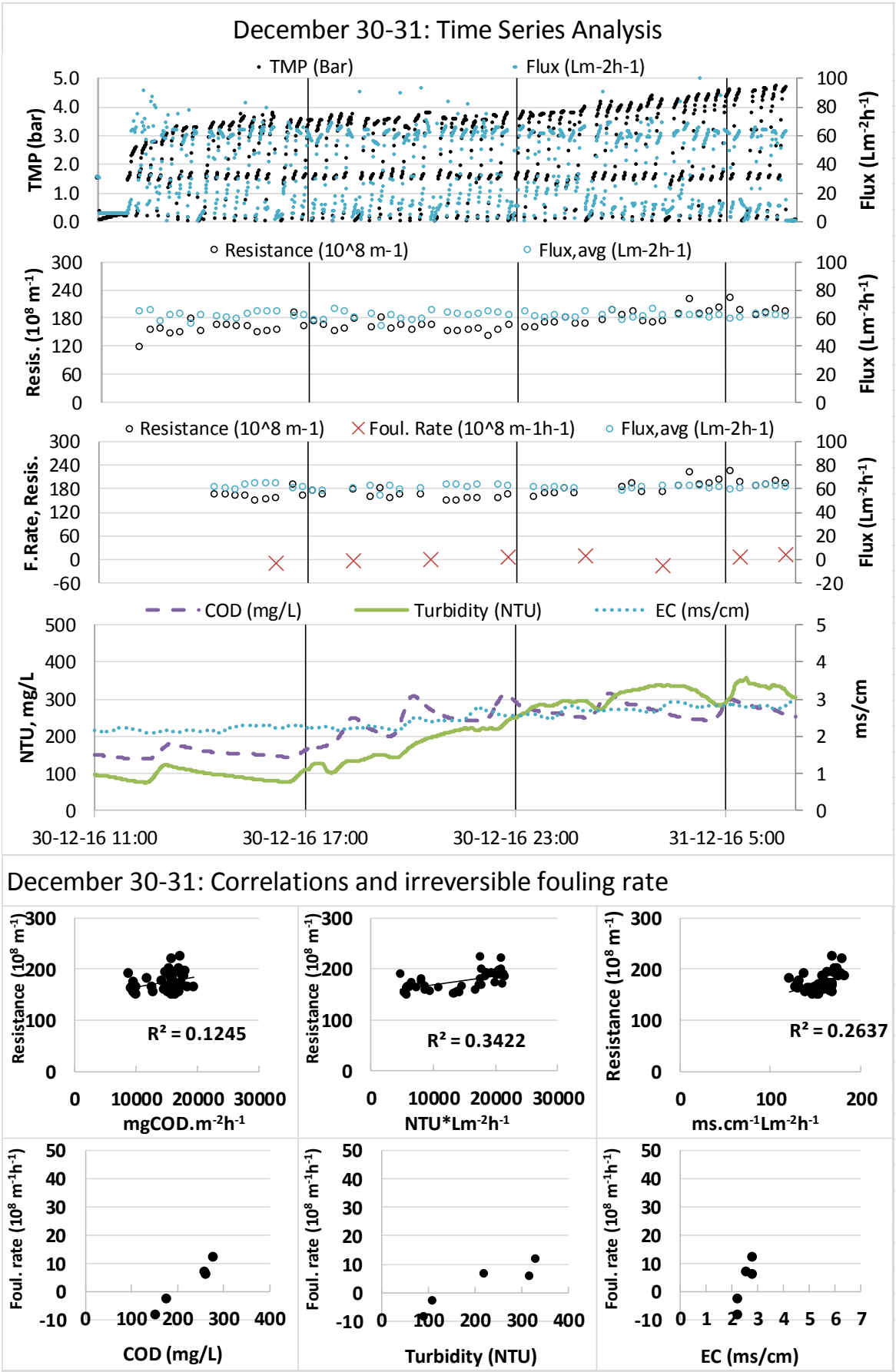

Appendix 7-7. Time series Dec 30-31

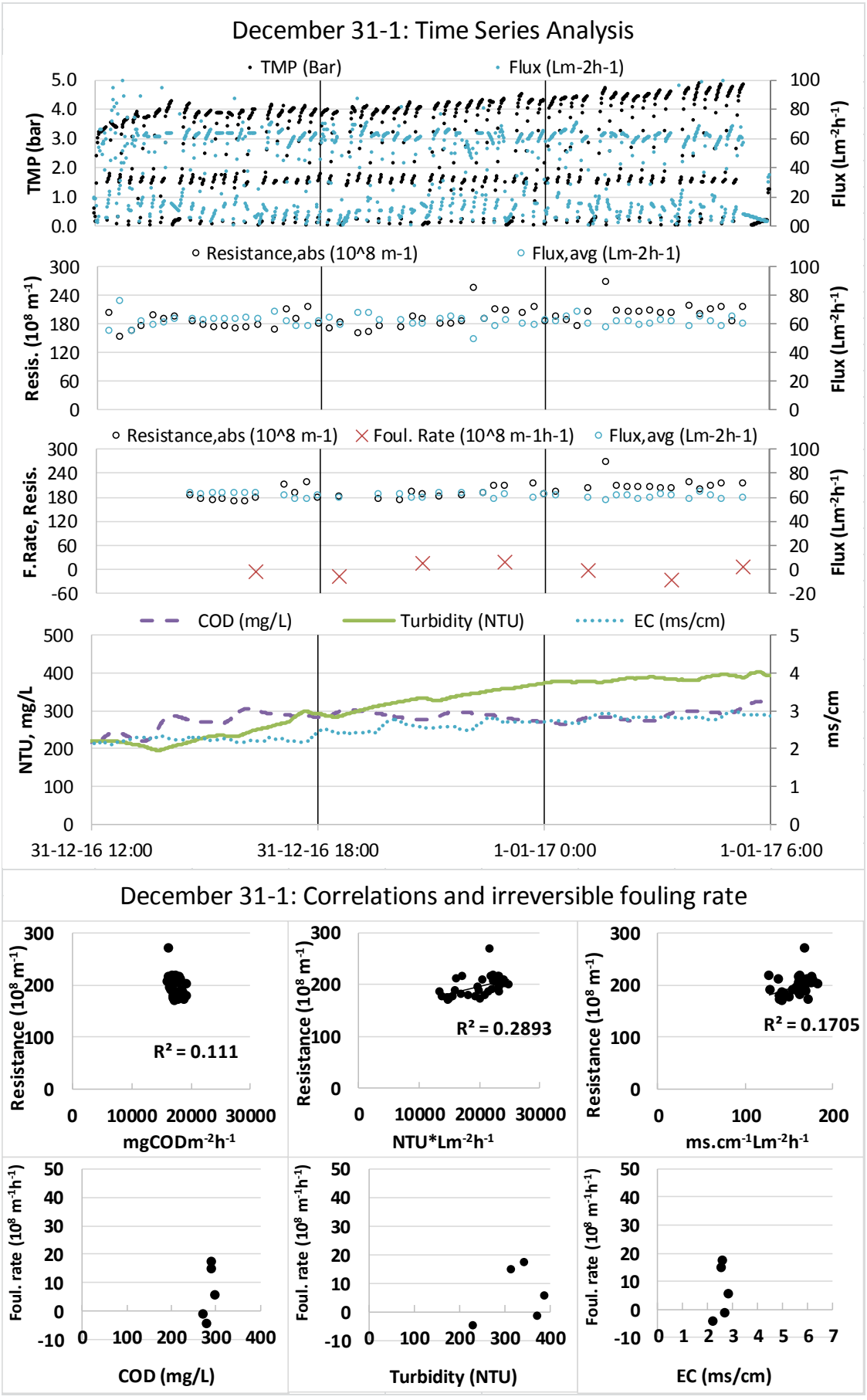

Appendix 7-8. Time series Dec 31-1

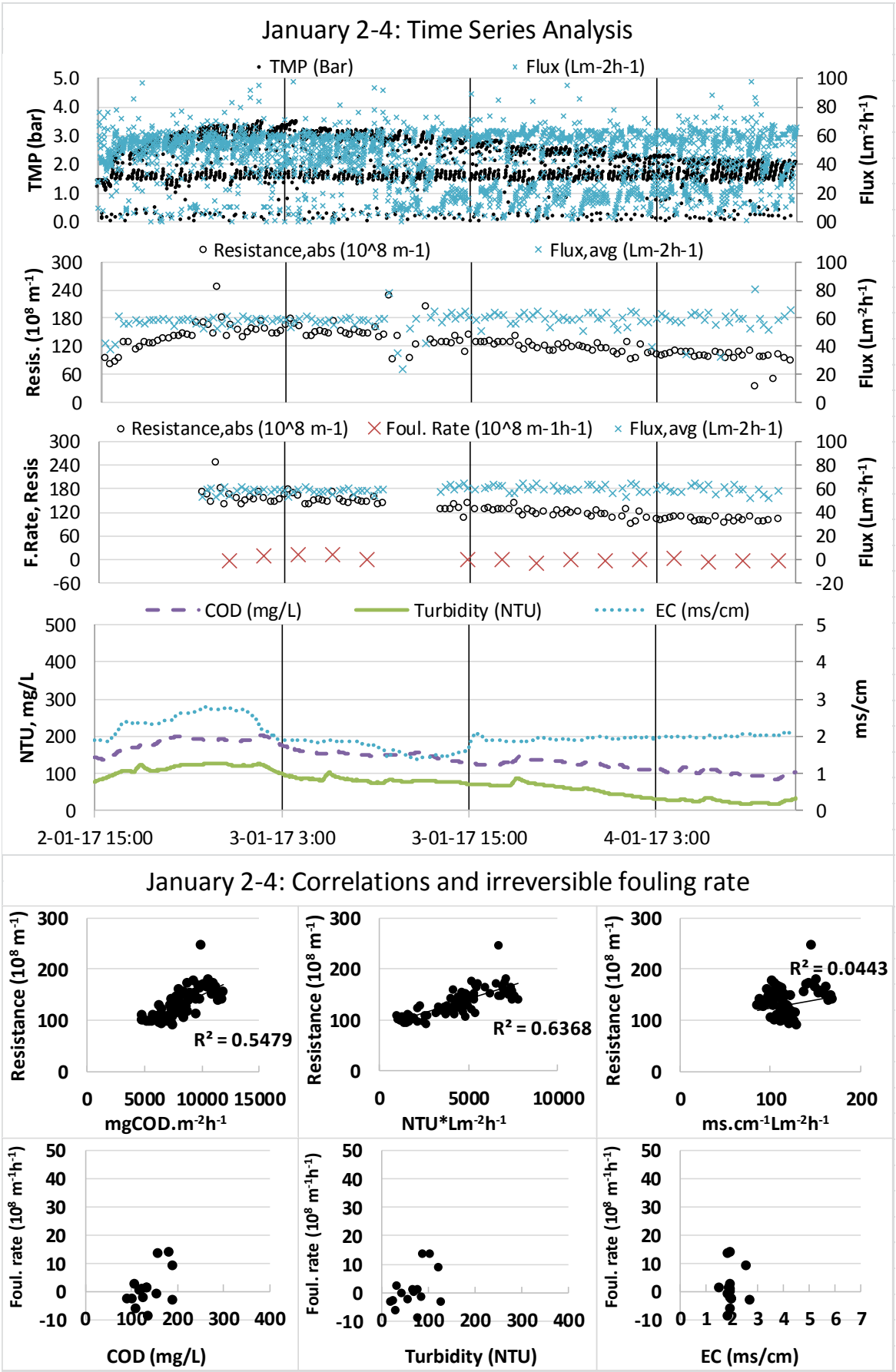

Appendix 7-9. Time series Dec 2-4

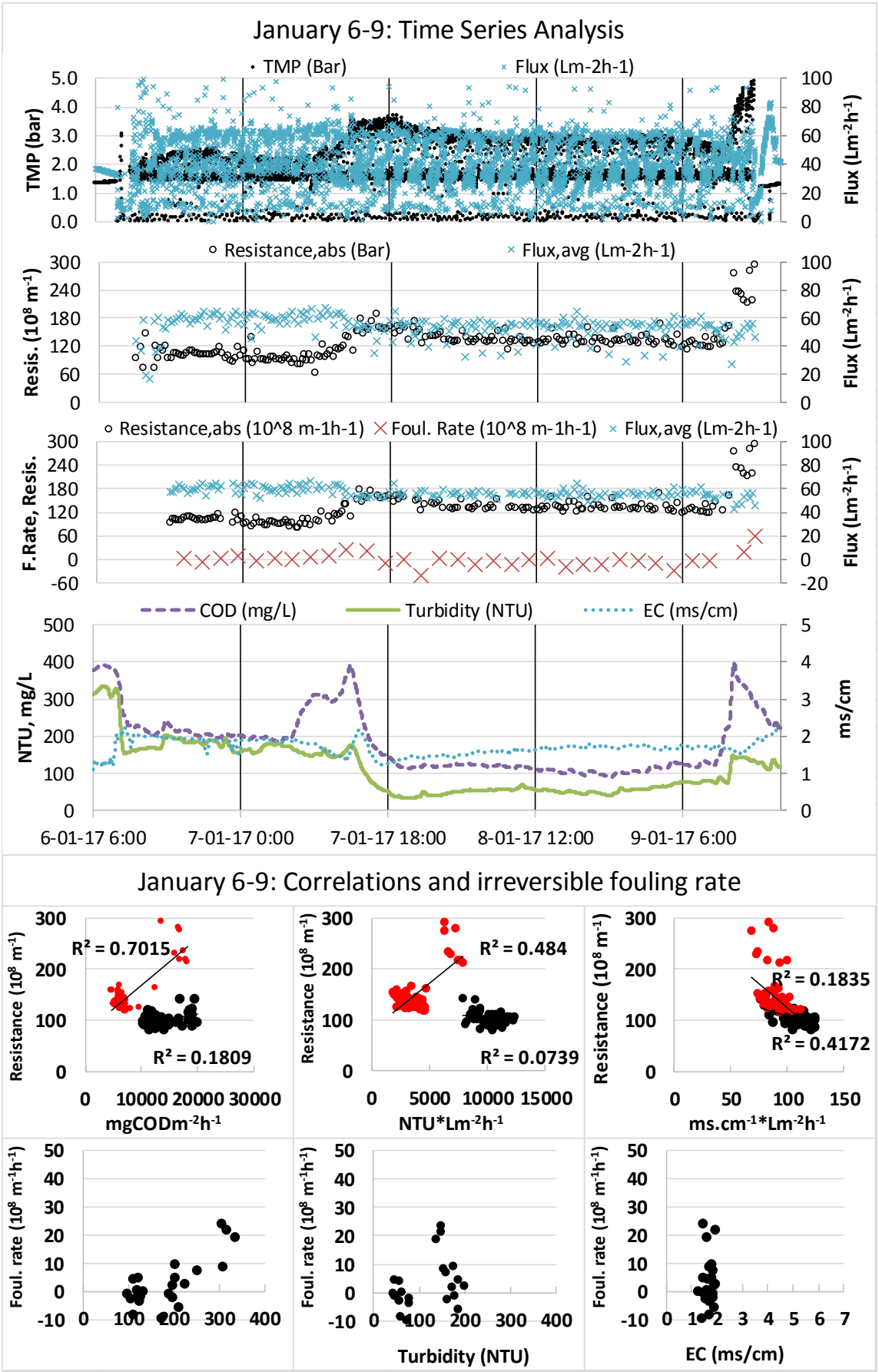

Appendix 7-10. Time series Dec 6-9

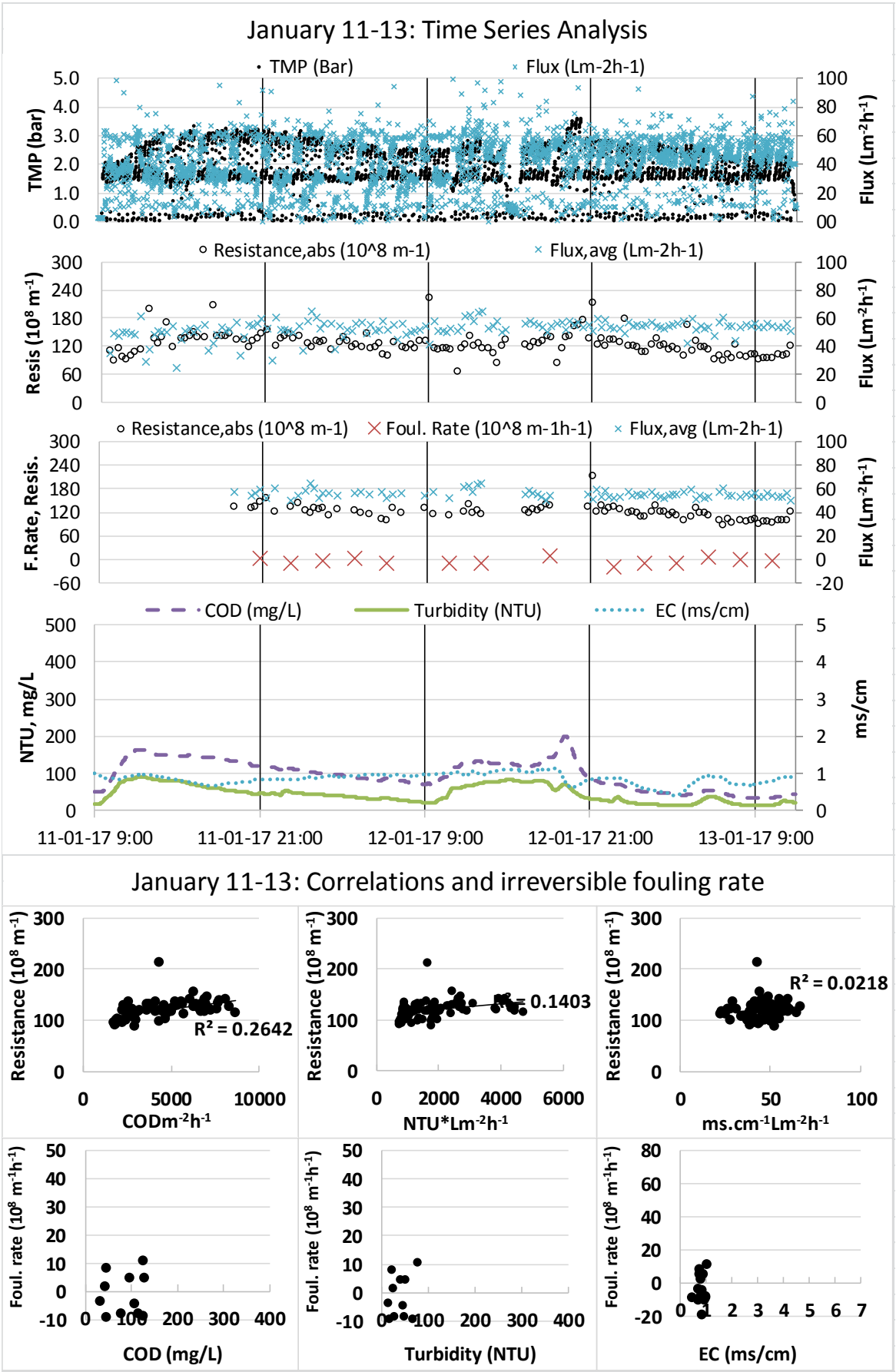

Appendix 7-11. Time series Dec 11-13

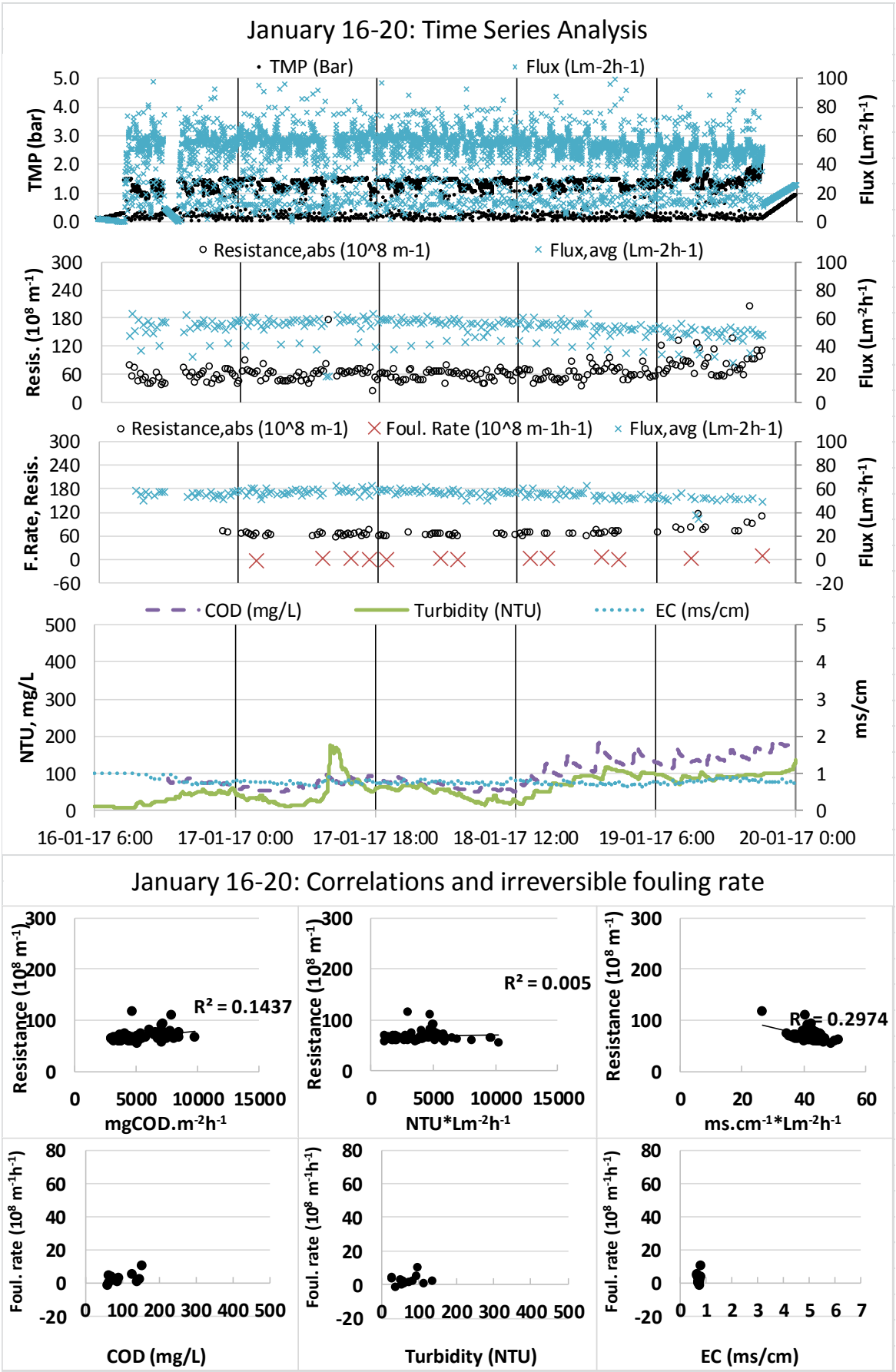

Appendix 7-12. Time series Dec 16-20

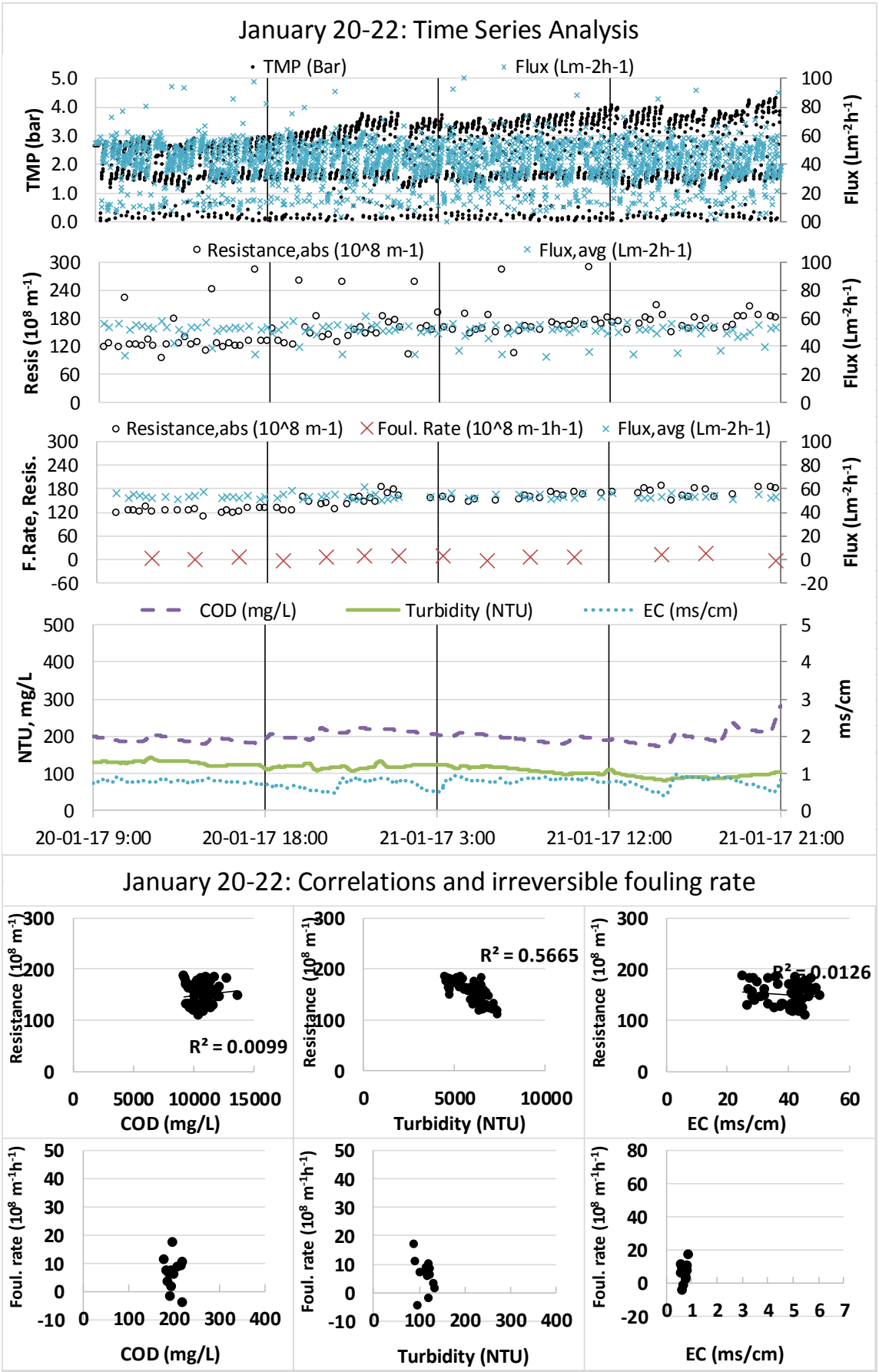

Appendix 7-13. Time series Dec 20-22

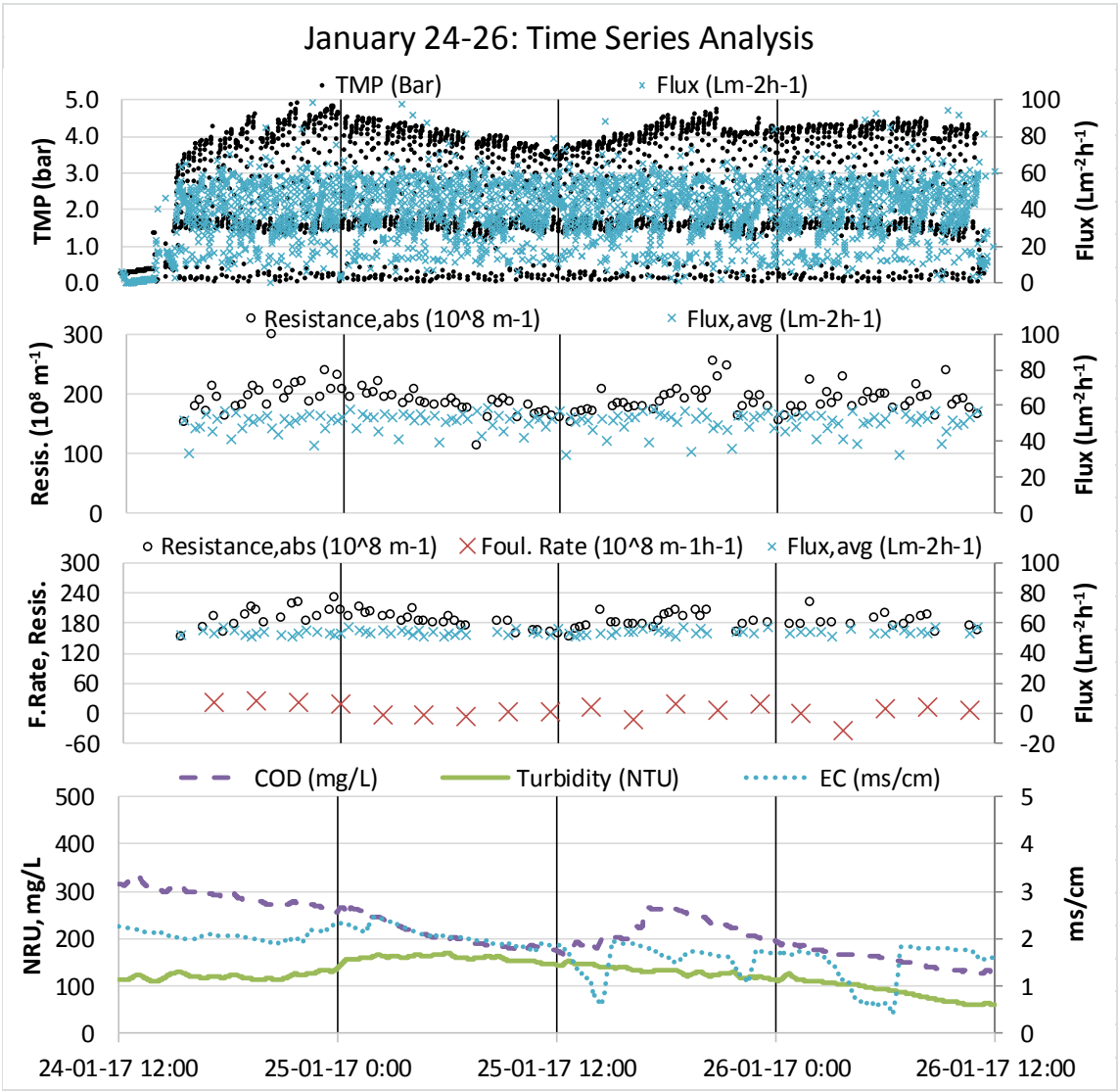

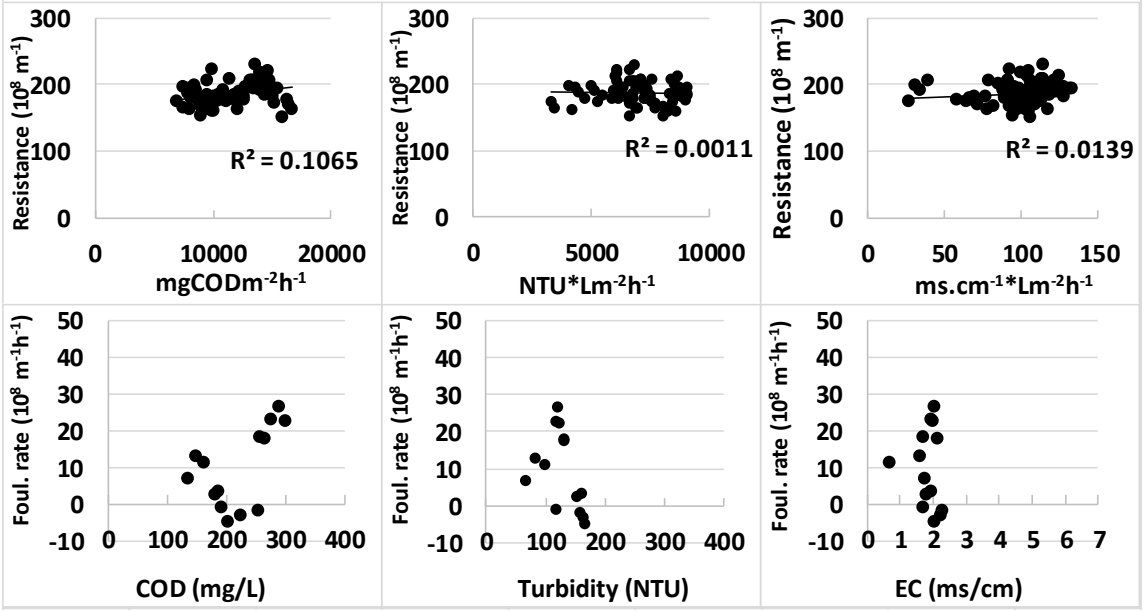

Appendix 7-14. Time series Dec 24-26

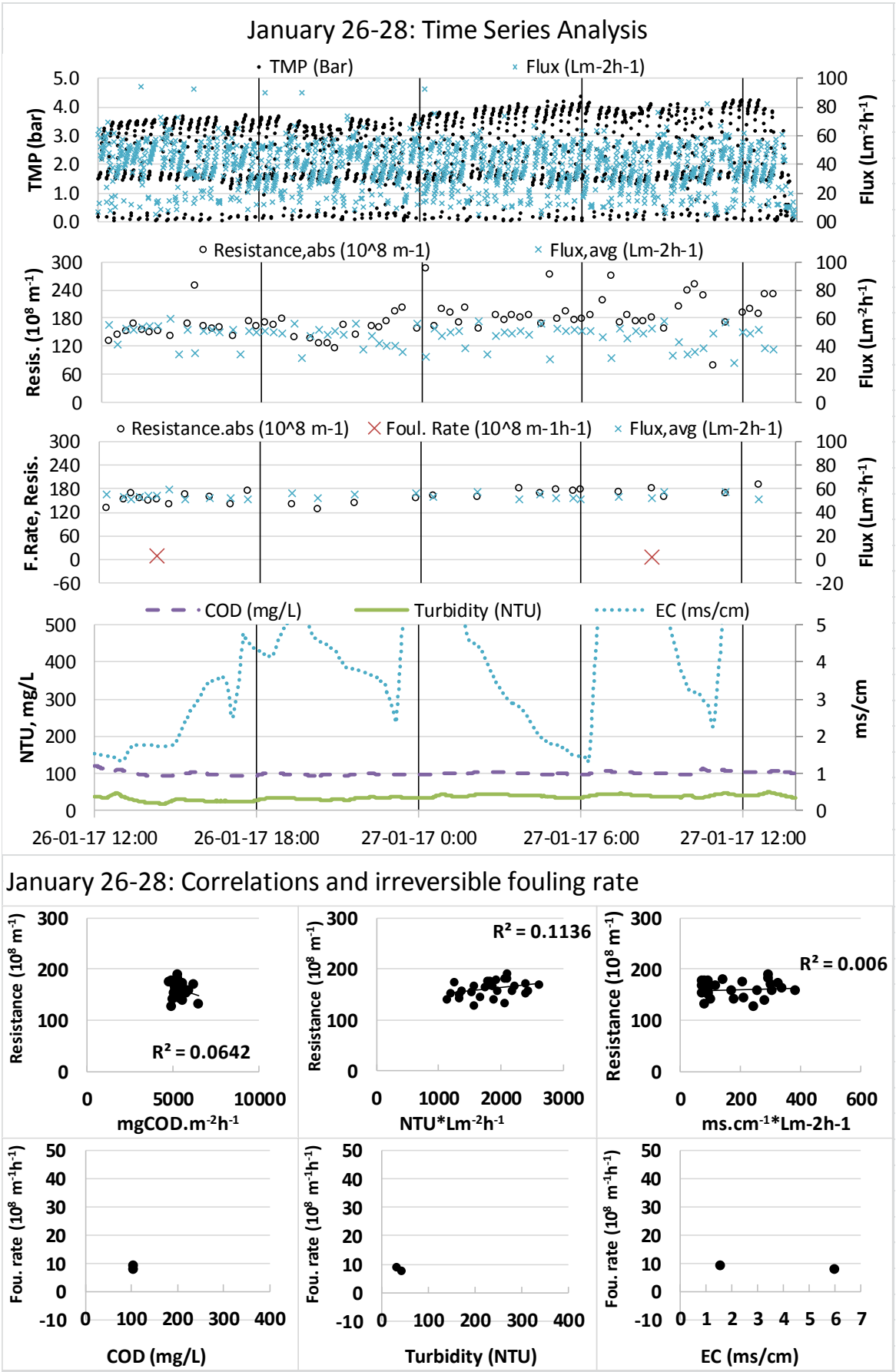

Appendix 7-15. Time series Dec 26-28

Appendix B RQ 2 results December

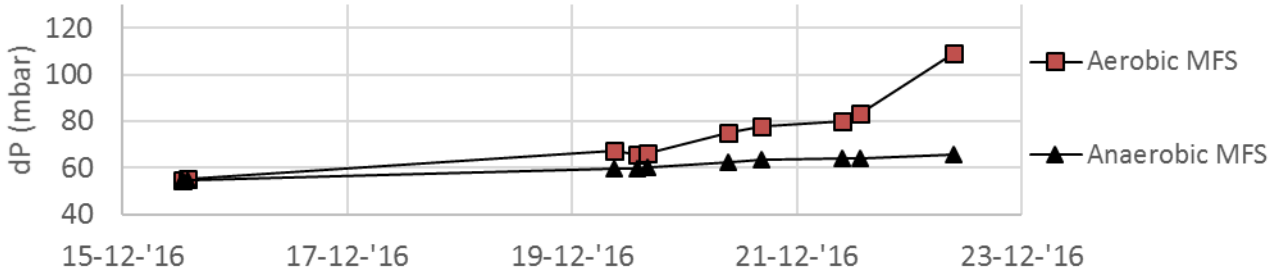

The parameters below are measured in samples taken from the MFS buffer tank

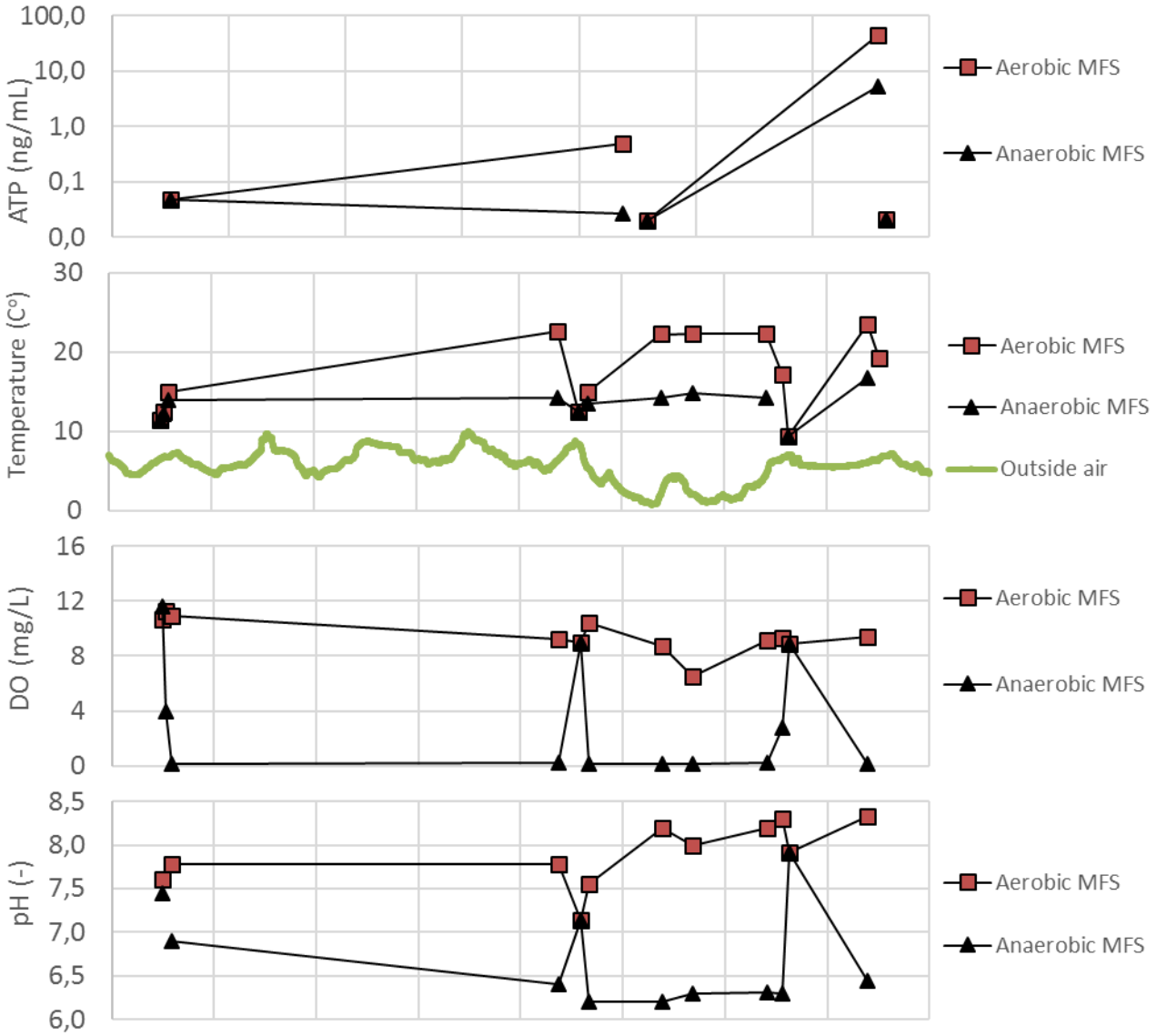

Appendix C RQ 2 results January

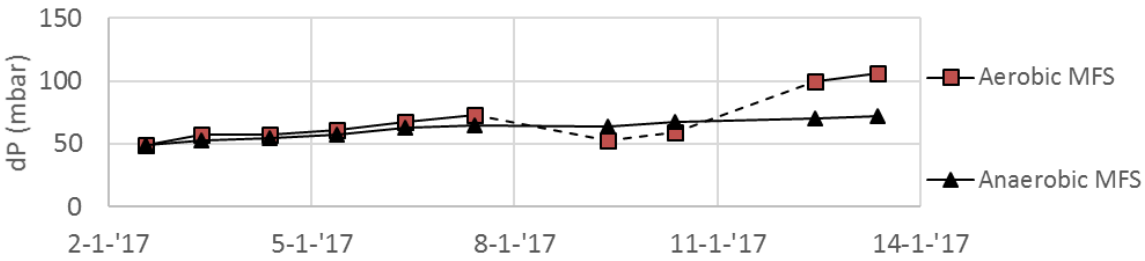

The parameters below are measured in samples taken from the MFS buffer tank

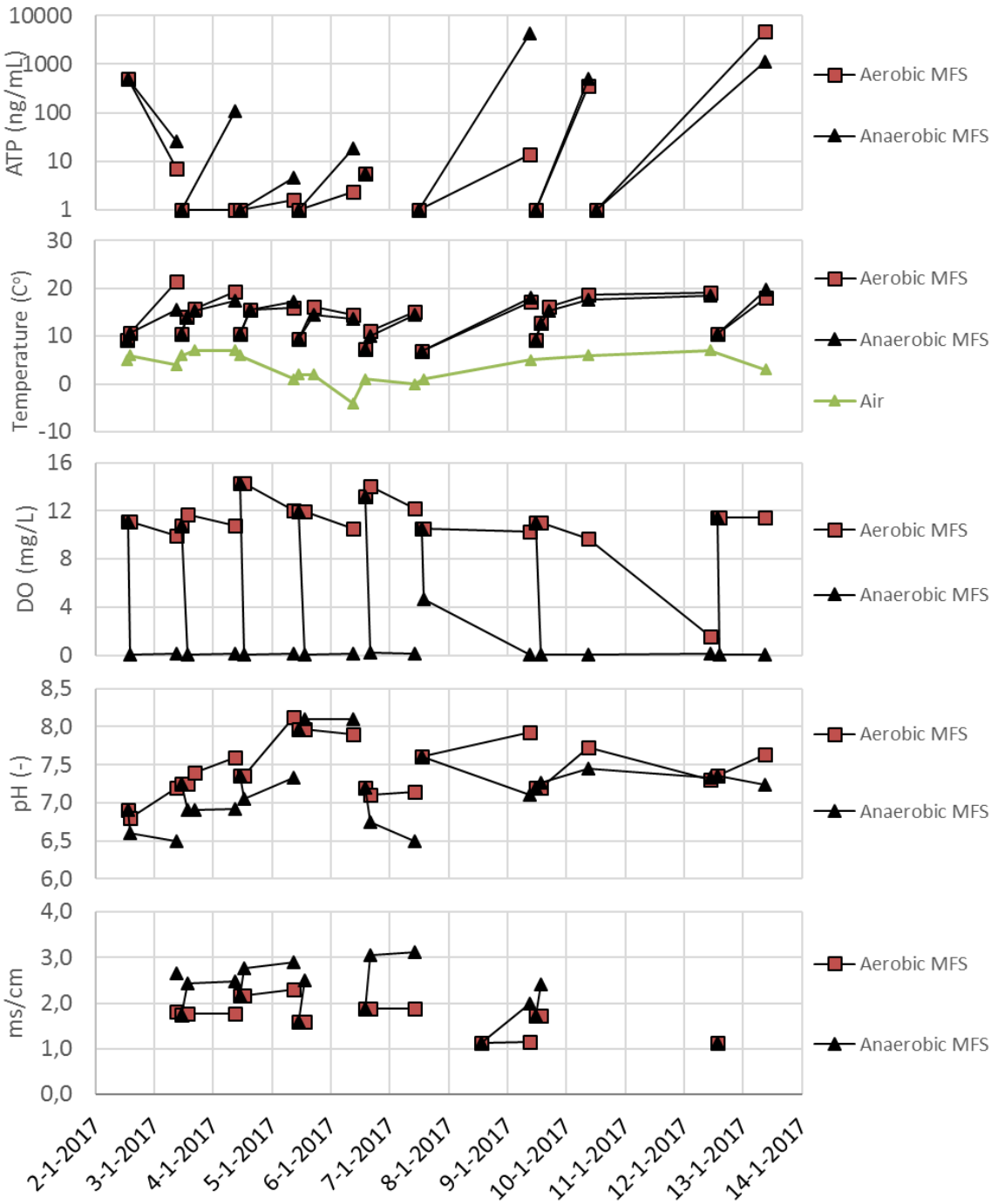

Appendix D SWTP cost calculation

The main goal in conventional biological treatment is to remove organic matter (BOD), nitrogen, and phosphate which requires anaerobic-, anoxic-, and/or aerobic conditions (Metcalf & Eddy, 2014). The removal principles are roughly explained below:

- The BOD in sewage water is removed in either aerobic or anoxic conditions by microorganisms. With the organic matter as carbon source and bound- or free oxygen the microorganisms are able to degrade/oxidize the organic matter into for example CO^2 and H_2O.
- For the removal of nitrogen (biologically) the processes nitrification and denitrification are needed. Nitrification occurs in aerobic conditions where ammonia and nitrite are oxidized by autotrophic bacteria. In subsequent anoxic conditions the formed nitrite is reduced to nitrogen gas by heterotrophic bacteria. In latter mentioned process organic carbon needs to be available.
- In anaerobic conditions Phosphate Accumulating Organisms (PAOs) consume readily available organic matter (rbCOD) by using energy made available from their stored polyphosphates. By the consumption cbCOD the PAOs produce intracellular poly-β-hydroxyalkanoate (PHA) storage products and release phosphates. Subsequently, in anoxic or aerobic conditions bounded- or free oxygen, respectively, oxidizes the PHA for cells growth and the formation of polyphosphate bonds so enhanced phosphate uptake will take place.

In order to make an estimate for the conventional biological treatment costs the cost tool ‘Afvalwatercalculator (Sewage calculator)’ is used (Padmos, 2012). The treatment system used for the cost tool is the ‘Carrousel’, an activated sludge circulation system. In a Carrousel biological BOD removal and denitrification can be integrated. The removal processes are performed in different zones inside the Carrousel. The optimal volume per zone depends on the oxygen concentration, water temperature and influent BOD. Thus the larger the Carrousel the more options for process operation control. Additionally, preceding the Carrousel an anaerobic tank will provide the operating conditions for biological phosphorus removal.

For the sewage cost tool, Padmos (2012) decomposed the conventional biological treatment as shown in Figure 7-1. The selector provides proper mixing of ‘fresh’ influent with the returned sludge from the secondary clarifier. Generally, the selector is considered as part of the anaerobic tank in cost calculations. Based on post calculation of realized project extrapolation lines are made for each of the elements. The extrapolation lines are made between the cost-determining parameter per element and constructional- and operational costs.

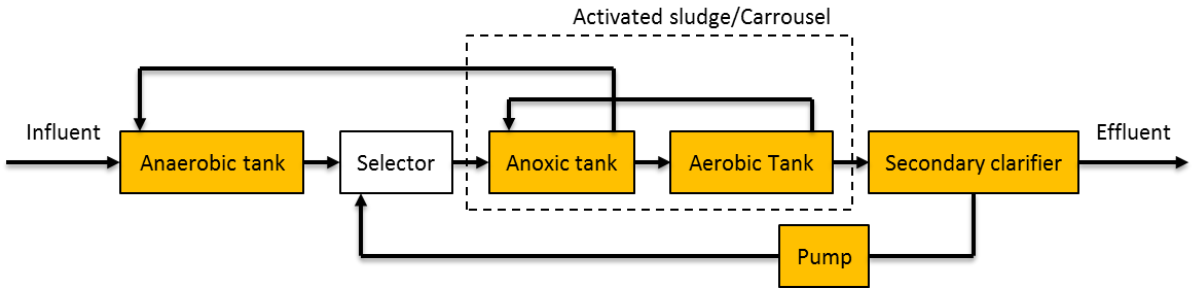

Figure 7-1. The different elements in the sewage treatment plant decomposition for the cost calculation.

The constructional costs are divided into civil-, mechanical-, and process automation- and electrical engineering costs (P&E). The average percentage of these three items in the total construction costs are given in Table 7-1. The studied operational costs include capital costs, energy consumption and maintenance for aeration. The process automation & electrical engineering costs are difficult to obtain since these are not well reported. Also the type of electrical installation per construction strongly varies which makes it difficult to quantify. Therefore only the civil- and mechanical engineering costs are considered in this report. Eventually, the P&E costs can be calculated since the average P&E percentage from the total construction costs are known.

Table 7-1. Division of the total construction costs in percentages

Costs item	Percentage (%) of the total construction costs			
	Anaerobic	Carrousel	Clarifier	Sludge circulation pump
Civil engineering	40	66	90-95	60
Mechanical engineering	40	13		22
P&E	20	21	5-10	18

Subsequently, Padmos (2012) obtained various cost formulas, in cooperation with Royal HaskoningDHV, for each treatment element. The cost formulas are given in the table below.

Table 7-2. Cost formulas for conventional biological treatment processes

		Costs (y) in euro	
Cost item	Variable x	Cost formula	Domain
Anaerobic tank	Volume (m^3)	y = 129x + 178.000	700 ≤ x ≤ 2800
Aeration tank	Volume (m^3)	y = 64x + 400,155	3300 ≤ x ≤ 10800
• Compressor	Flow (m^3h^{-1})	y = 7x + 34.000	1600 ≤ x ≤ 6400
• Aeration elements	Flow (m^3h^{-1})	y = 39x + 172.000	1600 ≤ x ≤ 6400
• Piping work	Flow (m^3h^{-1})	y = 27x+ 79.000	1600 ≤ x ≤ 6400
• Energy building	# Compressors	y = 33000x	-
• Lift	# Lifts	y = 20700x	-
• Propellers	# Propellers	Y = 25000x	-

Clarifier tank	Diameter (m)	y = 15,001x - 122,889	39 ≤ x ≤ 52
• Bridge	Diameter (m)	y = 3300x	39 ≤ x ≤ 50
Return pumping station	Flow (m^3h^{-1})	y = 17x + 167,128	485 ≤ x ≤ 4000
• Mortar	Flow (m^3h^{-1})	y = 29.436 ln(x) - 160.222	485 ≤ x ≤ 4000

In Table 7-2, it can be seen that numbers are required about the flow and tank dimensions in each phase of the treatment scheme, as given in Figure 7-1. With simple rules of thumb and general design numbers from the book 'Wastewater Engineering' (Metcalf & Eddy, 2014), all internal flows are determined, see schematically representation in Figure 7-2. As reference, the existing SWTP 'Kralingseveer' is used which treats 3500 m^3h^{-1} with a low loaded active sludge process. The internal flows and the tank dimensions with corresponding costs are calculated, see Table 7-3. From these costs the specific costs in $EURm^{-3}$ are calculated which is shown in Table 7-4. A specific cost of approximately 5 $EURct.m^{-3}$ is calculated. The process automation, civil-, mechanical-, and electric engineering costs is approximately 16.5 % of a total treatment plant (Drinkwater Kostenstandaard RHDHV, 2014). This results in a total treatment cost of ~0.31 $EURm^{-3}$.

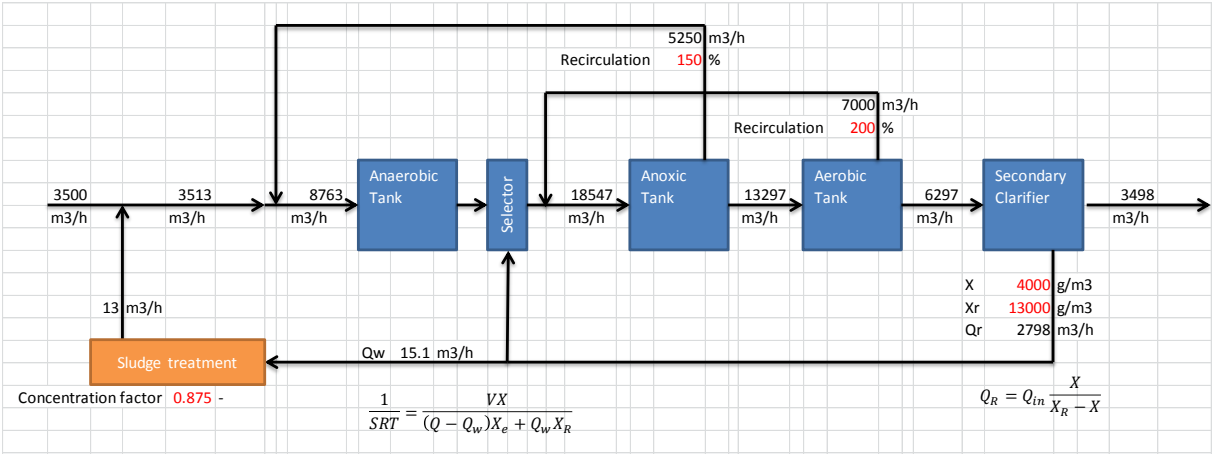

Figure 7-2. Schematically representation of the calculated flows in a conventional SWTP

Table 7-3. SWTP cost calculation

	Specific Energy cost		EUR/kWh	0.1	Source
	Influent flow (Qinf)		**m3/h**	**3500**	
	Influent BOD		mg/L	300	
	Return percentage from sludge treatment		%	87.5	Thickening from 1 to 8 percent SS content
Anaerobe tank	**Flow**	**Q**	**(m3/h)**	**8763**	
	Number of tanks		#	4	
	Residence time		h	1	Metcalf & Eddy, 2014 page 648
	Tank volume (single)		m3	2191	Domein: 700 < x < 2800
CT	Tank costs (total)		EUR	€ 1,842,456	
Seletor	**Flow**			**11547**	
AS system	**Flow**	**Q**	**m3/h**	**18547**	
	Number of Carrousels		#	5	Assumption
	Influent BOD	So	g/m3	300	
	MLSS anoxic tank	Xb	g/m3	4000	Metcalf & Eddy, 2014. Sludge conc is typically 4 g/m3
	Food to biomass ratio	F/M	g BOD/ gVSS*d	0.15	Metcalf & Eddy, 2014 page 755

	Tank volume (Single AS system)	V	m3	8400	Domein: 3300 < x < 10800
	Contact time			3.2	
	Recirculation		%	150	Metcalf & Eddy, 2014 page 873
	Sludge circulation		**m3/h**	**5250**	
Aerobic treatment	**Flow**	**Q**	**m3/h**	**13297**	
CT	Active sludge tank (EU)		EUR	€ 4,688,775	
	Compressors per Carrousel	n	#	1	Assumption
WTB	Costs compressor		EUR	€ 263,076	(Padmos, 2012)
WTB	Costs elements		EUR	€ 1,378,567	(Padmos, 2012)
WTB	Costs piping and appendages		EUR	€ 754,008	(Padmos, 2012)
WTB	Costs power building		EUR	€ 165,000	(Padmos, 2012)
	Propellors per Carrousel		#	6	Assumption
WTB	Costs lift		EUR	€ 621,000	
WTB	Costs propellors		EUR	€ 750,000	(Padmos, 2012)
	Effluent BOD	Ce	mgO2/L	10	Lozingseis Harnashpolder
	Oxygen requirement		kgO2/d	24360	
Compensation for fluctuation in oxygen requirement	Deficietfactor	β	-	1.21	Metcalf & Eddy, 2014
Difference between clear- and sludge water	Alpha-factor	α	-	0.70	Metcalf & Eddy, 2014
	Operation time of propellors	t	hour/d	12	Assumption
	Oxygen transfer efficiency	η_{O2}	kgO2/kWh	2	Metcalf & Eddy, 2014
	Power consumption per propellor	P	kW	1.5	Assumption
	Costs Compressor + Propellors		EUR/y	€ 788,181	(Padmos, 2012)
Manhours + oil costs	Costs maintenance		EUR/y	€ 31,950	(Padmos, 2012)
	Recirculation		%	200	Metcalf & Eddy, 2014 page 873
	Nitrite circulation		**m3/h**	**7000**	
Secondary settling	**Flow**		**m3/h**	**6297**	
	Number of tanks		#	6	Assumption
	SVI		mL/g	100	Metcalf & Eddy, 2014
	SVLR		m/h	0.3	Metcalf & Eddy, 2014
	Surface (single tank)		m2	1399	
	Diameter		m	42	Domein: 39 < x < 52
CE	Total Costs Tanks		EUR	€ 3,061,701	
WTB	Scraping bridge		EUR	€ 835,732	
	Solids Retention Time	SRT	d	7	Metcalf & Eddy, 2014, page 873
	Biomass in effluent	Xe	g/m3	1	Assumption
	Waste sludge flowrate	**Qw**	**m3/h**	**15.1**	
	Number of pumps		#	1	
	Sludge conc. In return flow	Xr	mg/L	13000	Metcalf & Eddy, 2014, page 1458
	Selector circulation		**m3/h**	**2783**	Domein: 485 < x < 4000
CE	Costs sludge return pump		EUR	€ 214,445	(Padmos, 2012) Regressielijn RHDHV
WTB	Costs mortar			€ 73,247	(Padmos, 2012) Regressielijn RHDHV
	Flow		**m3/h**	**3498**	

Table 7-4. Total SWTP costs

				Total	Yearly costs	
	Civil Eng.	Mech. Eng.	Process. Electric.	EUR	EUR/y	
Life time (year)	30	25	10			
Anaerobic	€ 1,842,456	€ 0	€ 0	€ 1,842,456	€ 61,415	
Aerobic	€ 4,688,775	€ 4,001,783	€ 2,310,148	€ 11,000,706	€ 547,379	
Secondary clarifier	€ 3,276,146	€ 908,979	€ 465,014	€ 4,650,139	€ 192,065	
Operational					€ 820,131	EUR/y
				Total	€ 1,620,990	EUR/y
				Effluent flow	3497	m3/h
					€ 0.05	EUR/m3

Appendix E Accuracy cost tool

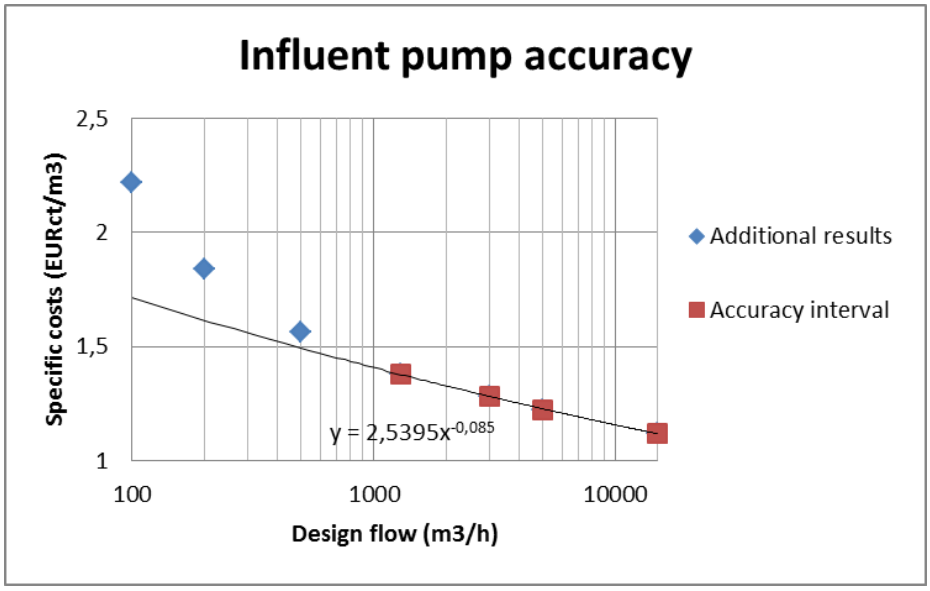

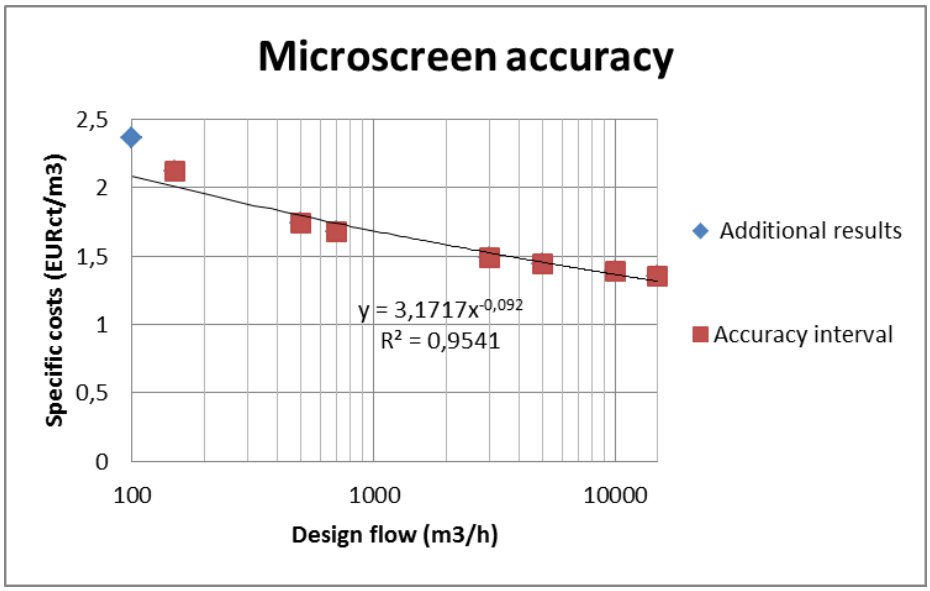

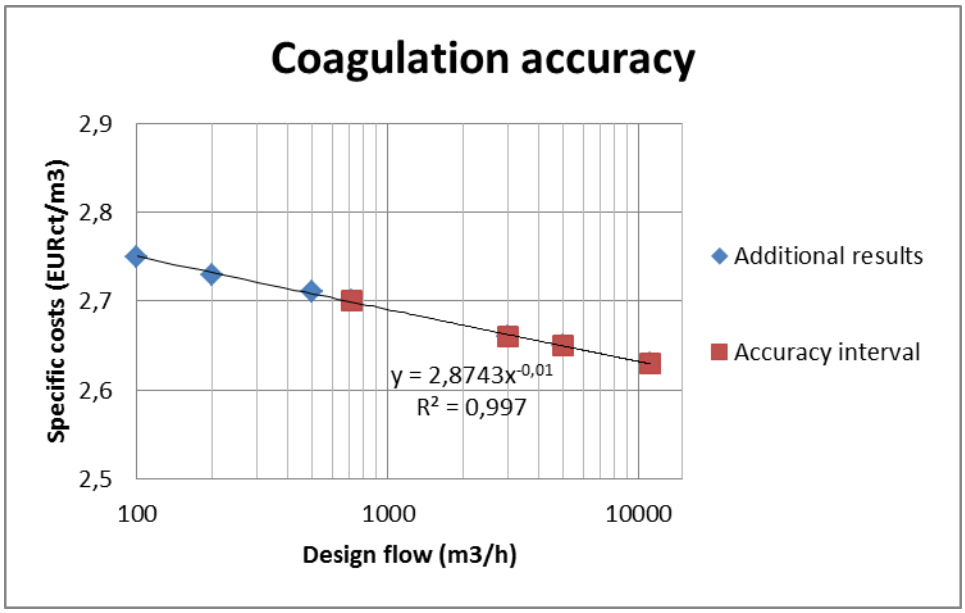
Coagulation accuracy
Specific costs (EURct/m3)
2,9
2,8
2,7
2,6
2,5
100
1000
10000
Design flow (m3/h)
y = 2,8743x-0,01
R² = 0,997
Additional results
Accuracy interval

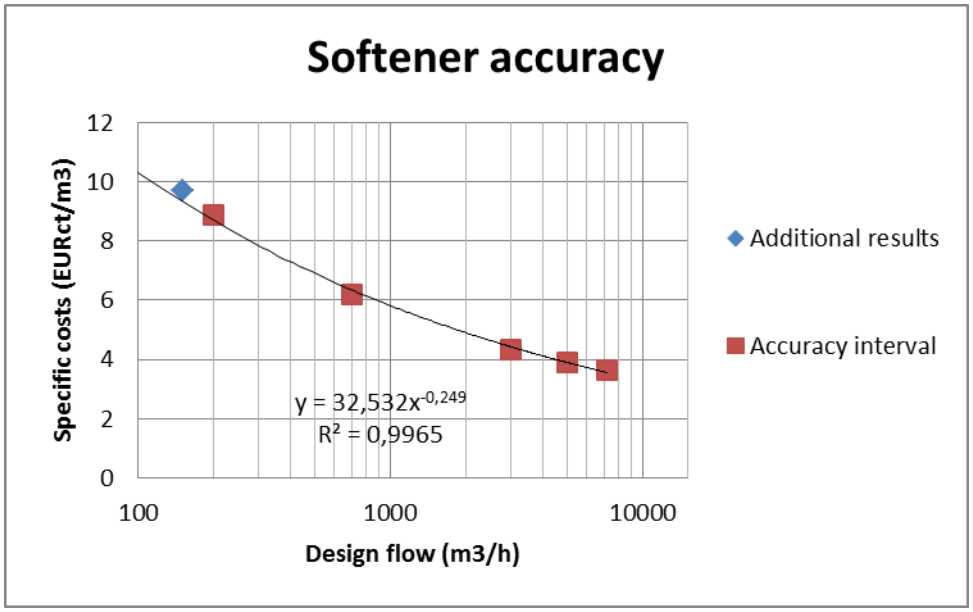
Softener accuracy
Specific costs (EURct/m3)
12
10
8
6
4
2
0
100
1000
10000
Design flow (m3/h)
y = 32,532x-0,249
R² = 0,9965
Additional results
Accuracy interval

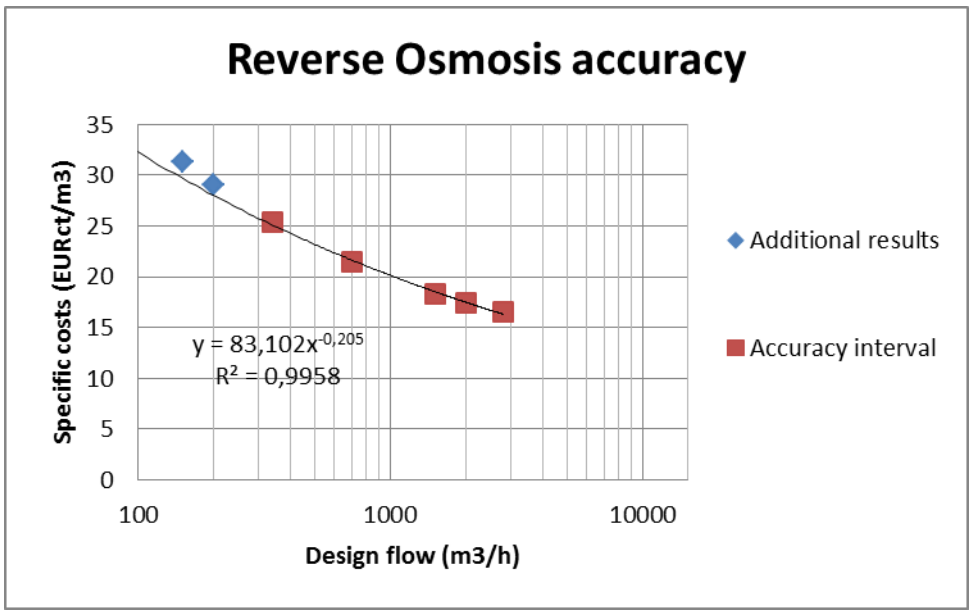
Reverse Osmosis accuracy
Specific costs (EURct/m3)
35
30
25
20
15
10
5
0
100
1000
10000
Design flow (m3/h)
y = 83,102x-0,205
R² = 0,9958
Additional results
Accuracy interval

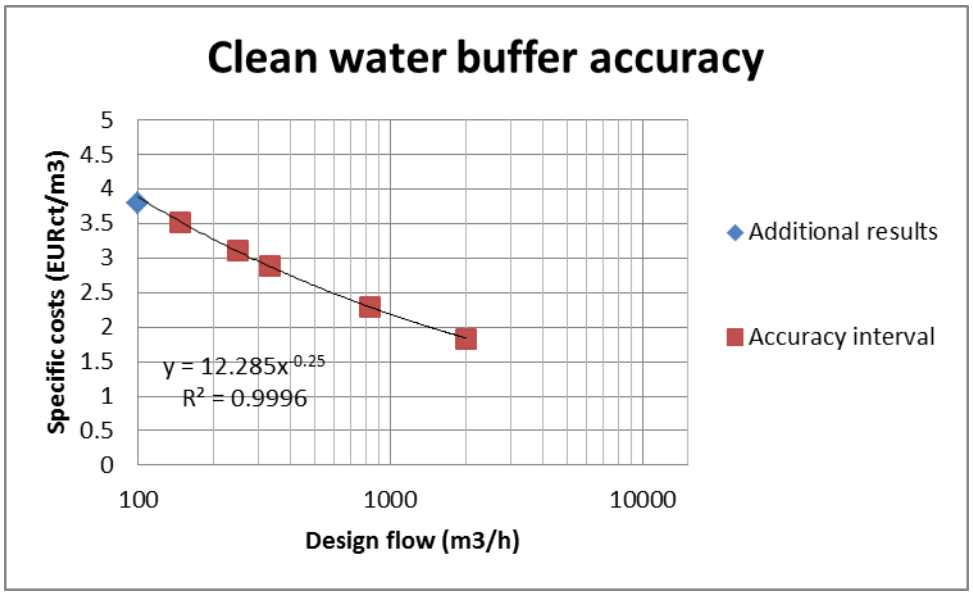
Clean water buffer accuracy
Specific costs (EURct/m3)
5
4.5
4
3.5
3
2.5
2
1.5
1
0.5
0
100
1000
10000
Design flow (m3/h)
y = 12.285x-0.25
R² = 0.9996
Additional results
Accuracy interval

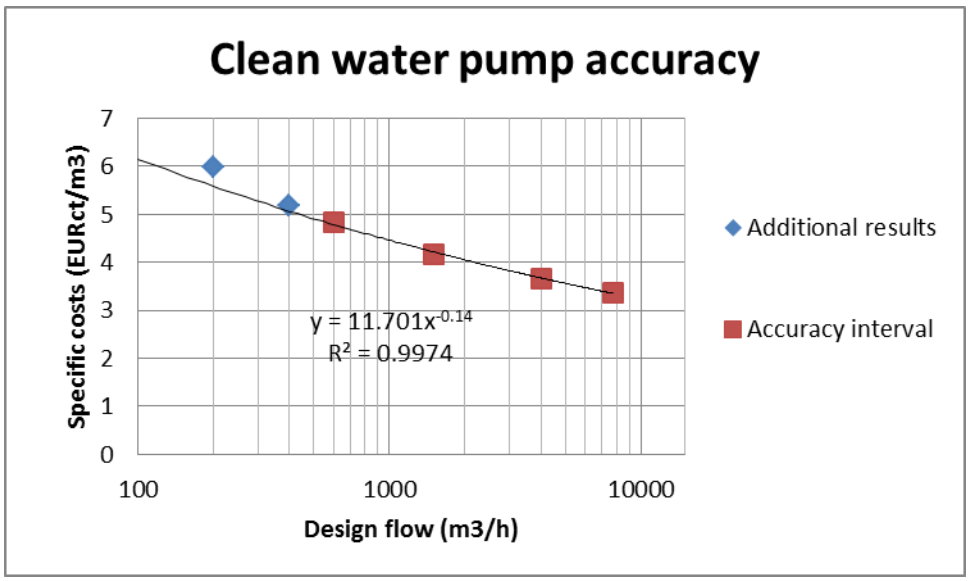
Clean water pump accuracy
Specific costs (EURct/m3)
7
6
5
4
3
2
1
0
100
1000
10000
Design flow (m3/h)
y = 11.701x-0.14
R² = 0.9974
Additional results
Accuracy interval